Graduate School Form 30
Updated 1/15/2015

PURDUE UNIVERSITY
GRADUATE SCHOOL
Thesis/Dissertation Acceptance

This is to certify that the thesis/dissertation prepared

By Tushar P. Bakhtiani

Entitled

OPTIMIZATION OF MODULAR DIE DESIGN IN EXTRUSION PROCESS

For the degree of Master of Science in Mechanical Engineering

Is approved by the final examining committee:

Hazim El-Mounayri
Chair

Jing Zhang
Co-chair

Sohel Anwar

To the best of my knowledge and as understood by the student in the Thesis/Dissertation Agreement, Publication Delay, and Certification Disclaimer (Graduate School Form 32), this thesis/dissertation adheres to the provisions of Purdue University's "Policy of Integrity in Research" and the use of copyright material.

Approved by Major Professor(s): Hazim El-Mounayri

Approved by: Sohel Anwar 2/13/2015

Head of the Departmental Graduate Program Date

OPTIMIZATION OF MODULAR DIE DESIGN IN EXTRUSION PROCESS

A Thesis

Submitted to the Faculty

of

Purdue University

by

Tushar P. Bakhtiani

In Partial Fulfillment of the

Requirements for the Degree

of

Master of Science in Mechanical Engineering

May 2015

Purdue University

Indianapolis, Indiana

ACKNOWLEDGEMENTS

I would like to acknowledge my utmost gratitude to the president of VIP Tooling Mr. Paul Nolting, for giving me the opportunity to work at VIP Tooling and helping me accomplish my master's thesis.

I would like to extend my special thanks to my mentors Dr. Pawel Kazanowski, and Mr. Kelby Graham for their insightful discussions that helped me achieve a better understanding of the extrusion process. Mr. Graham generously shared his years of extrusion experience and helped in guiding the objectives of the thesis.

I would like to thank Mr. Mike Foster, for constantly working with me on trouble shooting the DEFORM simulations errors and as well as helping me become an advanced user of the software.

I would like to thank my advisory committee members, Dr. Hazim El-Mounayri, Dr. Jing Zhang and Dr. Sohel Anwar for their advice and assistance.

I would like to thank all my co-workers at VIP Tooling for their help and support during this chapter of my life. I thank Akram El-Khatib and Ms. Valerie Lim Diemer for assisting me in formatting this thesis. Finally, I express my gratitude to my parents for their support and encouragement, and my brother for helping me out in time of need.

TABLE OF CONTENTS

Page

Page

LIST OF TABLES

LIST OF FIGURES

Figure Page

Figure Page

Figure Page

Figure Page

Figure Page

ABSTRACT

Bakhtiani, Tushar P. M.S.M.E., Purdue University, May 2015. Optimization of Modular Die Design in Extrusion Process. Major Professor: Hazim El-Mounayri.

Aluminum extrusion is a metal forming process used for the production of a large variety of solid, semi-solid and complex hollow products. During extrusion, the hot aluminum billet goes under severe plastic deformation as it is forced to flow through a smaller die cavity that defines the final shape of the extruding product. Surface finish and dimensional accuracy are the two most important criteria that specify the productivity and feasibility of the extrusion process which is highly influenced by the flow of aluminum through the deforming die. Therefore, die design is considered as one of the most important characteristics of the extrusion process that influences aluminum flow, quality of the extruding product and its dimensional accuracy.

Currently, development of extrusion dies is primarily based upon the empirical knowledge of the die designer gained through trial and error, which inevitability is an expensive, time consuming and ineffective method. However, owing to the technological advancements of this century in the field of finite element modeling, this decade old trial and error method can now be replaced by numerical simulations that not only save time and money but also, can accurately predict the flow of aluminum through a die as well as predict die deformation occurring during the extrusion process The motivation of this research project came from a private extrusion die manufactures need for improving their pioneered modular die based on good analytical and scientific understanding of the dies performance during the extrusion process.

In this thesis, a commercial simulation package Deform 3D is used to simulate the thermo-mechanical interactions of aluminum flow through the deforming modular die for the production of Micro Multi-Port (MMP) tubes. The attention of this thesis is focused on the following topics:

- Validation of extrusion model with the industrial measurements of extrusion load and profile exit temperature.
- Prediction of wear and stress concentration between a bilayer ($TiCN + Al_2O_3$) coated and non-coated H-13 tool steel; mandrel and die plate of the modular die.
- Understanding the effects and interactions of the mandrel and die cartridge geometric parameters with aluminum flow, extrusion load, welding pressure and die deformation.
- Optimization of the mandrel and die cartridge geometric parameters through design of experiments.

1. INTRODUCTION

1.1 Extrusion

The basic principle of extrusion is analogous to squeezing toothpaste through a tube, in which applying constant pressure at the closed end of the tube results in the toothpaste flowing out through the open end. Since the opening at the end of the tube is circular the paste emerges with a round shape.

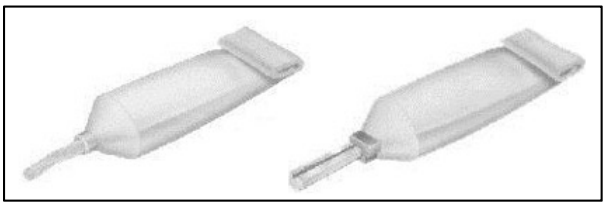

Figure 1.1 Extrusion analogy (reproduced from [1])

Similarly, extrusion is a metal forming process in which a cylindrical billet is plastically deformed by compressing it through a die that determines the cross section of the extruded product.

The earliest consideration of the principle of the extrusion dates back 1797; due to Joseph Bramah who patented the first documentation describing a process in which molten lead was forced through a die using hand-driven plungers for making pipes. In 1820, the extrusion process came into actual operation for the manufacturing of lead pipes due the invention of a hydraulic powered extrusion press invented by Thomas burr. In 1984 George Alexander Dick, invented the hot extrusion process a method applicable to almost all non-ferrous alloys by first heating the material to be formed and by controlling the temperature of the surrounding tools. Alexander Dick was able to reduce the force required to extrude materials of significant strength. His invention attributed to

a major breakthrough in the extrusion industry as the presses used for extrusion today are still based on his principle discoveries [2].

In the past extrusion was commonly used to produce cylindrical bars or hollow tubes. Today, due technological advancement, growing commercial need and better understanding of the fundamentals of extrusion a large variety of complex cross sections shown in Figure 1.2 are also produced by this process using dies of complex shapes.

(a) 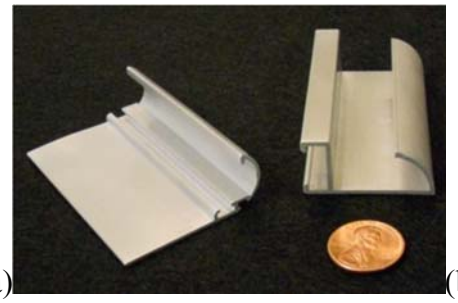 (b) 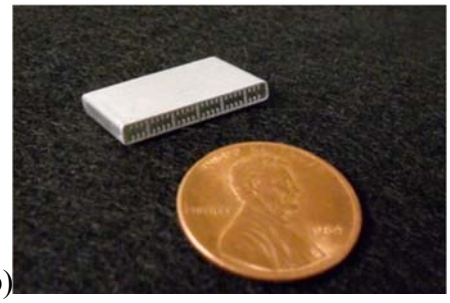

Figure 1.2 Examples of extrusion products; (a) solid profile and (b) hollow profile

1.1.1 Classification of Extrusion Processes

The two basic methods of extrusion processes utilized in the industry are direct and indirect extrusion. Direct extrusion shown in Figure 1.3 is the most important and common used method. In this process, the billet is placed in a container and is forced by the ram to flow through a stationary die. As the material moves in the direction of the ram displacement; it has to overcome the high resistance of friction caused by the motion of the billet against the container walls.

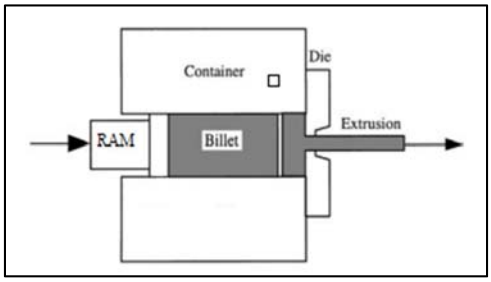

Figure 1.3 Direct extrusion (reproduced from [3])

In the indirect extrusion process shown in Figure 1.4, the billet is placed in a container that is completely closed off at one side and is pressed on from the open end of the container by the die which is placed on the ram. There are no frictional forces between the billet and container walls. As the ram pushes the die against the billet the extruded product flows in the opposite direction of the ram.

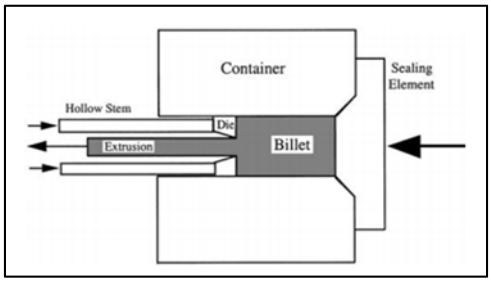

Figure 1.4 Indirect extrusion (reproduced from [3])

The only advantage of indirect extrusion process over the direct process is that it requires 25 to 30% lower energy due to the absence of friction. However, the main limitation of the indirect process is its inability to produce complex shaped extrusion products due to the rigidity and limited length of the hollow ram.

1.1.2 Aluminum Extrusion Process

The direct extrusion process is a widely practiced method for the extrusion of aluminum alloys due to its the versatility of producing long cross section of solid, hollow and shaped profiles without compromising the rigidity of the ram and ease of providing support to the extruded product when compared to the indirect process.

The typical sequence of operation for the direct extrusion method are:

1. Loading of the billet into the press.
2. Extrusion of the billet.
3. Decompression of the press and opening of the container to expose the discard.
4. Shearing the discard.
5. Returning the shear, container and ram to the loading position.

The basic schematic drawing of a direct extrusion press can be seen in Figure 1.5, where 1 is the feeder plate; 2 is die; 3 is the backer; 4 is the die ring; 5 is the bolster; 6 is the pressure pad; and 7 is the dummy block.

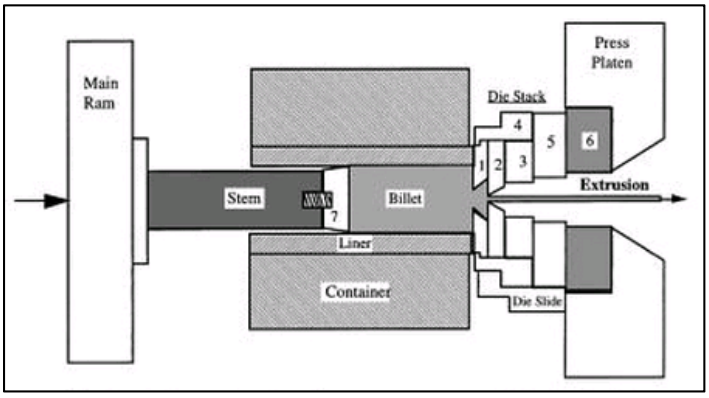

Figure 1.5 Schematic drawing of a typical direct extrusion press (reproduced from [4])

Before the extrusion process begins the aluminum billet, container and die are preheated to ease the deformation process and minimize the occurrence of work hardening. The preheated aluminum billet is sealed in the container with the help of a dummy block that prevents the aluminum from leaking backwards. The dummy block is used to transmit the force from the hydraulic ram on to the aluminum billet, causing it to plastically deform and flow through the die, thus causing high values of compressive forces at the container and die interface. To minimize die deformation and outlet shape distortion the die is housed within a support tooling stack which typically comprises of a backer, holder and bolster [5].

During the extrusion process the aluminum billet shears due to high friction between the billet and container interface adding to the force required to extrude the metal while accumulating a layer of oxides, magnesium silicide, dross etc. at the back end of the billet which could compromise the quality of the extruded shape. Therefore; not all of the aluminum billet is extruded at least one third of the compressed aluminum billet; also known as the discard or butt, is sheared off at the end of the extrusion cycle. A new billet is then inserted into the container and the whole process is repeated again, this is commonly known as billet-on-billet extrusion.

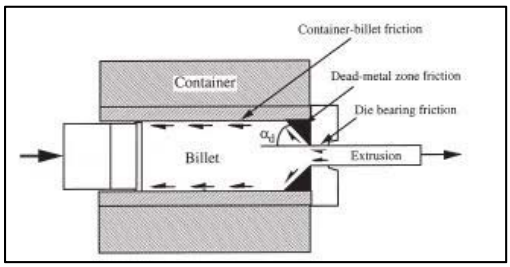

Figure 1.6 Metal flow of billet in direct extrusion (reproduced from[3])

The effect of friction between the billet and container results in an increase of force required by the ram to push the aluminum billet through the die. The typical trend of load-displacement curve of the ram during the direct extrusion process is shown in Figure 1.7 and is traditionally described in three stages:

1. Upsetting: the diameter of the billet is typically smaller than the inner diameter of the container, therefore, the rapid increase in load is due to upsetting of the billet to fill the container.
2. Breakthrough: this is the maximum amount of force required by the ram to fill the die cavity before the extruded product leaves the die.
3. Steady State: as the extruded product leaves the die steady state extrusion commences and the load gradually declines as the length of the billet decreases.

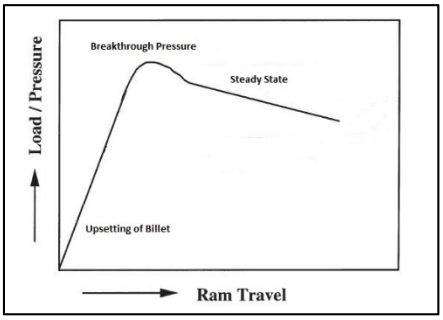

Figure 1.7 Extrusion load of a typical direct extrusion process

The aluminum extruded products made through the direct extrusion process can be categorized into two groups solid and hollow profiles as shown in Figure 1.2.

1.1.3 Micro-Multiport Tubing

Contemporary heat exchange applications such as air conditioning systems, evaporators, radiators and refrigerators use parallel flow tubes that are fabricated with aluminum extruded Micro-Multiport (MMP) tubes. This tubing, which is also referred to as condenser tubes, is typically made out of 1000 or 3000 series aluminum alloys due to their characteristic properties of high performance, low weight, low corrosion, and high recycling value. In general, the MMP tube is a flat body with a row of side-by-side passageways, which are separated by upright web walls as shown in Figure 1.8.

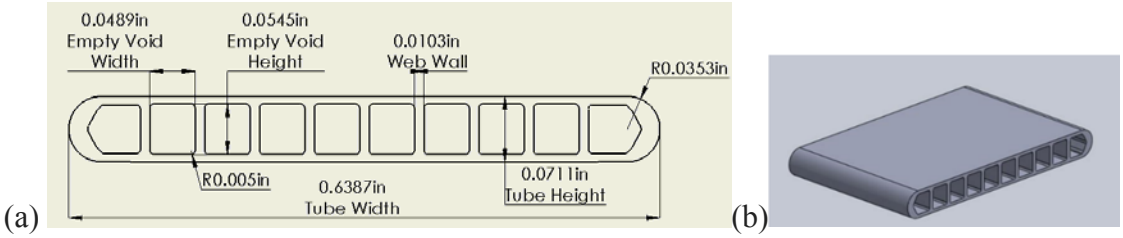

Figure 1.8 Micro-Multiport tube; (a) tubing dimension and (b) 3D profile

MMP tubes fall under the category of hollow extrusion profile that is produced with competitiveness in cost and good surface quality using the direct extrusion process. In the industry production of complicated hollow profiles are accomplished using special dies that consist of a mandrel and welding chamber such as porthole die, spider die and bridge die as shown in Figure 1.9.

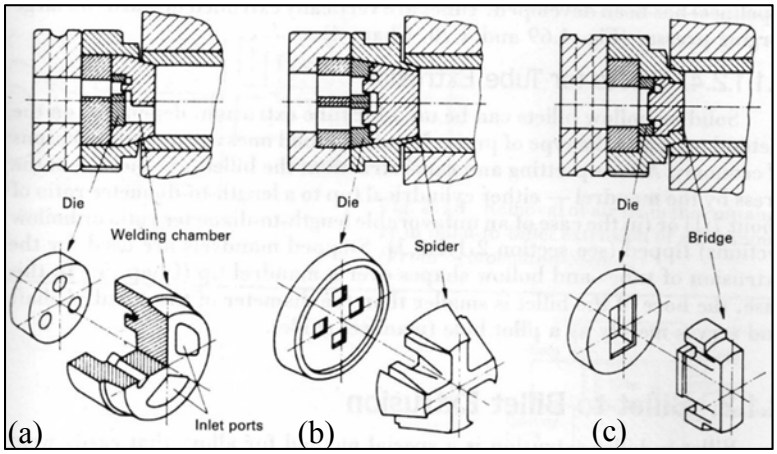

Figure 1.9 Porthole die; (b) spider die and (c) bridge die (reproduced from [6])

1.1.3.1 Modular Die and Tooling

The extrusion of hollow profiles such as the MMP tube shown in Figure 1.8 consists of ten empty voids separated by very thin web walls, which makes the die design even more sophisticated as the success of MMP tube extrusion depends on the die design, in order to achieve good quality of surface finish and high dimesional accuracy.

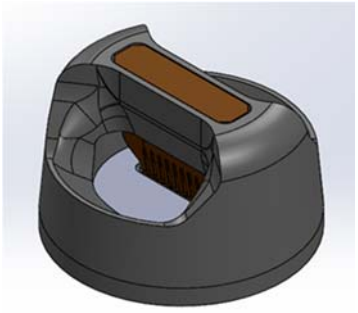

Figure 1.10 Modular die

The formation of the MMP tube is achieved through a combination of complex porthole and bridge die design, also known as the Modular die shown in Figure 1.10.

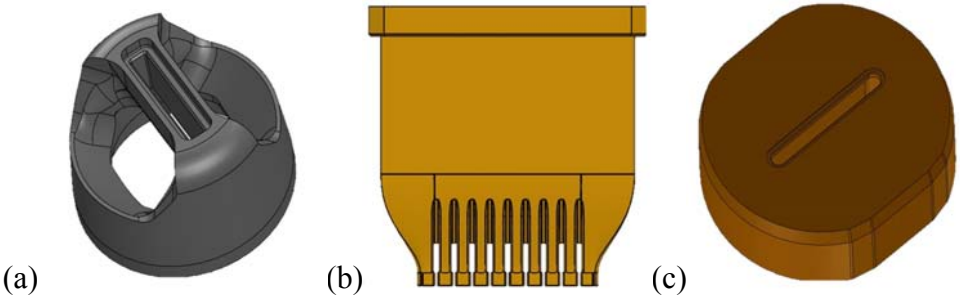

Figure 1.11 (a) Die cartridge; (b) mandrel and (c) die plate

The modular die consists of three critical components shown in Figure 1.11; a die cartridge which creates a welding chamber once placed into the holder thus forcing the aluminium to flow around the bridge into the porthole. The die plate helps in forming the outer dimension and the mandrel helps in creating the fine web walls separating the voids of the MMP tube. The mandrel and die plate are press fitted into the die cartridge carefully to avoid shifting of the components during extrusion. The modular die assembly

is then placed into its die tool stack; which comprises of a die ring, holder, spacer and backer shown in Figure 1.12a. All these components are assembled together to provide the structural strength needed for the tooling to withstand the high compressive forces of the extrusion process shown Figure 1.12b. The assembled porthole die tooling stack consist of eight portholes in order to increase productivity of the extrusion process, by extruding eight strands of MMP tubing from a single billet.

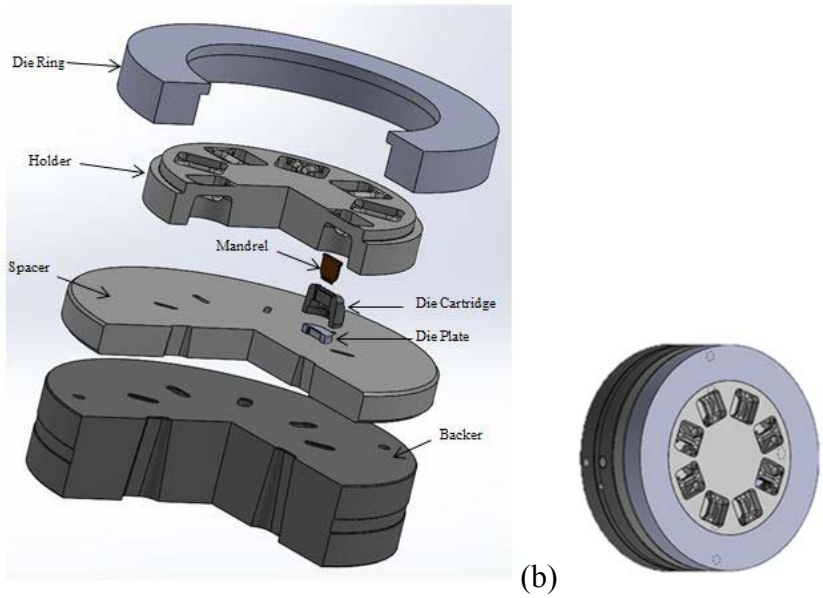

Figure 1.12 (a) Exploded assembly view; and (b) modular die tool stack

1.1.4 Die Design Process

Figure 1.13 shows a typical die designing process used in the industry today. The process of die designing starts with a drawing blueprint of the profile shape and its dimensions provided by the customer. The die designer uses his experience and personal judgment to design a CAD model of the die. This process typically takes about 4-6 weeks. Once the CAD model of the die is completed it is manufactured through different processes which also takes 4-6 weeks and is shipped to the extruder. The extruder then conducts die trials with the objective of obtaining good surface finish and tight dimensional tolerance. If the extruded profile meets these requirements it is used for production. However, if the extruded profile does meet these requirements it is either

corrected at the extruding plant depending on the extent of the issue or if the die has fatigued during extrusion it is scrapped and the die designer has to revise the die design.

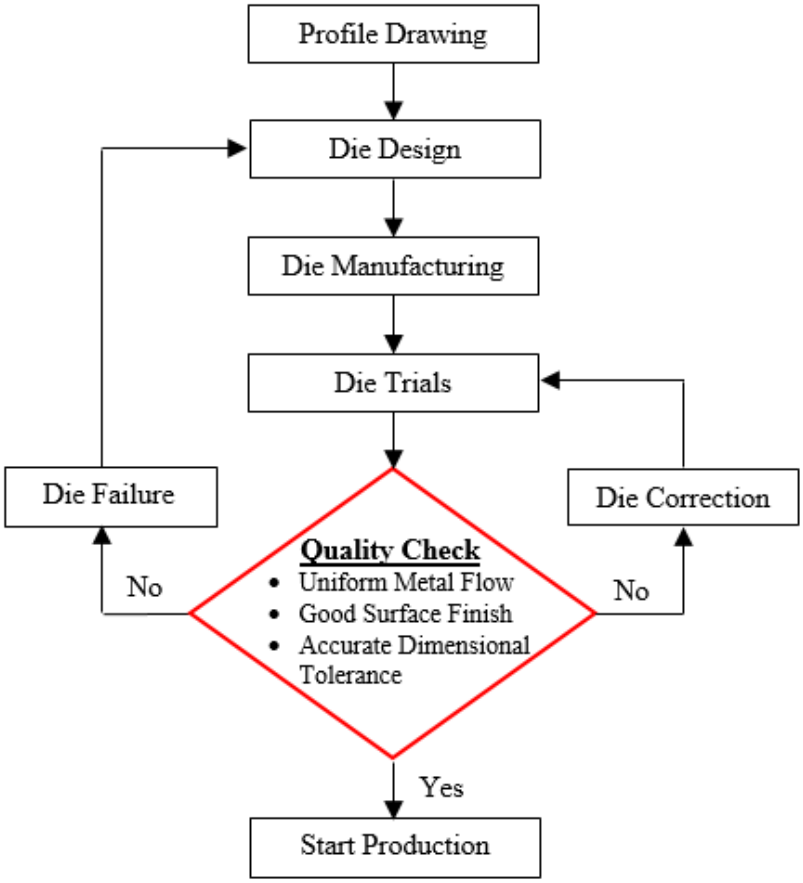

Figure 1.13 Schematic of a typical extrusion die designing process

1.2 Problem Statement

Die design is one of the most important and demanding aspects of the entire extrusion process that greatly influences performance of the die and productivity of the extrusion process. Ideally, development of a die should be based on profound understanding of metal flow and stress distribution occurring within the die during the extrusion process which is very difficult to analyze and study due to the complex thermo-mechanical conditions under which extrusion takes place. Therefore; currently in the extrusion industry a die is developed through trail-and-error that is solely dependent on

the experience, intuition and personal judgment of the die designer. Due to the competitive industrial environment of high productivity, low cost and low scrape rate, this traditional trial and error design approach is not only expensive and time consuming but greatly affects the productivity and efficiency of the extrusion process.

Owing to the advancement in the field of computational technology and finite element (FE) simulations over the last decade, many researches [7-10] have utilized FE simulations to understand the mechanics of metal flow and die stresses which is difficult to obtain experimentally. This being said the traditional trial and error approach needs to be replaced with a methodological design approach through the use of computer based extrusion simulations at an early design stage. In order to minimize cost and time but also help validate the intuition and personal judgment of the die designer by providing visual aid and fundamental understanding on how die geometry affects metal flow and die stresses occurring during the extrusion process.

1.3 Literature Survey

Currently, in the industry development of a new die geometry is solely based on empirical knowledge acquired through trial-and-error rather than deep scientific analysis and calculations[11]. In this chapter a comprehensive literature survey is conducted to identify different methods used in the industry and academic research to understand the interactions of metal flow and die geometry during the extrusion process. The literature survey can be classified into two sections, experimental studies and finite element simulations.

1.3.1 Experimental Studies

Preceding the development of finite element extrusion simulations knowledge on the mechanics of extrusion has been gathered mainly through experimental studies and analytical calculations [12].

Valberg et al. [13] has experimental investigated the contact conditions of the extruding aluminum over the whole volume of the billet and inside the bearing channel of a flat faced die used for the extrusion of a solid bar, using a transverse and longitudinal grid pattern technique. From his investigation Valberg has concluded that a complete sticking conditions prevails between the extrusion metal and die steel. However as aluminum flows through the die bearing, the inlet of the bearing is characterized by sticking conditions which then transitions into sliding contact due to the gradual development of an adhesive layer throughout the extrusion cycle.

Figure 1.14 Transverse and longitudinal grid patterns used for the investigation of aluminum from during the whole extrusion cycle [13]

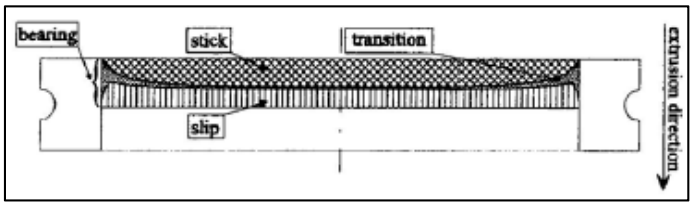

Figure 1.15 Flow of aluminum in the die bearing region described by Valberg [13].

Yuan el al. [14] has experimentally studied the effects of two different pocket dies one with a pocket guiding angle and one without a pocket guiding angle on metal flow during the extrusion of a solid bar, using a dissected extrusion billet. From his investigation Yuan, has observed that the dead metal zone; where material velocity is considered not moving, in the die pocket without the guiding angle was larger as compared to the dead metal zone of the die pocket with the guiding angle.

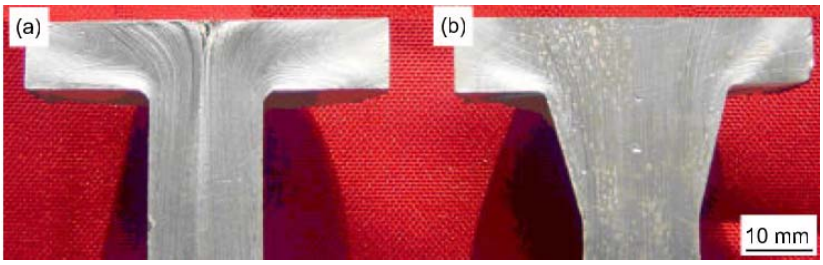

Figure 1.16 Flow lines of an extruded solid bar through a pocket die (a) without guiding angle & (b) with a guiding angle (reproduced from [14]).

A large number of experimental studies conducted in the past were mainly done to understand metal flow during extrusion using multiple reference-marking methods inside the experimental billet such as disc method[15], indicator method[16] and longitudinal grid method [6]. These experimental methods are time consuming, expensive, difficult to control and were confined to analysis of simple solid extrusion shapes.

1.3.2 Finite Element Simulations

Even though the aluminum extrusion industry is over a 100 years old, mathematical modeling and simulation of aluminum extrusion process has been established and exploited only during the last 35 years.

Using the implicit finite element codes FORGE2 and FORGE3, Flitta and Sheppard [17] have studied and experimentally validated the effects of friction on material flow in the extrusion of a solid rod. Through their investigation they have concluded that the friction coefficient between the billet and container interface has a significant effect on metal flow and internal material stresses which adversely has an effect on ram load and extrusion temperature. The investigation of this study provides fundamental information on the effects of friction between the billet and container interface during the extrusion process however, it is limited to explaining the mechanics of metal flow and no significance has been given to the effects of die geometry.

Zhang [18] has investigated and experimentally validated material flow in a porthole die cavity of a complex hollow aluminum profile using HyperXtrude, an arbitrary Lagrangian-Eulerian numerical model. The results from the study conclude that the non-uniform velocity of aluminum through the porthole cavity is dictated by the die design geometry. Utilizing numerical simulation models can be an effective tool in predicting final product defects such as twisting, waving, bending and cracking. However, making corrections to the die design in order to achieve uniform exit velocity does not provide enough detail on the effective stresses of the die geometry which could potentially lead to catastrophic failure.

Ceretti [8] has investigated the effects of material flow and stresses in a porthole-die using Deform 3D to improve die geometry, die wear and die tooling life. In this finite element study nine different die geometric configurations were analyzed in terms extrusion pressure, extrusion force, temperature, stresses on the die and uniformity of material flow. From the simulated results it is known that having webs with lower angle and width results in low stresses acting on the die, as well as enhances material flow thus reducing extrusion load.

Lee et al. [19] has investigated the effects of chamber shapes of porthole die for condenser tubes to evaluate material flow, welding pressure, extrusion load and the tendency of mandrel deflection using Deform 3D, an Updated Lagrange numerical model for the transient state aluminum flow and ANSYS 5.5 for die stress analysis.

Flitta and Sheppard [7, 20, 21] have studied and experimentally validated finite element model Forge2 and Forge3 to predict the effect of die geometry on maximum extrusion load and material flow during extrusion of a solid rod and shaped sections. In an another study they have utilized Forge3 to simulate the extrusion of 6063 aluminum alloy through a bridge die to predict extrusion load required, temperature and material flow during the extrusion process. They have also conducted a study using Forge2 to understand the effect of temperature change on deformation and surface finish of the extruded product.

Liu et al. [22, 23] has utilized HyperXtrude to optimize the die structure of a large multi-cavity and a large diameter thin-walled porthole die by studying and experimentally validating the material flow velocity of the extruded product. In their investigation modifications of the die structure are primarily dictated to achieve a uniform exit velocity of the material flow to avoid production defects such as twisting, warping and curving.

Jam et al. [24] has utilized Abaqus a general purpose finite element software to investigate the effects of die land on extrusion load of Tellurium-Lead alloy. Hosseini et al. [25] has also utilized Abaqus to simulate a 2D extrusion of a solid 2A12T4 aluminum alloy in order to optimize the extrusion process parameters by conducting a design of experiments to investigate the influence of die angle, friction coefficient and extrusion ration on extrusion pressure.

Tang et al. [26] has conducted a caste study of a flat extrusion die and a hemispherical extrusion die for the extrusion of micro-channel tubes using Deform 3D to understand the effects of die design on seam welding strength and microstructures of the extruded tube. Using a hydrostatic pressure test Tang has concluded that welding quality of tubes produced through the hemispherical die is higher than the flat extrusion die.

Fang et al. [27] has experimentally validated the results obtained from Deform 3D, to simulate the extrusion of a complex solid profile to investigate the effects of die bearing length and extrusion speed on extrusion temperature and pressure. From their investigation they have concluded that the extrusion speed and bearing length have a strong effect on the extrusion temperature and surface quality of the final product.

Forge3, HyperXtrude, Abaqus and Deform 3D are some of the commercial simulation software packages that have been identified in the literature survey utilized for simulating extrusion. Most of the simulation work done in the literature is confined to understanding the effects of material flow on the quality of extruded product for simple shaped solid or hollow profiles. Very few research work has been done on optimization

of a condenser tube die design to improve the performance a die and quality of extruded product.

1.4 Thesis Objective

The main objective of this thesis is to use finite element simulations to study the extrusion process of MMP tube through the modular die with the objective of helping the die designer understand how changing a certain geometric parameter in the die design will affect the material flow, extrusion force required and die deformation. In particular, this thesis focuses on the parametric optimization of the mandrel and die cartridge geometry of the modular die.

In this study of extrusion simulations to optimize the modular die a full factorial design of experiments is conducted using a commercial finite element code Deform 3D which is analyzed using a statistical tool Minitab to understand the main effects of the mandrel geometric parameters on welding pressure and to understand the main effects of the die cartridge geometric parameters on the deformation of the mandrel teeth during the extrusion process. Most importantly a methodological die design framework is established which can be used by die designers to replace their intuition based design approach using FE simulations.

1.5 Thesis Outline

Following the introduction of aluminum extrusion process and die design in Chapter 1, Chapter 2 defines the finite element modeling of the aluminum extrusion process using HyperXtrude and Deform 3D simulation software. Chapter 2 evaluates the capabilities and limitations of each software in respect to the thesis objectives. Finally, chapter 2 identifies the development of a finite element model of the modular die which is validated with experimental data provided by a local extrusion company that has previously used the Modular die for the extrusion of Micro-Multiport tubes. Chapter 3

discusses a case study comparing the advantages of bilayer coated tooling components vs. tooling components made out of H-13 tool steel. Chapter 4 introduces the use of design of experiments utilized for the parametric optimization of the mandrel and die cartridge geometry of the modular die. Chapter 4, also describes the different finite element models utilized to conduct a full factorial design of experiments. Chapter 5 describes in great detail the effect of each geometric parameter of the mandrel and die cartridge geometry on material flow, extrusion load, and effective stress and weld pressure. Statistical summary of the design of experiments is also conducted in Chapter 5 showing the importance of each geometric factor in regards to its response. Finally, results are concluded and future work is identified in Chapter 6.

2. ALUMINUM EXTRUSION SIMULATION

2.1 Overview

Due to the growing popularity of the extrusion process in multiple industries there is an increases in demand for the production of complex extrusion shapes while maintaining performance and economic feasibility. Thus, a better understanding of the metal flow in the extrusion process is required which is dictated by the initial process parameters and die geometry [7, 28]. With the advancement of technology over the last decade this demand has been met with the development of multiple finite element simulation packages that empowers researchers, die designers and press operators to enhance their understanding on the mechanics of extrusion to deliver quality products.

This main theme of this chapter is focused on utilizing FEM analysis tools such as HyperXtrude and Deform 3D to simulate the direct extrusion process of aluminum 3003 series alloy through the modular die for the extrusion of Micro-Multiport tubes. The objective of this chapter is to evaluate the capabilities and identify the limitation of HyperXtrude and Deform 3D that would best serve to the needs of this thesis. In order to proceed with the finite element simulations it is important to know the different finite element methods used for the formulation of the aluminum extrusion process

2.2 Governing Laws

The simulation of the extrusion process are governed by conservation laws based on the fundamental relations of continuum mechanics [29].

1. Conservation of Mass (Continuity Equation): states that the rate of change of mass in a fixed region is zero.

$$\frac{d}{dt}\int_V \rho\, dV + \int_S \rho(v - v_s)\cdot ds = 0 \quad (2.1)$$

Where V is the volume bounded by the domain S, ρ is the density of the deforming material, v is the velocity and v_s is the velocity of the bounded volume surface.

2. Conservation of Momentum (Equilibrium Equation): states that the rate of change of momentum is equal to the sum of external forces acting on a

$$\frac{d}{dt}\int_V \rho\, dV + \int_S \rho(v - v_s)\cdot ds = \int_S \sigma \cdot ds + \int_V f_b\, dV \quad (2.2)$$

In Equation (2.2) f_b is the body force, and σ is the Cauchy stress tensor. In the extrusion process, change in material density and body forces are neglected.

3. Conservation of Energy (First Law of Thermodynamics): states that the change in total energy is equal to the sum of the rate of work done by external forces and the change of heat content per unit time.

$$\frac{d}{dt}\int_V \rho c T\, dV + \int_S \rho c T\,(v - v_s)\cdot ds = \int_S q \cdot ds + \int_V \sigma : \nabla v\, dV \quad (2.3)$$

In Equations (2.3), c is the specific heat and T is the temperature.

2.3 Constitutive Relations

In order to complete the governing Equations (2.1)-(2.3) and to understand the flow of deforming material during the extrusion process utilization of constitutive models that can describe the material behavior are important. Extrusion is a complex thermo-mechanical process in which the elastic characteristic of the metal billet is neglected due to the large deformation of the metal billet occurring at high deformation (strain) rates. Therefore, rigid-visco-plastic constitutive laws are commonly used to describe the deformation behavior of material in the extrusion process [30, 31].

In the extrusion process the basic constitutive equations that postulates the flow rule is the Lévy-Mises yield criterion, which specifies the increment of plastic strain once the material has yielded [32].

$$\sigma'_{ij} = \frac{2}{3}\frac{\bar{\sigma}}{\dot{\varepsilon}}\,\dot{\varepsilon}_{ij} \tag{2.4}$$

$$\dot{\varepsilon}_{ij} = \frac{1}{2}(v_{i,j} + v_{j,i}) \tag{2.5}$$

$$\bar{\sigma} = \sqrt{\frac{3}{2}\sigma'_{ij}\sigma'_{ij}} \tag{2.6}$$

$$\dot{\varepsilon} = \sqrt{\frac{2}{3}\dot{\varepsilon}_{ij}\dot{\varepsilon}_{ij}} \tag{2.7}$$

Where $\dot{\varepsilon}_{ij}$ is the strain rate Equation (2.5), $\bar{\sigma}$ is the effective stress Equation (2.6) which is generally a function of strain, strain rate and temperature, $\dot{\varepsilon}$ is the effective strain rate Equation (2.7), σ'_{ij} is the deviatoric stress tensor is related to shape change which is defined by

$$\sigma'_{ij} = \sigma_{ij} - \delta_{ij}\frac{\sigma_{kk}}{3} \tag{2.8}$$

Where σ_{ij} is the stress, δ_{ij} is the Kronecker delta and $\frac{\sigma_{kk}}{3}$ is the hydrostatic stress related to volume change.

Using the governing Equations (2.1)-(2.3) and the constitutive relations of rigid-visco-plastic material flow shown in Equations (2.4)-(2.8) can be solved using different finite element formulation methods and numerical techniques given the appropriate boundary conditions.

2.4 Finite Element Formulation

Extrusion is a complex process which is difficult to solve using analytical techniques. However, using numerical techniques such as Finite Element Analysis helps in formulating a mathematical model that can be solved by a system of simultaneous equations. The metal forming process can be modeled using three different types of finite element formulations:

1. Updated Lagrangian Formulation
2. Eulerian Formulation
3. Arbitrary Lagrangian–Eulerian Formulation

The selection of a specific formulation is determined by two important factors, the problem to be solved and computation resource available.

2.4.1 Updated Lagrangian Formulation

The Updated Lagrangian (UL) formulation is most commonly used in the modeling of extrusion processes, which is divided into numerous time steps that solved sequentially. In the UL formulation the mesh is attached to the deforming material. The advantage of this, is that the transient behavior of material flow such as die filling, weld seam formations and profile exiting effects are accurately simulated, which helps in identifying all the different forming stages occurring during the extrusion process. The only disadvantage of the UL formulation is that large deformation causes the mesh to severely distort, thus leading to multiple re-meshes. Re-meshing, drastically increases computation time as it creates a new mesh at each iterative step and remaps the information from the old mesh onto the new mesh.

2.4.2 Eulerian Formulation

Eulerian formulation is most commonly used in the field of fluid mechanics but is also suitable for extrusion. In the eulerian formulation the mesh is fixed at a particular location in global coordinate of the system and only spatial variation of state variables is calculated. For utilizing the eulerian formulation the work piece has to be one integral piece that fills the die cavities, which is typically produced through a Boolean technique. The advantage of this method that the mesh does not distort thus saving computational time. However, tracking material flow after it has left the die is difficult to model using the eulerian formulation due to the assumption that the rate of change of strain is zero.

2.4.3 Arbitrary Lagrangia–Eulerian (ALE) Formulation

The ALE formulation is a combination of Lagrangian and Eulerian formulation. In this formulation the displacement of the material and mesh are decoupled which means that the mesh can move independently of the material reducing mesh distortion which is a major drawback of the lagrangian formulation and increasing accuracy of the free surface of material flow which is a short coming of the eulerian formulation.

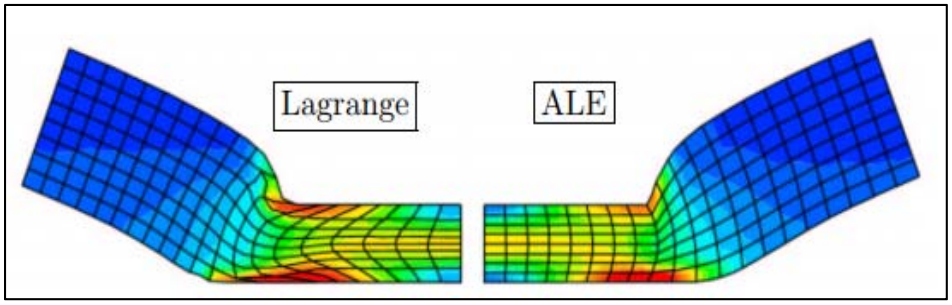

Figure 2.1 Numerical simulation of coining test (reproduced from [33])

2.5 Simulation Modeling Process

In this section details of aluminum extrusion modelling process used in HyperXtrude and Deform 3D are presented. The general principles of the numerical modelling process can be categorized into three categories:

1. Pre-Processing: it is used for creating, assembling or modifying geometries, generating meshes and applying boundary conditions.
2. Simulation Engine: its main purpose is to perform the complex simultaneous numerical calculations and solve for the physical problem being simulated.
3. Post-Processing: the results generated from the calculations of the simulation engine due to the input parameters of the pre-processing can be represented graphically and exported into data in the post processor.

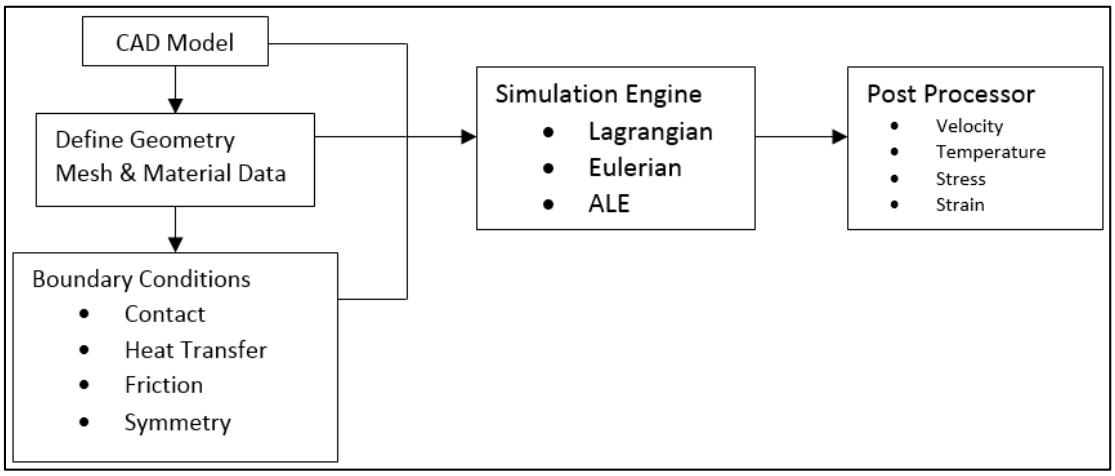

Figure 2.2 Schematic drawing of a numerical modelling process

2.5.1 Geometric Model

The original modular die tool stack comprises of eight porthole cavities which would take a lot of time to simulate and generate results. Thus, in order to save computation cost and time the modular die tool stack was reduced to 1/16th of its original geometry due to symmetry.

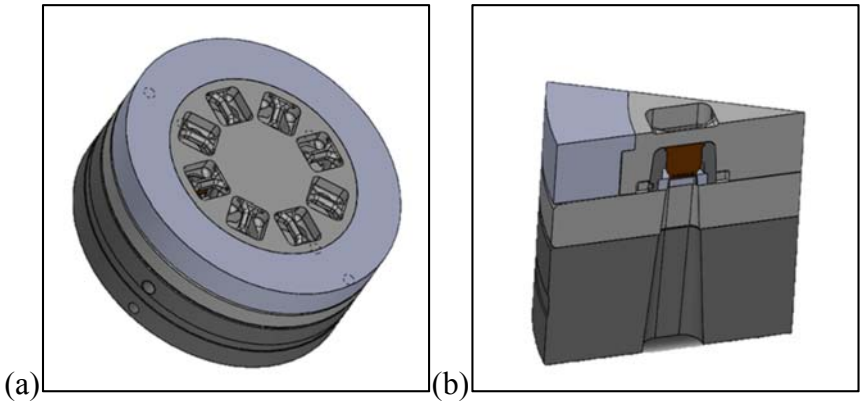

Figure 2.3 (a) Original modular die tool stack and (b) 1/16th model

The simulation model also consists of a ram, container and billet. Aluminum alloy 3003 series and H-13 tool steel were designated as the material properties of the billet and tooling components.

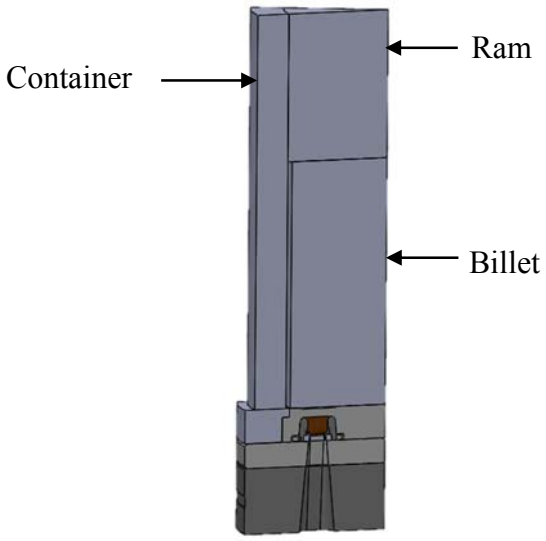

Figure 2.4 Simulation model

2.5.2 Deform 3D

Deform 3D, developed by Scientific Forming Technologies Corporation (SFTC) is finite element software, which uses an adaptive meshing technique to predict large scale plastic deformation, three dimensional (3D) material flow, heat transfer and die stresses that occur during a complex bulk metal forming process. Deform 3D is specifically designed to meet the analysis and optimization needs of the cold, warm and hot manufacturing operations in all industries. Deform 3D has the option to select either Lagrange, Eulerian or ALE formulation depending on type of manufacturing process to be simulated and computational resources available.

2.5.2.1 Deform 3D Modeling Process

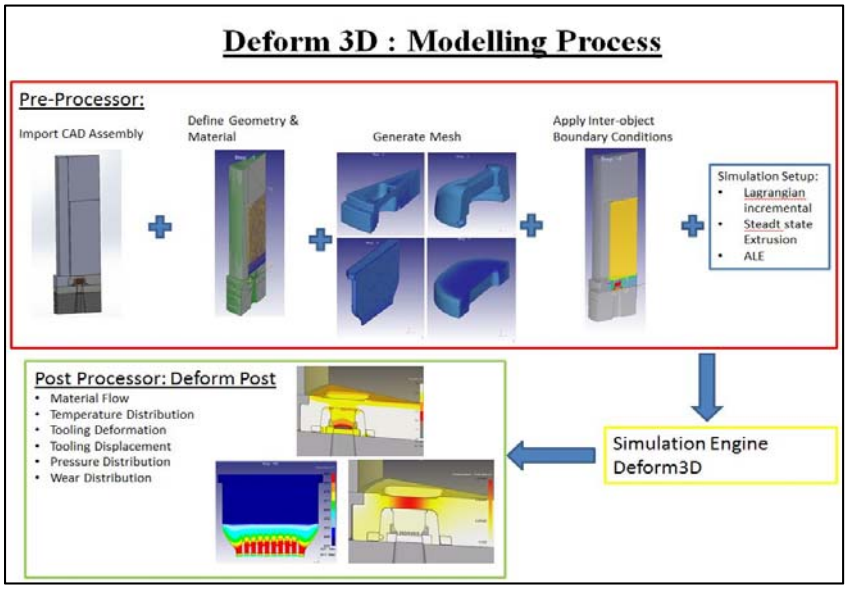

Figure 2.5 Deform 3D simulation modelling schematic

A graphical representation of the sequence of steps required for modelling the extrusion process in Defomr3D is shown in Figure 2.5. The recommended sequence for modelling an extrusion simulation process is:

1. CAD Model: Using any computer aided design tool extrusion die tooling geometries can be imported into Deform graphical user interface using an STL file format.
2. Defining Die Geometry:
   (a) Die Tooling Model: During extrusion the billet deforms and is therefore modelled as a plastic object. Depending upon the objective of the simulation study die tooling components can be modelled as either rigid, elastic or plastic objects.
   (b) Mesh Generation: Deform has the capability to use several meshing techniques such as lagrangian, eulerian and combination of arbitrary lagrangian eulerian and coupled eulerian lagrangian. In Deform mesh density can be controlled using two methods:
      (i) System-Defined: This is an automatic mesh generation method in deform that uses a system of weights and assigns windows to control the size of

elements during the initial mesh generation and subsequent automatic re-meshing.

(ii) User-Defined: this is a manual mesh generation method that allows the user to specify areas on the object to have higher element sizes relative to other areas of a given object during the initial mesh generation and subsequent automatic re-meshing.

(c) Assigning Material Data: Deform has a vast material data library of common extrusion tooling and billet material information, that consist of both mechanical and thermal properties. New material data can also be added if the constitutive equation is known.

3. Boundary Conditions

(a) Inter-Object Relationship: In Deform the purpose of the inter-object relation is to define how the different die tooling components in a simulation interact with the deforming billet. With the help of inter-object boundary conditions thermal and mechanical behavior of each die tooling component with itself and the billet can be defined. The inter-object relation include the following boundary conditions to be defined :

(i) Friction Model: The shear friction models available in deform are Shear, Coulomb and Hybrid.

(ii) Heat Transfer Coefficient: specifies the heat transfer between two objects in contact

(iii) Tool Wear: deform has the capability to calculate tool wear of an object which is in contact with another object based on two predefined models used for predicting wear: Archards and Ususi.

4. Simulation Settings: in order to get accurate results from the simulation it is important to define the simulations settings such as:

(a) Type of simulation: Lagrangian incremental, Steady-state machining, Steady-state extrusion, ALE rolling, Ring rolling and ALE extrusion are some of the different simulation types that are available in Deform.

(b) Solution Method: Conjugate gradient, sparse, GMRES and MUMPS.

(c) Iteration Method: Direct iteration or Newton-Raphson.

5. Generate simulation database and submit it to solve by the simulation engine.
6. Review the results generated in Deform post processor.

2.5.3 HyperXtrude

HyperXtrude is a finite element analysis software that is used to solve complex fluid and heat transfer problems encountered in polymer and metal extrusion processes. It is one of the five engineering performance optimization software packages developed by Altair, that uses the Arbitrary Lagrangian-Eulerian (ALE) formulation to predict material flow stresses, material velocity, extrusion load, temperature distribution in tooling and billet, seam weld strength, transverse weld. The ALE method utilized in HyperXtrude, uncouples the Eulerian (displacement) and Lagrangian (material) mesh thus allowing the mesh to move independently of the material which reduces mesh distortion and increases accuracy [34].

2.5.3.1 HyperXtrude Modelling Process

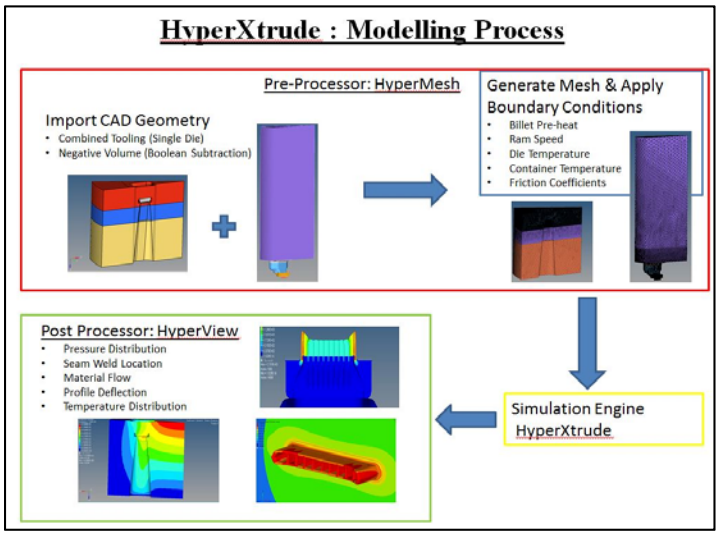

Figure 2.6 HyperXtrude simulation modelling schematic

A graphical representation of the sequence of steps required for modelling the flow analysis for extrusion process in HyperXtrude is shown in Figure 2.7. The recommended sequence modelling an extrusion simulation process in Hyperxtrude is:

1. CAD Model: Using any CAD tool the geometries required for simulation can be imported into HyperXtrudes graphical user interface using a SAT file extension.
   (a) Material Flow Analysis: only the negative volume of the die cavity needs to be imported to conduct flow analysis.
   (b) Die Stress Analysis: all the modular die tooling components needs to be combined into a single solid and imported into HyperXtrude to conduct stress analysis.
2. Create Components: The imported negative volume of the billet is split into multiple components to define the volume of the profile, bearing, welding chamber, portholes and the billet.

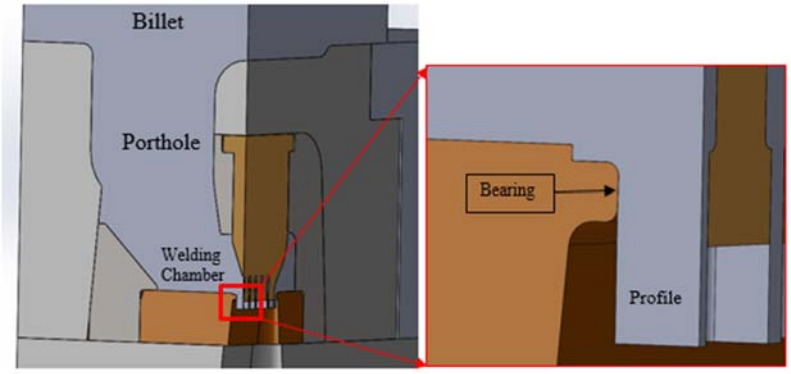

Figure 2.7 Negative volume components

3. Extrusion Wizard: helps the user step by step to input the process parameters
   (a) Specify database directory
   (b) Setup model units: length, velocity, temperature and stress.
   (c) Setup analysis parameters:
      i. Profile type: hollow or solid
      ii. Extrusion method: direct or indirect extrusion
      iii. Analyze profile deformation
      iv. Apply friction conditions between billet and tooling

v. Billet movement: fixed or moving
vi. Single or multiple cycle
vii. Analyze for skin tracking
viii. Compute weld length
ix. Meshing: automatic or manual
x. Select billet components for meshing

(d) Assign Material Data: HyperXtrude has a vast material data library for common extrusion tooling and billet material that consist material density, specific heat, thermal expansion ratio, Young's modulus and Poisson's ration.

(e) Generate Mesh: HyperXtrude give the user the ability to either automatically mesh the negative volume or the element size can be specified for manual meshing.

(f) Boundary Conditions:
i. Billet pre-heat
ii. Ram speed
iii. Die temperature
iv. Container temperature

4. Define Bearing: this enables HyperXtrude to optimize the bearing lengths in order to achieve uniform exit velocity of the profile.
5. Save and export model to radios which is the simulation engine for HyperXtrude
6. The results of the simulation model can be viewed in HyperView, which is the post processing graphical user interface.

To conduct die stress analysis in HyperXtrude, the forces from the flow simulation are interpolated on the combined modular die tooling assembly and the same sequence of steps is followed.

2.6 Software Evaluation

To evaluate the capabilities and identify the limitations of Deform 3D and HyperXtrue the extrusion simulation of MMP tubes through the modular die was conducted. The results obtained from each software is compared in terms of extrusion load, exit velocity, exit temperature, and most importantly die tooling stresses of the modular die.

2.6.1 Extrusion Load

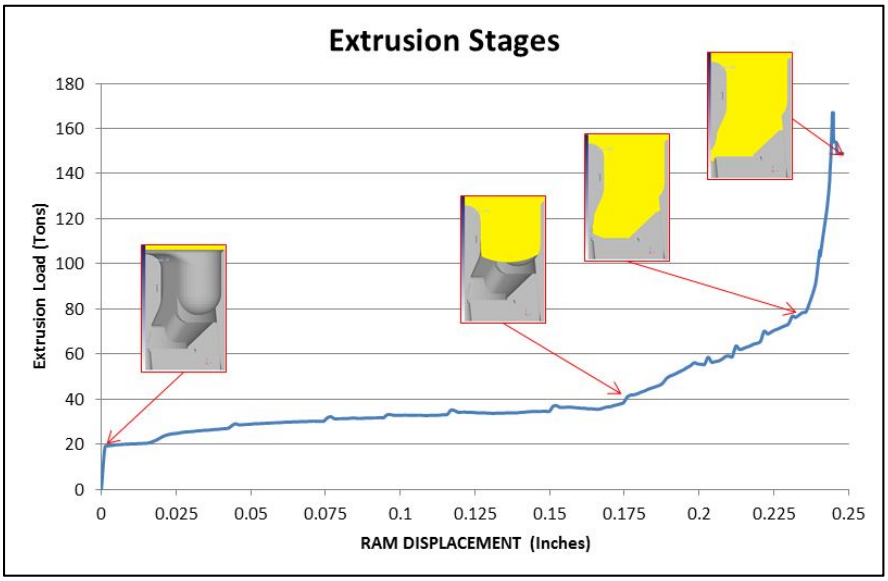

Figure 2.8 Deform 3D extrusion load

Figure 2.8 shows the extrusion load produced through deform simulations. Due to the lagrangian formulation used in deform the entire extrusion load-displacement curve is identified, which shows all the forming stages as the aluminum fills the die cavity.

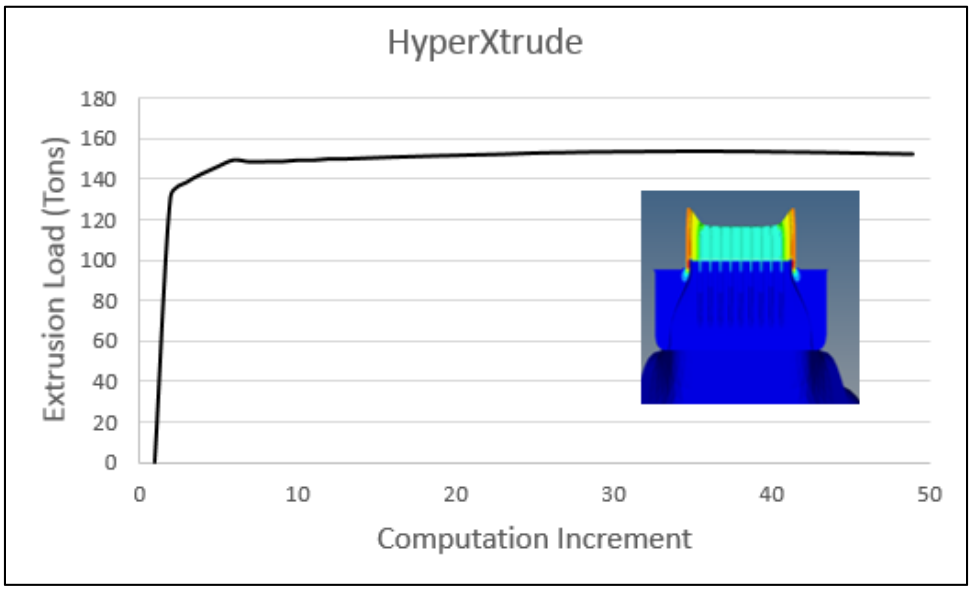

Figure 2.9 HyperXtrude extrusion load

Figure 2.9 shows the extrusion load obtained from the HyperXtrude simulations. Due to the use of ALE formulation only the steady state extrusion process is simulated in HyperXtrude which is observed in the extrusion load.

2.6.2 Exit Velocity

Figure 2.10 shows a samples of the extruded micro-multiport tubes. It is observed that the edges of the tube flow faster than the top and bottom walls.

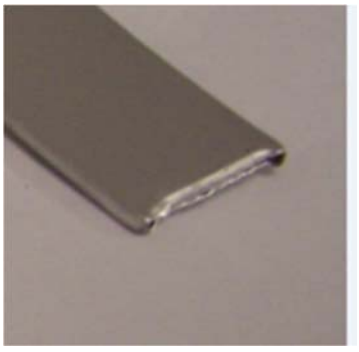

Figure 2.10 Micro-Multiport tube sample

This characteristic of non-uniform flow was also observed in both simulations, where the exit velocity obtained from HyperXtrude and Deform 3D were approximately 38.65in/sec and 45in/sec, respectively.

(a) 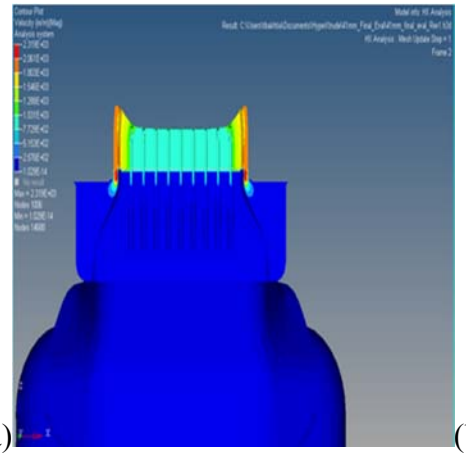 (b) 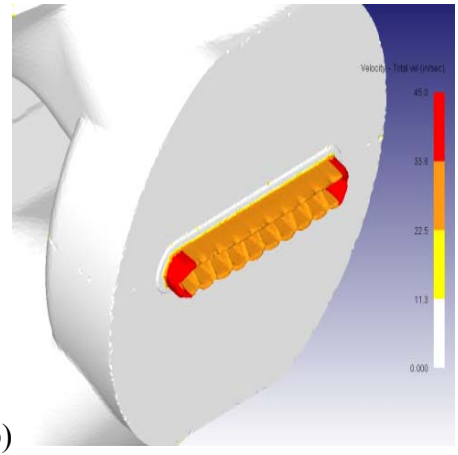

Figure 2.11 Exit velocity profile (a) HyperXtrude and (b) Deform 3D

2.6.3 Exit Temperature

Temperature change during the extrusion process is affected by many factors, including initial billet temperature, initial tooling temperature, extrusion speed, extrusion ratio and friction. However, the maximum temperature is always observed to be close to the bearing region due to the smallest cross sectional area characterized by maximum plastic deformation which generate heat due to loss of energy shown in Figure 2.12 [7]

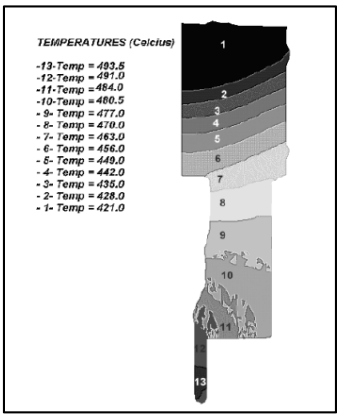

Figure 2.12 Exit temperature of a hollow profile cross section (reproduced from [7])

Figure 2.13 shows the exit temperature of the MMP tube obtained from HyperXtrude and Deform 3D. It is observed that maximum temperature of the extruding profile starts in the bearing region and extends till the outlet of the profile. The values obtained from HyperXtrude (1070˚F) and Deform 3D (1000˚F).

(a) 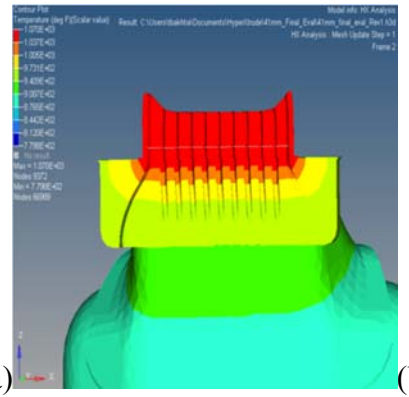 (b) 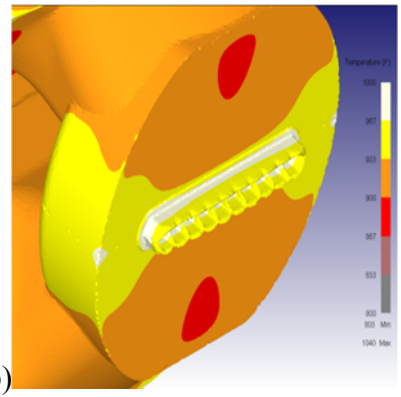

Figure 2.13 Exit temperature profile (a) HyperXtrude and (b) Deform 3D

2.6.4 Die Stress

Figure 2.14 shows the stress distribution produced in Deform 3D for each individual components of the modular die. This is very useful information for a die designer or a die manufacturer because it shows the areas where the design improvement is needed before the model is manufactured and used for extrusion.

(a) 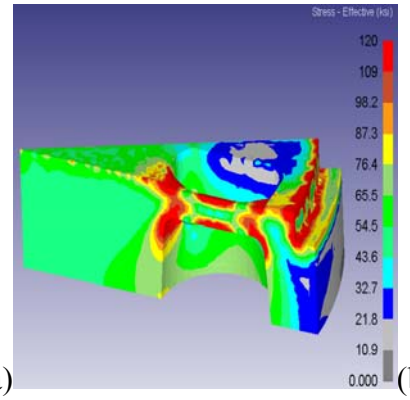

(b) 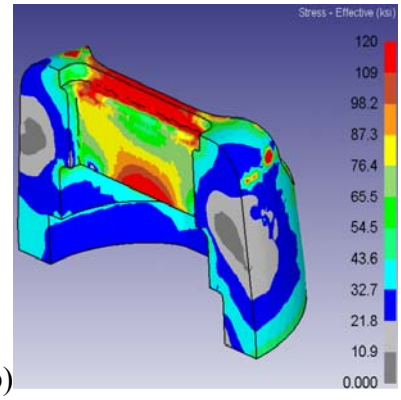

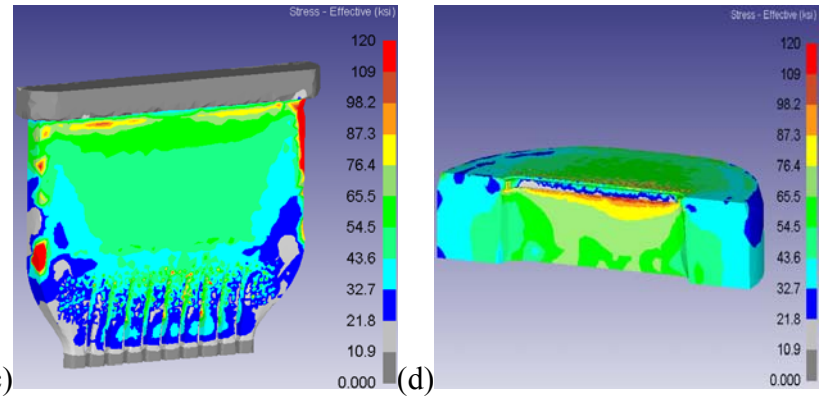

Figure 2.14 Deform 3D simulation stress distribution in modular die tooling components; (a) Holder; (b) Die Cartridge; (c) Mandrel and (d) Die Plate

Figure 2.15 shows the stress distribution produced in HyperXtrude for the combined modular die tooling geometry. In order to conduct die stress analysis in HyperXtrude a Boolean addition of all the different components is needed. The effective stress values obtained in HyperXtrude (4.191E+12 psi) were significantly larger than the predicted values of Deform 3D (178,000 psi). Comparing these results to the yield strength of H-13 tool steel (120,000 psi [35]) at elevated temperatures shows that the values obtained from HyperXtrude are far from the yield strength of H-13 tool steel as compared to the simulated results of Deform 3D.

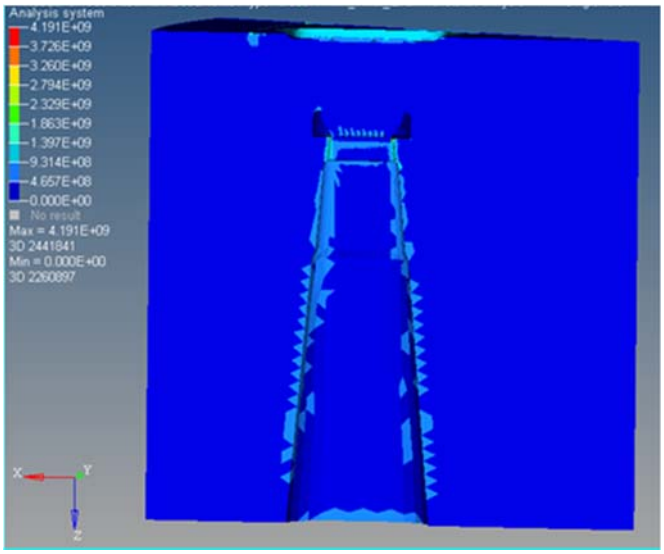

Figure 2.15 HyperXtrude simulation stress distribution of modular die tool stack

2.6.5 Conclusion

The aluminum extrusion process is an attractive metal forming process in the manufacturing industry due to its ability to produce quality products with minimal energy and secondary manufacturing operations. Currently, in the industry development of complex aluminum extrusion dies are solely based on the experience of the die designer which is continuously corrected after a number of trail extrusion runs before going into production. This trial and error method makes it difficult to guarantee product quality, reduces productivity and cost effectiveness. Utilization of numerical simulations such as HyperXtrude and Deform 3D play an important role in replacing the decade old trial and error approach by empowering extruders to extrude complex profiles with minimal defects and provides the die designer with accurate and theoretical guidance for design improvements at minimal cost.

HyperXtrude is an effective finite element simulator that helps the extruder in optimization of process parameters such as ram speed, initial billet temperature, initial tooling temperature and bearing length to ensure balanced material flow in order to eliminate product defects thus reducing production costs by eliminating die trails. Deform 3D; on the other hand, is an effective tool that can not only be utilized by die manufacturers to access the quality of their die by studying stress of tooling components to make appropriate die improvements such as increasing or decreasing the height of the welding chamber, mandrel teeth height, web shape and porthole angle with accurate guidance, but also be utilized by extruders to visualize and understand the different forming stages during the extrusion process.

Keeping the goals of the thesis in mind Deform 3D is an appropriate software that will help achieve the objectives of this thesis as it is not only capable of handling the flow analysis simulations which is vital information for the extrusion process but it is also is capable of handling tool deflection analysis for our complex die geometry with multiple components of different materials, as it allows us to mimic the real world scenarios of geometric gaps, press fit and die coating.

2.7 Deform 3D Model Development and Validation

Aluminum extrusion is a complex thermo-mechanical process during which the flow of the deforming aluminum billet is primarily dictated by frictional forces at the billet container and tooling interface. Bulk deformation of the aluminum billet occurs in the container as compared to the die cavity therefore, frictional forces at the billet and container interface are of utmost importance. Due to high temperatures and pressures occurring during the extrusion process, it is difficult to obtain experimental data of friction. As a result, friction mechanism during aluminum extrusion has not been thoroughly understood and mathematically expressed, therefore it has been acknowledged as the most uncertain parameter in the finite element simulation for aluminum extrusion [36].

A local extrusion company that has previously used the modular die for the extrusion of MMP tubes has provided the initial input parameters of the extrusion process as well as experimental data of the exit temperature and extrusion load. Since, friction is the only unknown parameter a comparative study with different friction parameters (Table 2.1) is conducted to validate the accuracy of the simulated results with the experimental data provided.

2.7.1 FEM Formulation

In order to accurately predict the material flow during a forming process, the formulation must consider large plastic deformation, incompressibility, interface contact between tooling and deforming metal and temperature. The FEM formulation in Deform 3D is based on minimum work rate principle [30, 32, 37], which is determined using the variation principle equation shown by mixed formulation Equation (2.9), employed for the 3D tetrahedral elements to obtain the variable solution for velocity and pressure.

$$\delta\emptyset(v,p) = \int_V \bar{\sigma}\delta\dot{\bar{\varepsilon}}dV + \int_V p\delta\,\dot{\varepsilon}_V dV + \int_V \dot{\varepsilon}_V\delta p - \int_S F_i\delta v_i dS = 0 \quad (2.9)$$

Where $\int_V \bar{\sigma}\delta\dot{\bar{\varepsilon}}dV$ is the variational form of the plastic work done, $\int_V p\delta\,\dot{\varepsilon}_V dV + \int_V \dot{\varepsilon}_V \delta p$ is the dilatation work rate integrated by parts, which together form the constant volume constraint and $\int_S F_i \delta v_i dS$ is the surface traction work. $\dot{\varepsilon}_V$ is the volumetric strain rate, $\bar{\sigma}$ is effective stress, $\dot{\bar{\varepsilon}}$ is the effective strain rate, p is the pressure, V is the volume of the deforming material and S is the surface of the deforming material. This variation equation is converted into simultaneous non-linear algebraic equations utilizing FEM discretization procedure which is solved numerical either using direct iteration method or Newton-Raphson.

Temperature is an important characteristic of the extrusion process that influences the material flow stress. Therefore, the temperature distribution occurring between the deforming material and die tooling can be obtained by rewriting the thermal energy balance equation using weighted residual method shown by Equation (2.10)

$$\int_V kT_j\delta\,T_j dV + \int_V \rho c\dot{T}\delta\dot{T}dV - \int_V \alpha\,\bar{\sigma}\bar{\varepsilon}\delta\dot{T}dV - \int_S q_n\delta T dS = 0 \qquad (2.10)$$

Where $\int_V kT_j\delta\,T_j dV$ is the conductive term, $\int_V \rho c\dot{T}\delta\dot{T}dV$ is the heat capacity term, $\int_V \alpha\,\bar{\sigma}\bar{\varepsilon}\delta\dot{T}dV$ is the heat lost due to plastic deformation, $\int_S q_n\delta T dS$ is the heat flux occurring between the deforming material and die tooling components, k is the thermal conductivity, T is the temperature, ρ is the density of the deforming material, c is the specific heat, α is the percentage of deformation energy that converts into heat and q_n is the heat flux normal to the boundary.

2.7.2 Friction Model

Much experimental research and theoretical modelling has been conducted to understand the friction phenomenon occurring during the extrusion process. However, assigning accurate frictional coefficients and models is one of the key issues for the finite element analysis of the extrusion simulations [17, 38, 39]. Shear and Coulomb friction,

are the two of the oldest and widely used classical frictional models in most commercial FE codes, due to their theoretical and numerical simplicity.

The coulombs frictional model can be described as a function of normal pressure between two contacting bodies.

$$f = \mu p \tag{2.11}$$

Where f is frictional stress, μ is the friction coefficient and p is the interface pressure between two bodies.

The shear friction model can be described as a function of the yield stress of the deforming body.

$$f = mk \tag{2.12}$$

Where f is frictional stress, m is the friction coefficient and k is the shear yield stress of the deforming body.

Both friction models are equally popular and have been utilized by many researchers. Sofuoglu et al. [40], and Arentoft et al. [41] , among many others have successfully utilized the coulomb friction model. Xianghong et al. [42] and Khansai et al. [43], among many others have successfully utilized the shear friction model. Both of these frictional models are numerically implemented and readily available to the user in deform. However, selection of the friction coefficient is based on an educated guess [38] as it is not easy to determine these values through experimentation due to the dynamics of the aluminum extrusion process. Therefore; for the comparative study the shear and coulomb friction models are both evaluated and can be seen in Table 2.1.

Table 2.1 Comparative study friction coefficients

Case	Friction Coefficient	
	Billet Container Interface	Billet Tooling Interface
1	Coulomb 0.9	Coulomb 0.4
2	Shear 0.9	Shear 0.4

The coulomb friction parameters for trial 1 were provided by a research scientist from a local extrusion company who had based these parameters from his experience in the industry and empirical knowledge of conducting extrusion simulations. The shear friction parameters in Trial 2, was referenced from the works of Jian et al. [44].

2.7.3 Validation Criteria

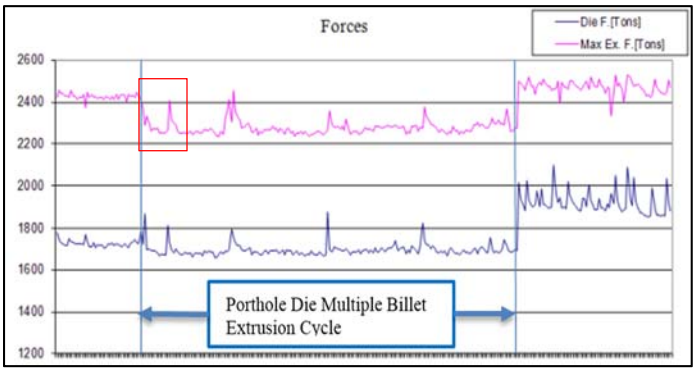

Figure 2.16 MMP tube multiple billet production extrusion force

.

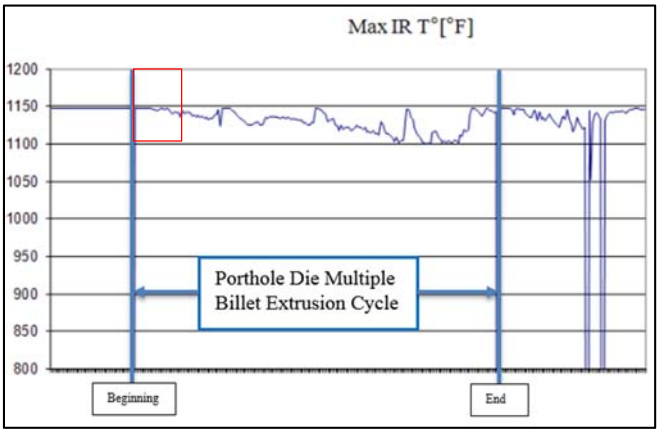

Figure 2.17 MMP tube multiple billet production extrusion temperature

Figure 2.16 shows the extrusion force required by the hydraulic extrusion press to push multiple billets through the porthole die tooling assembly that consist of eight die cavities. The extrusion process is a continuous process; therefore, the peaks shown in the figure for maximum extrusion force are considered to be the breakthrough forces that

marks the onset of steady state extrusion after which the maximum extrusion forces reduces gradually as the length of the billet decreases. In this study the extrusion of the first billet is simulated therefore, we compare the simulated results with the experimental data for the first few billets which shows the first peak of maximum extrusion at 2400 tons. Similarly Figure 2.17 shows the temperature of the MMP tube extruded from the porthole die which is measured after the tube exits the die through an infrared thermometer. The maximum temperature in the experimental data of the first few billet is close to 1150°F which is also considered as the validation criteria for the simulated results.

2.7.4 Deform 3D Simulation Model

One sixteenth of the modular die geometry was utilized for this comparative study validation. In the actual extrusion process the length of a single billet is 40 inches which would need a lot more number of elements to model. Therefore, to save time and computational costs (reducing mesh and total number of elements) only a 4 inch long aluminium billet was simulated as shown in Figure 2.18.

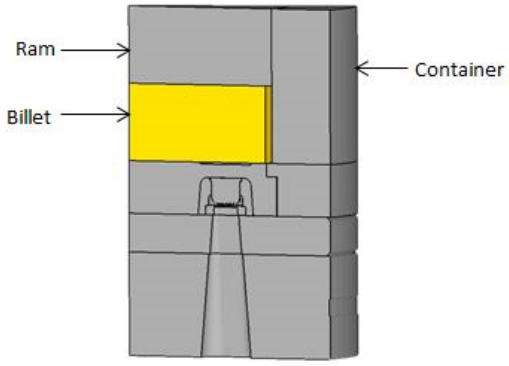

Figure 2.18 Modular die FEA model

A local extrusion company that had previously used the modular die for the extrusion of MMP tubes, provided the input parameters for this simulation. The billet was modelled as a plastically deforming 3003 series aluminum alloy whereas, the porthole die tool stack, container and ram were defined as rigid H-13 tool steel material. The

extrusion ram speed was defined at 6mm/s; whereas, initial temperature of the billet and tooling was defined at 900ºF, respectively. The heat transfer coefficient are readily available in deform for forming and free resting objects. Therefore, the heat transfer coefficient between the forming billet and die tooling components is 0.002 $\frac{Btu}{\sec in^2 °\mathrm{F}}$ and the heat transfer coefficient between resting objects which is the tooling components and die is 0.0003$\frac{Btu}{\sec in^2 °\mathrm{F}}$. In addition, symmetric planes were assumed to be fixed with no material moving across due to the use of one-sixteenth of the model. The simulation was setup to stop after the ram has been pushed down 0.45 inch, and the simulation information was setup to save every 10 steps. The length of the simulation step was defined in terms of ram displacement, and each step is defined as a constant value of 0.01 in/step. The diameter of the billet used in the simulation is 8 inches and the inner diameter of the container was set at 8.375 inches. This was done to mimic the upsetting stage of the extrusion process.As the ram forces the billet through the porthole cavity the billet will undergo severe plastic deformation due to the reduction in cross sectional area. Therefore; to control the element number and ensure calculation accuracy; several local mesh windows with a higher element density are applied on the billet in accordance with the extent of local deformation shown in Figure 2.19.

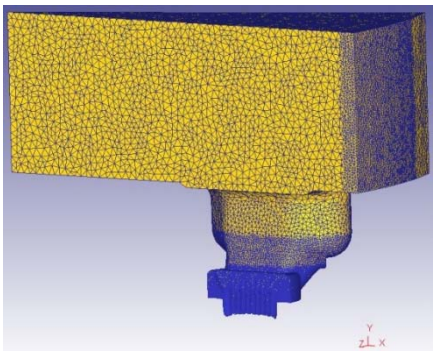

Figure 2.19 Deformed billet with several mesh window

A windows operating with 32GB of RAM and four 3.4Ghz Intel Core i7 processors was utilized to conduct the numerical simulation of the extrusion process in Deform 3D. The total computational time for each simulation is approximately 16 hours mainly due to re-meshing of the billet due to large scale deformation.

2.7.5 Deform 3D Simulation Results

A summary of the comparative study results can be seen in the Table 2.2. Both the simulations results are in good agreement with the experimental data.

Table 2.2 Friction model validation table

Case	Friction Parameter		Max Extrusion (Tons)	% Load Difference	Max Temperature (Degree ˚F)	% Temperature Difference
	Billet Container Interface	Billet Tooling Interface				
1	Coulomb 0.9	Coulomb 0.4	2338	2.667%	1090	5.333%
2	Shear 0.9	Shear 0.4	2201	8.602%	1095	4.888%

2.7.5.1 Effect of Friction on Extrusion Load

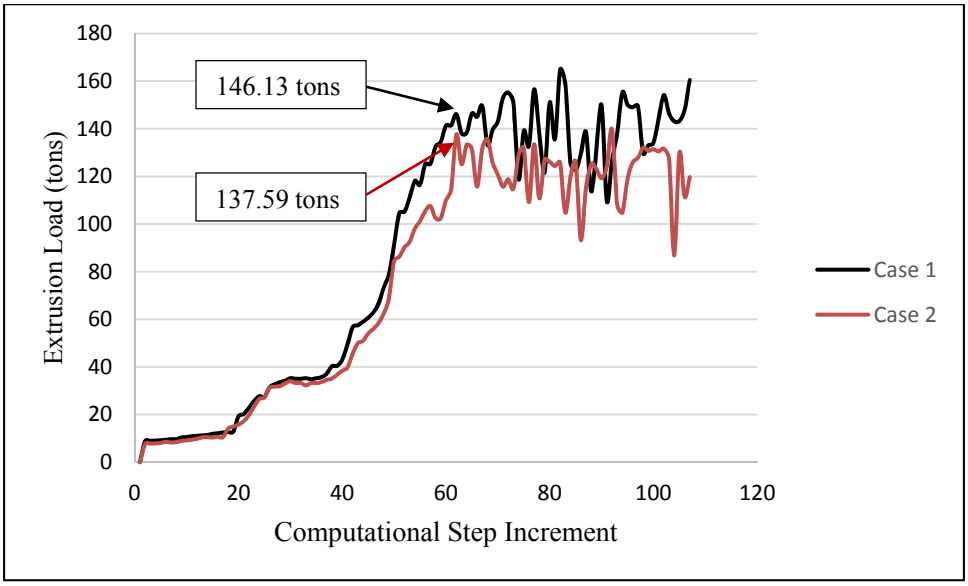

Figure 2.20 Deform 3D simulation extrusion load curve

Figure 2.20, compares the extrusion load stroke of coulomb and shear friction models. The extrusion curves observed in figure 8 are not smooth and show fluctuations at each step after the breakthrough pressure, this is due to the use of UL formulation in Deform, that causes multiple re-meshes of the deforming billet once the elements reach the small dimension of the MMP tube web walls in mandrel port opening. However, from

the simulated results it is observed that the breakthrough force occurs at the same computational step increment and is 146.13 tons for trial 1 and 137.59 tons for trial 2. The simulated results of extrusion load is for one sixteenth of the actual porthole die model, which is approximately 2338 tons for trial 1 and 2201 tons for trial 2 of the entire porthole die model due to symmetry.

The results obtained from this simulation is only for the first billet cycle; therefore, when comparing these results to the multiple billet cycle experimental data, we compare the simulated breakthrough loads with the average value of the experimental extrusion load observed in Figure 4, which is 2325 Tons. Both the simulated results are in good agreement with the experimental data provided. However, coulomb friction present in trial 1 has a breakthrough pressure close to the average value of the experimental extrusion load.

2.7.5.2 Effect of Friction on Exit Temperature

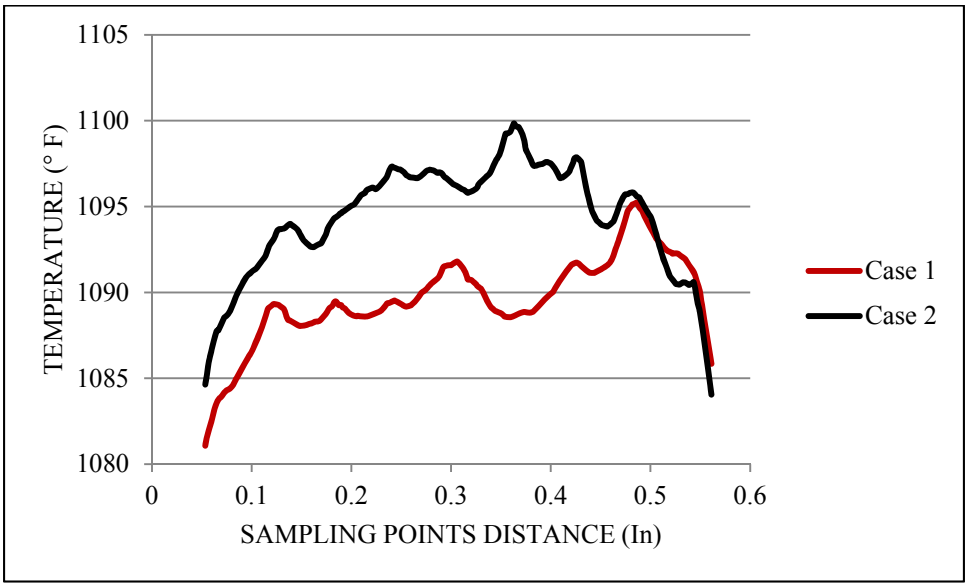

Figure 2.21 Exit temperature measured on the outer surface of MMP tube

Figure 2.21, shows the temperature distribution obtained from each simulation trial. The data represented in Figure 2.21 was calculated using sampling points along the outer wall of the condenser tube as shown in Figure 2.22.

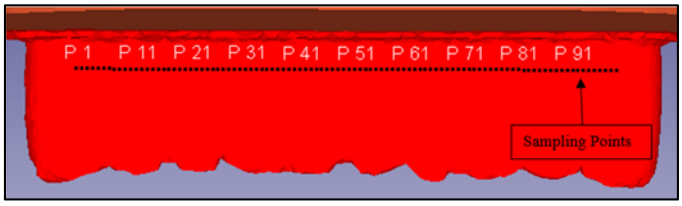

Figure 2.22 Exit temperature sampling points on surface on MMP Tube

From the graphs of the exit temperature measured on the surface of the MMP tube. It is observed that the difference in exit temperature is very minute, as the exit temperature in trial 1 is close to 1090°F and trial 2 is 1095°F. Friction greatly influence the flow of aluminum, extrusion load and temperature in the extrusion process where bulk deformation occurs; i.e. where contact is more intimate and pressure are significantly higher, such as the container and porthole [4, 39]. However, the same is not true in the bearing region as this region is characterized by maximum extrusion velocity and minimum pressure due to the drastic reduction in cross sectional area. As a result the two frictional models in consideration lose their influence in the bearing region due to its small size. The results from both the simulations are below the exit temperature values obtained in the experimental data, due to the assumed value of heat transfer coefficient.

3. CASE STUDY: COATING WEAR

3.1 Overview

In aluminum extrusion, the service life of a die is mainly limited by wear and plastic deformation; thus, reliable predictions on the amount of wear and stress distribution of a die helps improve the economics of the extrusion process. In this study temperature, wear depth and stress concentration of the modular die; mandrel and die plate were calculated using the Archards wear model; based on abrasive wear theory, implemented in the Deform 3D finite element code. A comparative study was conducted on the mandrel and die plate in order to predict the service life of dies without coating and with a bilayer ($TiCN + Al_2O_3$) chemical vapor deposition (CVD) coating.

3.2 Introduction

Productivity, cost and quality of the extruded profile are significantly affected by the service life of die tooling components, due to the repeated thermo-mechanical properties of the extrusion process. The service life of a die is dependent on wear; which affects the dimensional accuracy of extruded product, and plastic deformation; which causes the die components to fail due to fatigue. According to an investigation carried out by Stahlbergh and Hallstorm [45] more than 70% of die replacements are due to wear in the hot aluminum extrusion process. Therefore; to achieve cost effectiveness and production feasibility, it is important to predict wear of die components at the early stage of product development.

Wear is a complex phenomenon which can simply be described as the gradual removal of surface material, due to the interaction of two solid objects in motion relative

to each other. Wear on dies surface is an unwanted effect which needs to be prevented to improve the overall efficiency the aluminum extrusion process. In order to prevent wear, we must first predict the mechanics under which wear occurs. Thus, solving of engineering problems related to wear can be classified broadly into two categories: prediction and prevention. The prediction of wear has led to the development of theoretical wear models established on the mechanics of wear commonly identified as [46-48]:

(a) Abrasive Wear: asperities of harder material rubbing against a softer material.
(b) Adhesive Wear: welding of asperities on the rubbing surface of counter bodies.
(c) Surface Fatigue Wear: cyclic loading of materials leading to fatigue
(d) Corrosive Wear: chemical reaction of rubbing surfaces leading to corrosion.

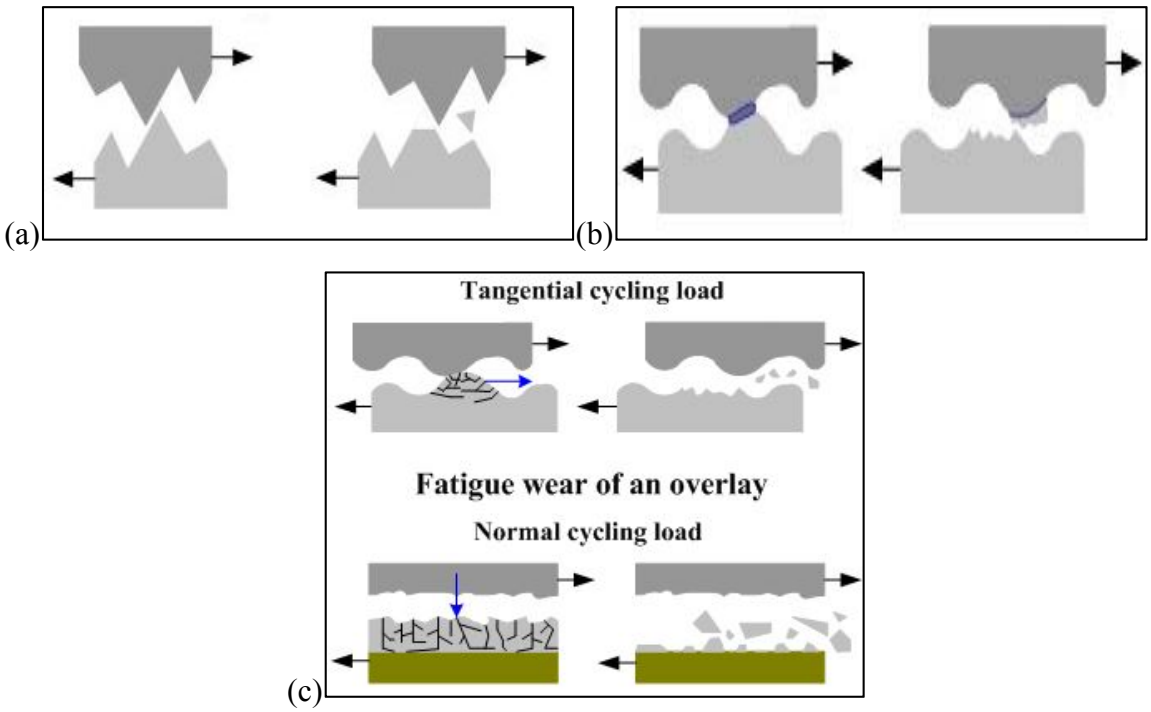

Figure 3.1 (a) Abrasive wear; (b) Adhesive wear and (c) Surface Fatigue wear [48]

In the extrusion process these wear mechanisms are not strictly segregated, but usually occur in combinations leadings to a more complex overall wear mechanism. Understanding, the mechanics of wear has led to the development of wear prevention

methods through surface treatment technologies such as nitiriding and different combinations of chemical and physical vapor deposition (CVD and PVD) coatings. So far, prevention and prediction of wear in the extrusion industry is exclusively established on experimentation and experience through trial and error; which is expensive, time consuming and difficult to control. However, in the recent years, finite element simulations have become a powerful tool in the extrusion industry due to its capability to predict wear based on the wear model discussed; thus, leading to prevention of wear and improved die life.

Currently, many researchers have numerically [49-51] and experimentally [2, 52, 53] investigated the effects of metal forming conditions on die wear in order to improve die service life. Zhang el al. [49] has investigated the effects of ram speed, initial billet temperature and initial die temperature to predict the die wear behavior during the hot extrusion of 7075 aluminum tube in Deform 3D using Archards wear model. From his studies Zhang has concluded that wear depth increases when ram speed and initial billet temperatures are increased and wear depth decreases when initial temperature of the die is increased.

Choi et al. [50] has utilized Deform 2D to analyze and predict abrasive wear and plastic deformation in forging dies. From his investigation Choi has concluded that die failure of forging dies occurs due to abrasive wear and plastic deformation at elevated temperatures.

Lee at al. [51] has modified the Archards wear model in a rigid-thermo-visco-plastic finite element program to predict wear depth profiles of dies during cold extrusion. From his investigation lee has concluded lower extrusion lead to die failure due to wear; whereas, high extrusion ratio had a greater risk of sudden fatigue fracture.

Bjork el al. [52] has studies the effects of wear on nitride and duplex ceramic coated hot works tool steel (H-13) dies during experimental extrusion die trials. From his investigation Bjork has concluded that duplex ceramic coatings are expensive and

prolongs die life by about one order of magnitude compared to nitride dies as they initially protect the die from chemical and mechanical attack.

Bjork et al. [2] has utilized a block on disc test to simulate the tribological interactions on the die bearing surface during hot aluminum extrusion. The aim of his study was to compare the mechanics of wear between nitride dies and a Chemical Vapor Deposited (CVD) Titanium-Carbide + Titanium-Nitride ($TiC + TiN$) coating. From his studies Bjork concluded that the mechanics of wear in both cases occurs by a combination of abrasive, chemical and delamination wear. However; $TiC + TiN$ coated dies improve die life as they have a better wear resistance due to its high hardness and chemical stability.

Lugscheider et al. [53] has experimentally investigated the effects of varying PVD (Cr, Al)N coating thickness, of a typical pressure casting mold by arc ion plating on surface roughness and cracking of surface coating due to thermal and residual compressive stress. Through his investigation it has been concluded that PVD coatings show a substantial increase in life span of dies with growing coating thickness. However, residual compressive stress is limited to certain height after which flaking of the surface coating will occur leading to local imperfections hence increasing wear.

From the above survey, much research has be done on predicting die wear using the Archards wear model which accurately takes into account the mechanics of abrasive wear occurring during the extrusion process; only a few experimental studies have been done on different combinations CVD or PVD coatings that help prolong die life; and, to the authors best knowledge no research until now has been done on numerically predicting the amount of wear of a bilayer coated die for the extrusion of Micro-multiport tubes. Therefore, the aim of this present study is to predict service life of modular die mandrel and die plate by simulating the extrusion of MMP tube in Deform 3D while comparing the wear depth , temperature and stress concentration of a bilayer ($TiCN + Al_2O_3$) coated mandrel and die plate against a non-coated modular die mandrel and die plate.

3.3 Wear Simulation

The aluminum extrusion process is a complex thermo-mechanical process, during which wear occurs on die surfaces due to the interaction of soft aluminum rubbing against the hard coated tooling components at elevated temperatures. Prediction of wear of the modular die components during extrusion can be modelled in Deform 3D, using the Archards wear model which is based on the mechanics of abrasive wear.

3.3.1 Coating FEM Model

The FEM model of the modular die tooling assembly mentioned in the earlier chapters for the extrusion of Multi-micro port tubes has been utilized for this investigation.

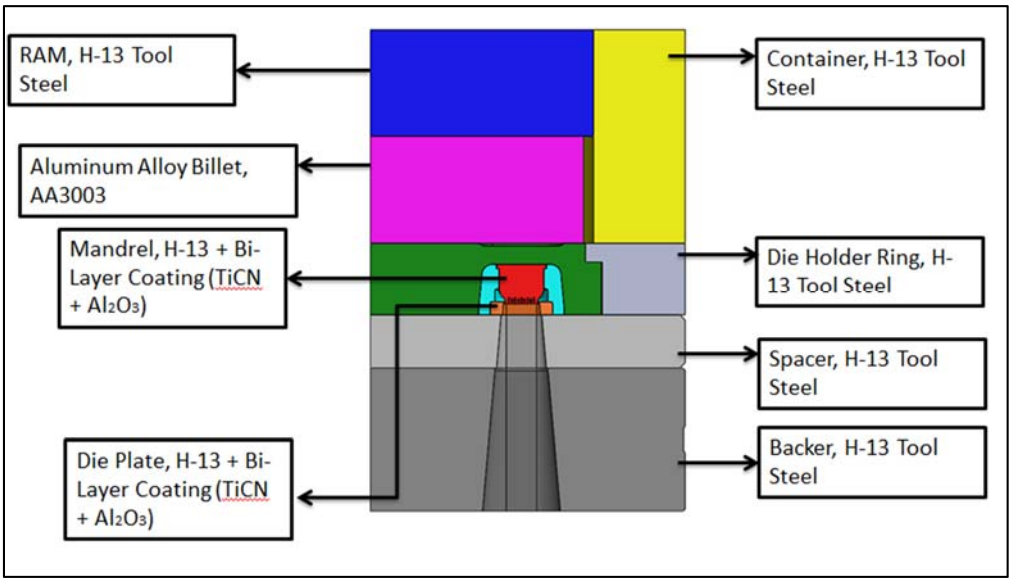

Figure 3.2 FEM model tooling description

In this study, prediction of wear depth and stress concentration of the mandrel and die plate is of primary concern during the extrusion process. Therefore, to numerically achieve this objective the mandrel and die plate of the modular die are considered to be elastically deforming; H-13 tool steel, with a surface mesh depicting the bilayer Titanium Carbo-Nitride ($TiCN$)+ Aluminum Oxide (Al_2O_3) coating and the billet is modelled as a

plastically deforming AA3003 alloy while the other tooling components are considered to be rigid.

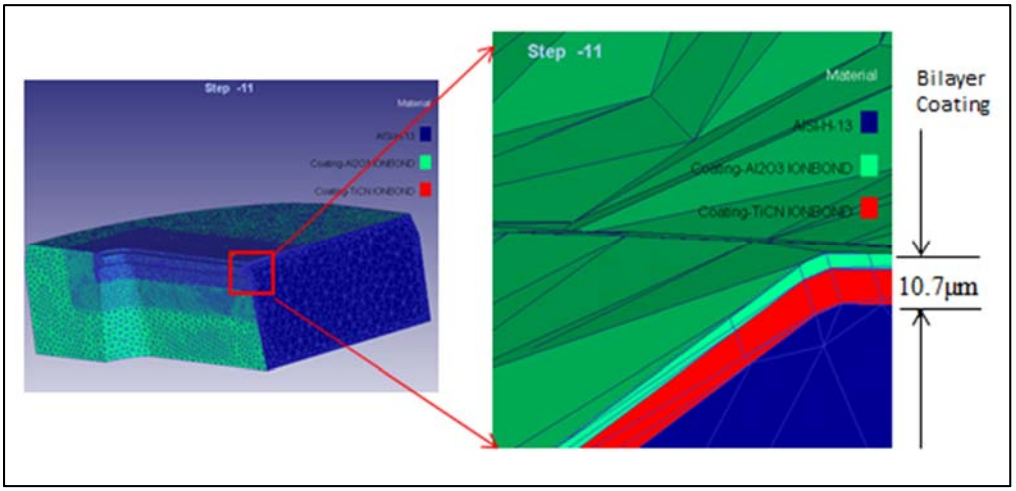

Figure 3.3 Bilayer coating thickness

The total thickness of the bilayer coating applied on the die plate and mandrel is 10.7µm (Figure 3.3); 7.4µm thick $TiCN$ adhesive layer; characterized by its toughness at elevated temperatures and 3.3µm thick Al_2O_3 working layer; characterized by low friction and high resistance to thermal stresses. In Deform 3D, each coating layer is modelled as a surface mesh within the geometry of the component thus keeping the volume of the object unaffected. Table 3.1 provides coating material data for the surface mesh applied on the mandrel and die plate in Deform 3D.

Table 3.1 Material data used in the model provided by a coating company

Mechanical/Thermal Property	Unit	TiCN Coating	Al2O3 Coating	H-13 Tool Steel
Young's Modulus	Ksi	3907.75	60190.7	30500
Poisson's Ratio		0.23	0.22	0.3
Thermal Expansion	1/°F	4.444e-06	4.25e-06	6.5e-06
Thermal conductivity	$Btu/\sec in^2$ °F	0.0003356	0.0003607	0.0003264
Density	Klb/in^3	1.83346e-04	1.43245e-04	7.28773e-07

In the present study, a coulomb friction model Equation (2.11) was utilized to represent the friction among the billet and tooling components. A coulomb friction coefficient (µ) of 0.4 was assumed at the billet and tooling component interface to

represent the sliding contact, while a coulomb friction coefficient (μ) of 0.9 was assumed at the billet container interface to represent sticking contact since no lubrication is applied among the billet and container. The friction coefficients were provided by a local extrusion company based on empirical knowledge of the extruder which has been validated in Section 2.5.

Established on the mechanics of abrasive wear, the Archard's wear model Equation.(3.1) implemented in DEFORM, is commonly used in finite element analysis of extrusion simulations to predict tool wear of a die [54]. In this model, tool wear (W) is a function of the interfacial pressure (p), the sliding velocity (v) and the hardness of the tool material (H)

$$W = \int K \frac{p^a v^b}{H^c} dt \tag{3.1}$$

The exponents, a, b, and c, for interface pressure, sliding velocity and hardness are experimentally calibrated, since no experimental data was available the exponents for interface pressure and sliding velocity is assumed to be 1; whereas, the exponent for hardness is assumed to be 2 for common tool steels [55]. 50 RC, was the measured hardness of the non-coated mandrel and die plate whereas, 54RC was the measured hardness of the bilayer coated mandrel and die plate. The wear coefficient is generally calculated through experimentation of the material, however, in this study no such data was available for the CVD ($TiCN$+ Al_2O_3) bilayer coating, hence the wear coefficient ($k = 2.426\, e^{-5}$) was calculated from the modified Archard's wear model present in [49] in which die wear behavior during aluminum extrusion was experimentally validated.

Table 3.2 Coating simulation process parameters

Billet Length (in)	8.00
Billet Diameter (in)	8.375
Initial Billet Temperature (˚F)	900
Initial Die Temperature (˚F)	850
Ram Velocity (Extrusion Speed) (in/s)	0.236220472
Heat Transfer coefficient billet/tooling interface ($\frac{Btu}{\sec in^2 {}^\circ\mathrm{F}}$)	0.002

The Updated Lagrangian formulation has been utilized for the simulation of this case study along with the extrusion process parameters mentioned in section 2.5; summarized in Table 3.2. The simulation was setup to stop after the ram has been pushed 0.45 inch and the simulation information was setup to save every 10 steps. The length of the simulation step was defined in terms of ram displacement, and each step is defined as a constant value of 0.01 in/step. The total simulation time required to complete one simulation is approximately 16 hours.

3.4 Wear Simulation Results and Discussion

In this case study, the aluminum extrusion process of a Micro-Multiport tube has been simulated to predict and compare the service life of a coated and non-coated mandrel and die plate using Deform 3D.

3.4.1 Temperature

Temperature distribution during the extrusion process is an important factor that influences product quality and tooling feasibility. Therefore, temperature distribution of the billet and tooling components should be analyzed. Figure 3.6 shows the difference in exit temperature of the MMP tube measured in Deform 3D using the state variable distribution of 100 sampling points along the width of the tube.

(a) 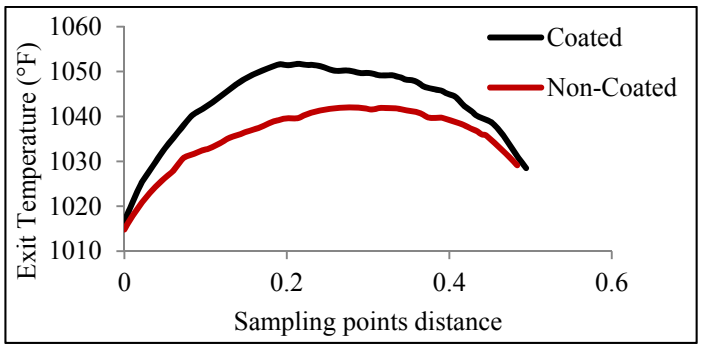

(b) 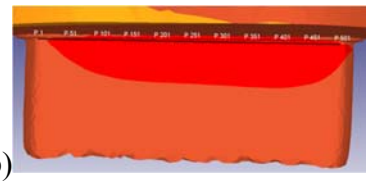

Figure 3.4 (a) Profile exit temperature and (b) Sampling points along the width of the MMP tube.

From the above graph it can be noticed that the exit temperature distribution is not uniform because the ends of the MMP tube move faster thus having less contact time with the die plate and mandrel bearing region to transfer heat. Also, the exit temperature of the MMP tube is higher in the bilayer coating simulation due to thermal barrier of the coating which reduces the amount of heat transfer occurring between the billets and tooling.

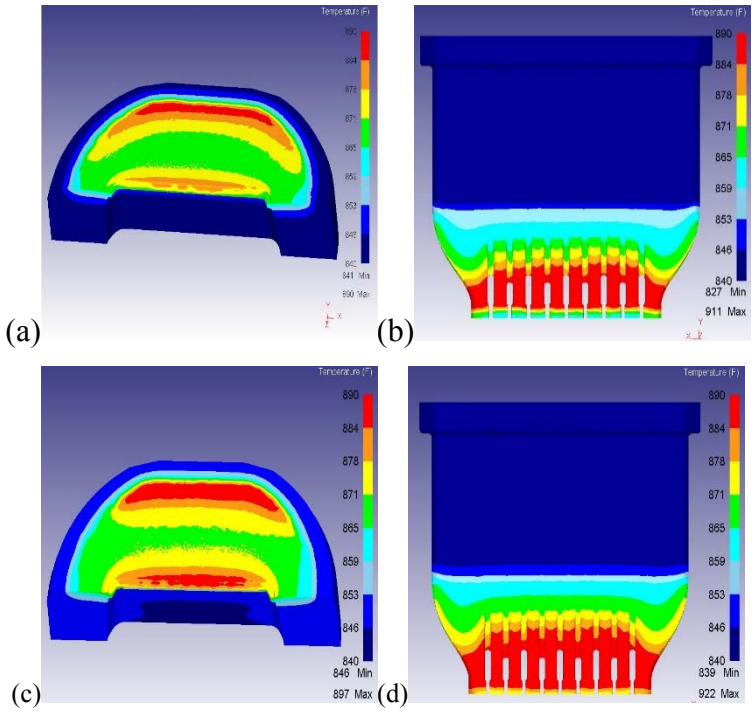

Figure 3.5 (a) Non-coated die plate temperature distribution; (b) Non-coated mandrel temperature distribution; (c) Coated die plate temperature distribution and (d) Coated mandrel temperature distribution

Figure 3.5 shows the temperature distribution of the die components. It is observed that the maximum temperature of the non-coated die plate and mandrel is 890˚F and 911˚F, whereas the maximum temperature of the coated die plate and mandrel is 897˚F and 922˚F. The higher temperature of the coated dies is due to the higher thermal conductivity of the combined coating layers. Having a higher temperature of die tooling components is beneficial in avoiding any surface defects thus leading to good quality surface finish of the extruded product; however, higher temperature of tooling components causes the die to have a shorter service life [56].

3.4.2 Wear Depth

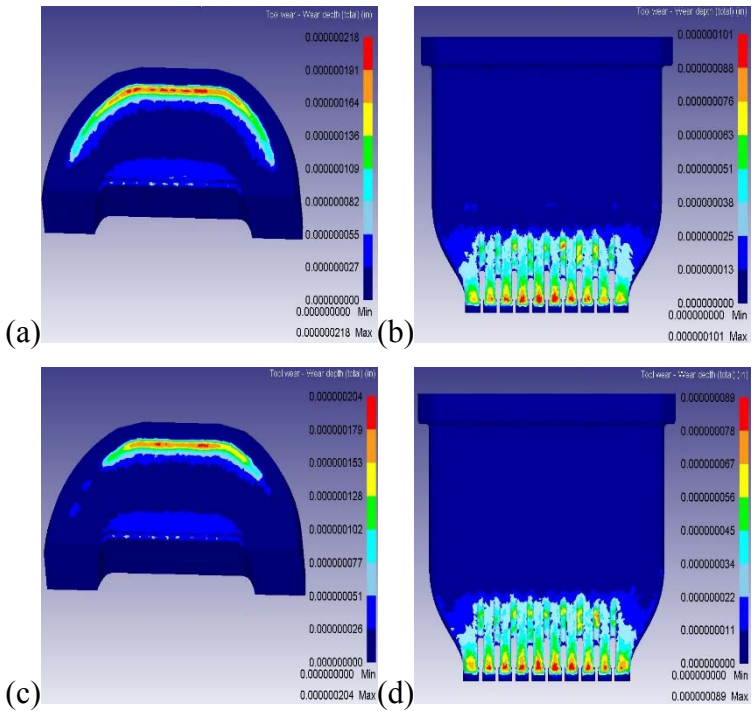

Figure 3.6 (a) Non-coated die plate wear depth; (b) Non-coated mandrel wear depth (c) Coated die plate wear depth and (d) Coated mandrel wear depth

Figure 3.6 compares the wear distribution in the mandrel and die plate. According to the Archards wear model, the wear coefficient (k), sliding velocity (V) and interface pressure (P) is directly related to wear while the hardness is indirectly related to wear. To understand the simulated results it is assumed that the sliding velocity and interface pressure is constant at each step, the wear coefficient is a constant value set forth by the user based on the literature review conducted, and the hardness of the coated and non-coated components have been measured at 54 RC and 50 RC.

From the simulated results it is observed that the coated mandrel has a wear depth of 8.95e-08 inch, the coated die plate has a total wear depth of 2.04e-07 inch; whereas, the non-coated mandrel has a total wear depth of 1.01e-07 inch and the non-coated die plate has a total wear depth of 2.18e-07 inch. In both of the tooling components it is observed that the non-coated parts have a higher tool wear than the coated parts, thus the coated die tooling components will have longer service life. The tool wear profile

observed in the simulation matches the localized areas of maximum wear of a previously used modular die as shown in Figure 3.7.

Figure 3.7 Image of modular die showing the wear pattern

An assumption made for the deform simulation is that the coating layer is free from cracks and burs. When the mandrel and die plate are coated the surface generally has small cracks or burs which during aluminum extrusion increase the wear rate due to abrasion, adhesion and chemical reactions thus leading to wear. The results generated from the simulation provide a benchmark for the extruder to test the die design and compare it with the results generated for the coating simulation thus giving the die manufacturer a rough estimate of the service life of the die.

3.4.3 Effective Stress

(a) 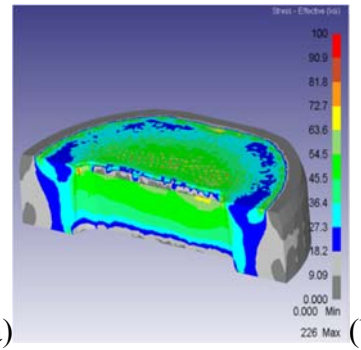

(b) 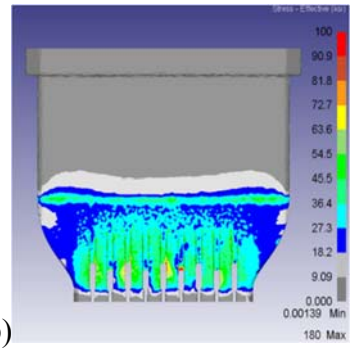

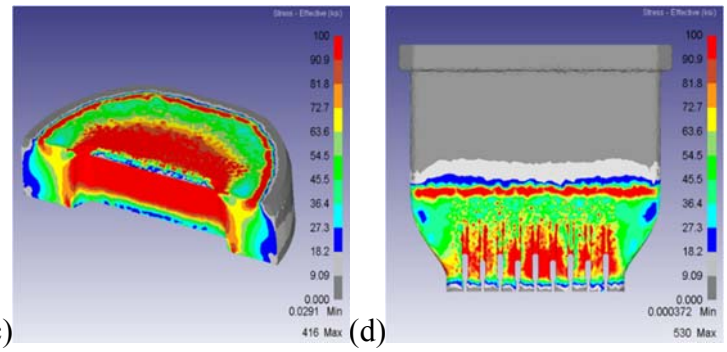

Figure 3.8 (a) Non-coated die plate effective stress; (b) Non-coated mandrel effective stress (c) Coated die plate effective stress and (d) Coated mandrel effective stress

Figure 3.8 shows the effective stress of the die components experienced during extrusion. It is observed the average effective stress of the non-coated mandrel is 20.062 ksi, and die plate is 25.894 ksi; whereas the average effective stress of the coated mandrel is 29.871 ksi and the die plate is 35 ksi. Knowing that the compressive forces applied in each simulation is the same; it was rather odd noticing such a high stress concentration zone on the coated parts. Upon, cross sectioning the die components it was evident that the high stress concentration was specific to the coating layers shown in Figure 3.9.

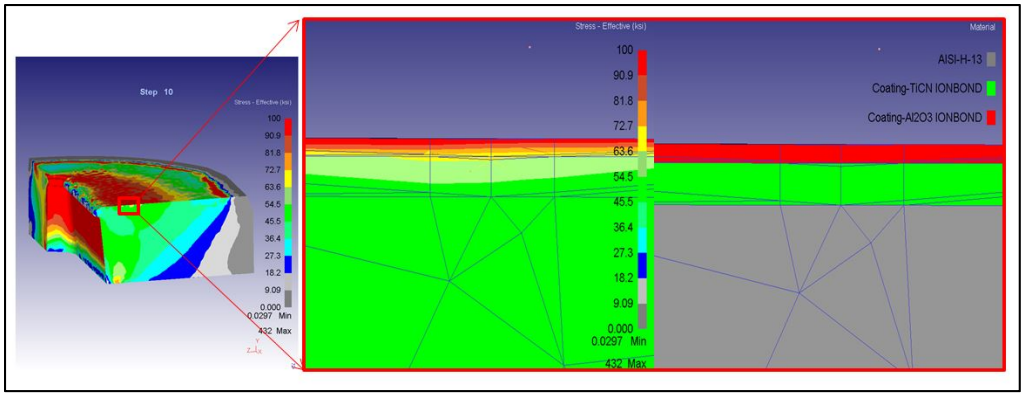

Figure 3.9 Die Plate stress concentration in coating layers

The modulus of elasticity (E) for the bilayer coating is difficult to determine due to the coatings low thickness. On the other, it has a strong influence on contact stress, coating delamination and detachment, fracture and residual stress within the coating. Usually, the young's modulus of the adhesive layer is higher than the base material [57].

(a) 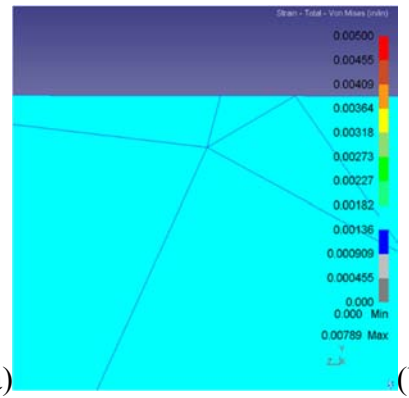

(b) 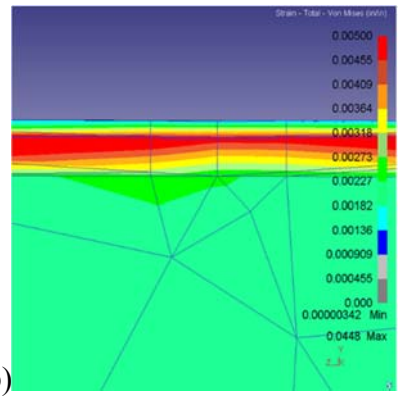

Figure 3.10 (a) Non-coated die plate strain and (b) Coated die plate strain

However, based on the material information (Table 3.1) provided for this case study; the adhesive layer ($TiCN$) has a relatively lower modulus of elasticity compared to it substrate (H-13); whereas, the working layer (Al_2O_3) has a higher elasticity. Thus, the simulated results of stress and strain concentration are in good agreement with characteristics of young's modulus for each coating layer. High stress and strain concentration in the adhesive layer of the coating will eventually lead to coating fracture, thus compromising the adhesion of the working layer leading to delamination and detachment of coating.

3.5 Conclusion

A finite element model incorporating Archards (abrasive) wear model was successfully used to simulate aluminum die extrusion process from which the following can be concluded:

1. The service life of a coated mandrel is 12.07% higher than the non-coated mandrel, whereas the service life of the coated die plate is 6.63% higher than the non-coated die plate.
2. The working layer of Aluminum Oxide (Al_2O_3) in the coated tooling creates a thermal barrier which causes the exit temperature and tooling temperature to be high, thus reducing the risk of generating surface defects.

3. Higher hardness increases wear resistance of coated tooling compared to non-coated tooling, thus increasing die service life.
4. Due to the high compressive forces of the extrusion process the adhesive layer of Titanium Carbo-Nitride ($TiCN$) showed high strain, which could lead to the generation of micro-cracks, compromising the adhesion of the working layer leading to increased surface wear, hence reducing die life.

The result generated from this simulation provides valuable information to a die manufacturer to predict the service life of a die. It also provides a frame work that can be used to eliminate the expensive trial and error method to measure performance of a die and quality of extruded product.

4. DIE DESIGN OPTIMIZATION

4.1 Overview

In this work first, based on the extruders feedback on the performance of the modular die used for the extrusion of MMP tubes; three geometric parameters, each in the mandrel and die cartridge are identified. Second, a full factorial design of experiment of the three geometric parameters each at three levels is established in Minitab. Third, using steady state FE analysis in Deform 3D, aluminum extrusion is simulated through the modular die for each parametric set, to collect numerical data of the identified responses in the first step. Fourth, Minitab is utilized to statistically analyze the main effects and interactions of the geometric parameters on the responses. Finally, the response optimization in Minitab is utilized to optimize the geometric parameters identified by the die designer based on the objective of the optimization problem.

4.2 Introduction

Aluminum Extrusion is a continuous metal forming process where a billet of hot aluminum is compressed through a die of relatively smaller cross sectional area to produce long shaped aluminum profiles. During the extrusion process, the die has to overcome high values of compressive forces at elevated temperatures in order to produce high quality products that meet tight geometrical tolerances thus, die design is one of the most important and demanding aspects of the entire extrusion process that greatly influences die failure and extrusion quality.

Currently in the extrusion industry development of a new die design is solely dependent on the die designers experience, personal judgment and intuition. Some of this

experience is captured in empirical design rules which are quite valuable in the production of efficient dies; however, a large part of the die design is still dependent on the traditional trial-and-error approach. In today's modern industrial environment of high productivity, low cost and low scarp rate, these traditional methods consume time and money. In addition, these methods are not effective or economical as the die cannot be repaired in some instances and have to be discarded.

Due to the complexity of the extrusion process, a systematic die design approach is required that will help the die designer better facilitate their empirical knowledge as well as provide some resourceful information on the feasibility and performance of the die design during extrusion; in terms of die failure and quality of extruded product. This objective for a systematic die design approach can be fulfilled by conducting design of experiments along with the use of numerical models that can simulate the extrusion process. According to Wu and Hamada, [58] a Design of Experiments (DOE) *is "a body of knowledge and techniques that enables an investigator to conduct better experiments, analyze data efficiently, and make the connections between the conclusions from the analysis and the original objectives of the investigation."* In other words, DOE is a statistical tool that is used to develop experimentation strategies that maximizes knowledge while using minimal resources. DOE's are helpful in statistically studying and building a cause-and-effect relationship between a number of independent design factors and their dependent output. However, to establish a relationship between the die design factors under investigation and their effect on die failure or extrusion quality it is important to experimentally test the design change. Experimental tests of extrusion dies are expensive, time consuming and difficult to analyze due to the rigorous temperatures and forces involved in the extrusion process.

However, with the modern technological advances in finite element methods to numerically simulate the extrusion process; fundamental understanding and optimization of the die design can be done with the help of numerical simulations and DOE [59]. Many researchers have performed some simulations work on aluminum alloy extrusion to provide accurate and theoretical guidance for die design optimization using Finite

Element (FE) analysis. Jung et al. [19] has investigated the effects of chamber shapes of porthole die for condenser tubes to evaluate material flow, welding pressure, extrusion load and the tendency of mandrel deflection using updated lagrange method for aluminum flow and ANSYS 5.5 for die stress analysis. Lee et al. [60] has investigated the effects of chamber shape dimensions and initial temperature of tool and die on the forming load, welding pressure and stress analysis of the die using finite element simulation and experimental validation of a 12 cell al3003 condenser tube. Tang et al. [26] has studied the effects of flat and hemispherical extrusion die design in a micro channel extrusion tube by investigating the seam weld strength and microstructures of the extruded tube using numerical simulations and experimental validation. Ceretti et al. [8] has investigated the geometrical effects of a porthole die using finite element simulation to optimize material flow and stresses acting on the die.

Despite the technological advancement and success of numerical simulations to help improve the design process, the modular die used for the extrusion of MMP tubes has been designed based on the experience, intuition and personal judgment of the die designer. Although, the modular die design has significantly improved, due to the knowledge gained from previous experimental trials some failure modes still exist. Therefore utilization of DOE's and numerical simulations will better facilitate the knowledge of the die designer for future designs.

The novel concept of this chapter is to utilize Deform 3D a finite element code to simulate the extrusion process of a MMP tube through the modular die and to conduct a set of design of experiments in order to help the die designer understand how changing a certain geometric parameter in the die design will effect a specific response of the extrusion process.

4.3 Design of Experiments

A DOE is an optimization method that lets us study the effects of several factors for a specific response. When conducting a DOE, varying the levels of each factors at the

same time helps in studying the interactions between factors. For example, estimating the influence of two factors (Factor1 and Factor2) each at two levels (Level1 and Level2) on the response of interest (Response1), is shown in Table 4.1. The total number of experiments necessary for a full factorial design of experiments can be calculated using an exponential formula where n is the number of factors and k is the number of levels.

$$Full\ Factorial\ \#\ of\ Experiements = n^k$$

Table 4.1 Example of a 2-level full factorial DOE layout

Number of Experiments	Factor1	Factor2	Response
1	Level1	Level1	$Interaction\ of\ Factor1{,}2_{\ Level1,1}$
2	Level1	Level2	$Interaction\ of\ Factor1{,}2_{Level1,2}$
3	Level2	Level2	$Interaction\ of\ Factor1{,}2_{Level2,2}$
4	Level2	Level1	$Interaction\ of\ Factor1{,}2_{Level2,1}$

The modular die, is used for the extrusion of MMP tubes (Figure 4.1) used for Contemporary heat exchange applications such as air conditioning systems, evaporators, radiators and refrigerators.

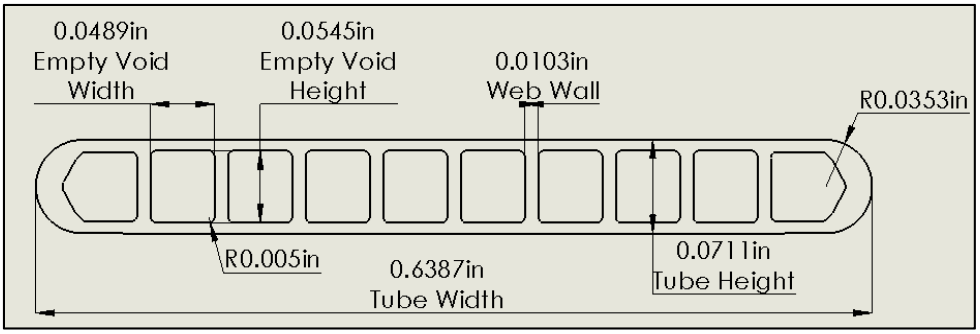

Figure 4.1 Micro-Multiport tube dimensions

The success of MMP tube extrusion depends on the surface quality and tight geometric tolerances, which is achieved through proper designing of the modular die. The modular die is the assembly of three components the die cartridge, mandrel and die plate. The design of each component is defined through a number of different geometric parameters which has been revised multiple times through trial and error, intuition of the die designer and feedback provided from the extruder. Therefore; the parameters to be

considered for the optimization of the modular die design is based on current issues reported by the extruder which is:

- Under fill of aluminum in mandrel port opening causing no formation of web walls.
- Breaking of mandrel teeth

Based on these reported issues, along with the die designer's experience and examination of the failed modular die parts it is identified that the mandrel and die cartridge designs are the primary reason for these failures. Therefore, 3-level full factorial DOE was developed to understand the interactions of aluminum flow on modular die deformation. In order to optimize the CAD geometries the results obtained from the DOEs through finite element analysis, were then analyzed using statistical knowledge to better facilitate the knowledge of the die designer. The methodology used in this improved die design process is summarized in Figure 4.2.

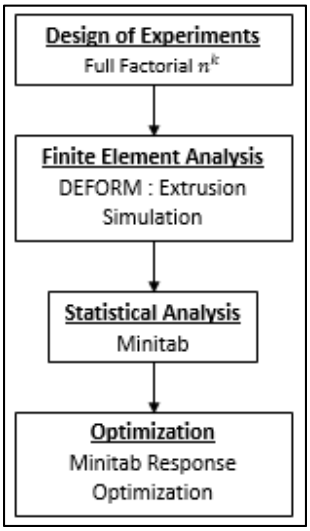

Figure 4.2 Methodological die design process

4.3.1 Mandrel Design of Experiments

The Mandrel is one of the critical components in the modular die design. The function of a mandrel is to help create the thin web walls (shown in Figure 4.1) on the

insides of the MMP tube that are separated by fine voids. The Port Opening (PO), Port Lead Angle (PLA) and Angle Intercept Distance (AID) are the key characteristics of the mandrel CAD geometry that allow the formation of the thin web walls of the MMP tube.

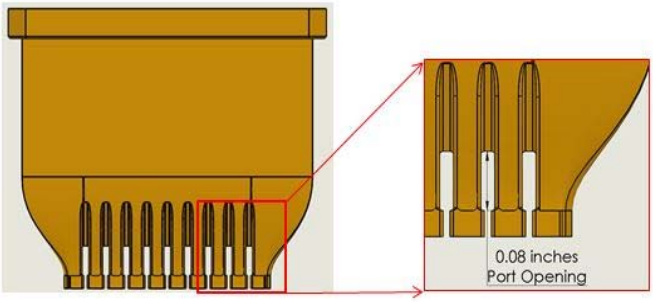

Figure 4.3 Port opening

The port opening feature was designed to allow sufficient amount of aluminum to flow in between the teeth's to form a good weld before the actual dimension of the web walls are defined in the bearing.

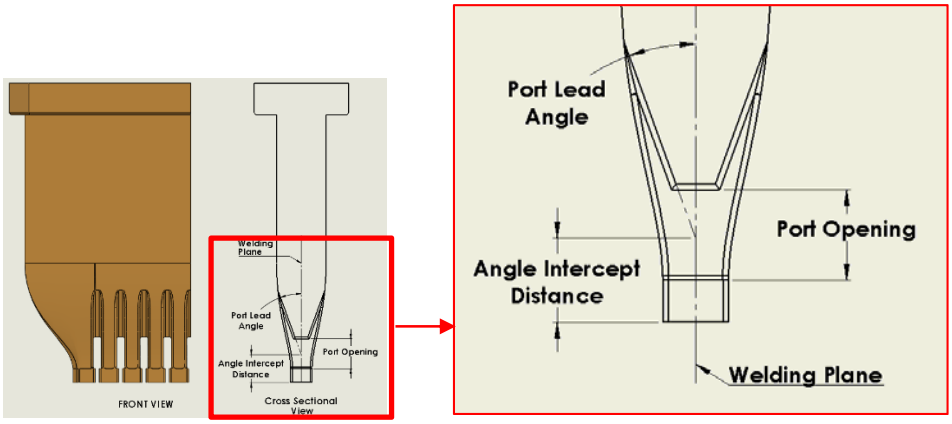

Figure 4.4 Cross sectional view of the three parameters that influence aluminum flow into the porting geometry distance

The port lead angle and angle intercept distance was designed with the intuition that the aluminum would flow along the angled walls and start welding at the specified angle intercept distance. These three parameters of the mandrel help in forming the port geometry that allows to increase the amount of aluminum flowing into the porting geometry. Therefore, using a full factorial DOE approach, three factors (port opening,

port lead angle and angle intercept distance) each at three levels were statistically analyzed to understand the effects of the mandrel CAD geometries on aluminum flow into the porting geometry in order to maximize weld pressure

Table 4.2 Mandrel full factorial design of experiments

Trial	Port Opening (inch)	Port Lead Angle (°)	Angle Intercept Distance (inch)
1	0.06	15	0.04
2			0.07
3			0.1
4		20	0.04
5			0.07
6			0.1
7		25	0.04
8			0.07
9			0.1
10	0.07	15	0.04
11			0.07
12			0.1
13		20	0.04
14			0.07
15			0.1
16		25	0.04
17			0.07
18			0.1
19	0.08	15	0.04
20			0.07
21			0.1
22		20	0.04
23			0.07
24			0.1
25		25	0.04
26			0.07
27			0.1

4.3.2 Die Cartridge Design of Experiments

The die cartridge is the main component of the modular die. Its functional responsibility is to create a porthole once placed into the holder; as well as, house the mandrel and die plate. There are many geometrical features that make up the die cartridge. However, the Angle Guide Curve (AGC), Bridge Mandrel Angle (BMA) and

Die Plate Covering (DPC) were the parameters chosen by the die designer, to investigate their effects on the stresses of the mandrel teeth.

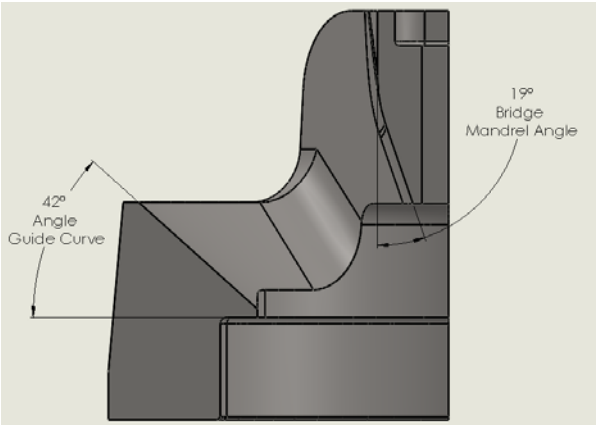

Figure 4.5 Die cartridge DOE showing angle guide curve and bridge mandrel angle

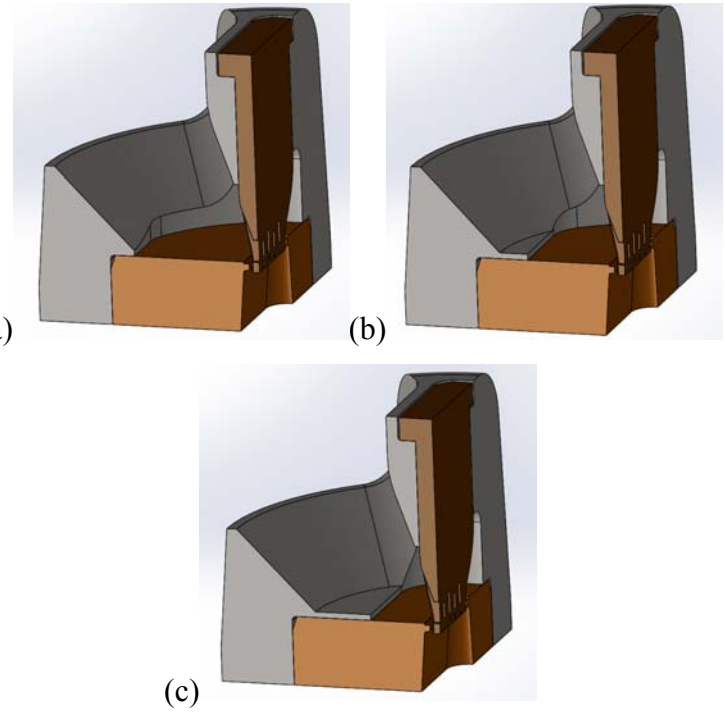

Figure 4.6 Die cartridge DOE showing die plate covering (a) 0.9 inch; (b) 0.7 inch; and (c) 0.5 inch.

Using a full factorial DOE approach the three factors (angle guide curve, bridge mandrel angle and die plate covering) each at three levels were statistically analyzed to understand the effects of these geometric features on the stresses of the mandrel teeth.

Table 4.3 Die cartridge full factorial design of experiments

Trial	Angle Guide Curve (°)	Die Plate Covering (inch)	Bridge Mandrel Angle (°)
1	45	0.9	20
2			15
3			10
4		0.7	20
5			15
6			10
7		0.5	20
8			15
9			10
10	30	0.9	20
11			15
12			10
13		0.7	20
14			15
15			10
16		0.5	20
17			15
18			10
19	15	0.9	20
20			15
21			10
22		0.7	20
23			15
24			10
25		0.5	20
26			15
27			10

4.4 DOE Simulation Model

While conducting a DOE it is important that the only parameters under investigation change while all the other auxiliary boundary conditions remain the same. The contact boundary condition of the die filled aluminum needed to be same in all the 27 DOE's; therefore, the Steady State (SS) extrusion model available in Deform 3D was utilized for the mandrel and die cartridge DOE's. The modeling is based on the Eulerian

formulation of the finite element method with the assumption that the extrusion process has reached the steady state thermo-mechanically. Each of the simulation steps is solved in an uncoupled way, which consists of two stages: the Lagrangian calculation and remapping of state variables. The Lagrangian calculation is where the equilibrium is achieved and the former remapping is done to obtain the convective values. A few steps of simulation are conducted iteratively until the solutions converge. In these steps, the nodes do not march forward as in the updated Lagrangian formulation but the free surface of the extrudate will be corrected so the surface is tangential to the material flow and the strain and temperature will be calculated [55]. In order to utilize the steady state extrusion model; Deform requires specific details of the CAD geometries to be enhanced such as: the work piece should entirely fill the die cavities, initial surface of the extrudate part should be parallel to the extrusion direction and the top of the billet and the end of the extrudate should be perpendicular to the flow direction.

4.4.1 Mandrel

Due to the linear design of the mandrel a simplified cross sectional model was utilized to conduct the 27 mandrel DOE's. The three features under investigation are consistent between each mandrel tooth. Therefore; this model was created focusing only on one port opening to help reduce computation time.

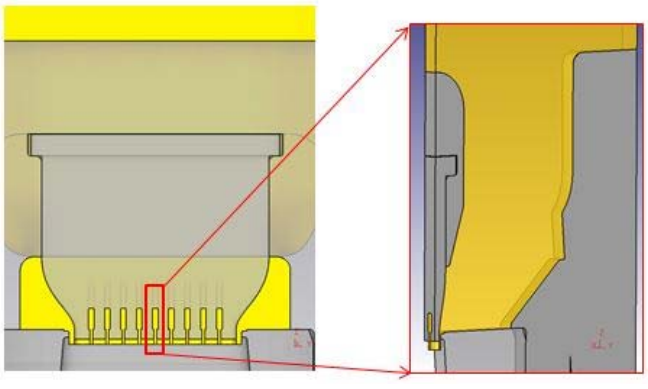

Figure 4.7 Cross sectional mandrel DOE model

The cross sectional model consisted of 200,000 elements in the cavity filled work piece; which consisted of multiple mesh windows of higher mesh density to gain good accuracy in results of the critical features under investigation. All the tooling components were considered to be rigid as the billet was modelled as a plastically deforming 3003 series aluminum alloy. The FEA model was considered to be isothermal as the main focus of this study is to obtain welding pressure results in the welding plane.

4.4.2 Die Cartridge

Due to the complexity of the die cartridge parameters under investigation a quater-domain model ($1/4^{th}$) of the modular die tooling components was utilized for the investigation of the Die Cartridge DOE's.

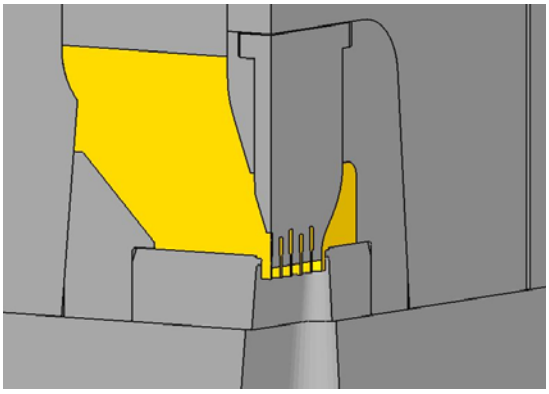

Figure 4.8 Quarter domain die cartridge DOE model

As it can be seen in the image above the angle guide curve for the Die cartridge DOE's is revolved features that greatly influence the flow of aluminum towards the mandrel thus influencing its stresses. Therefore, a quarter-domain symmetric model was considered for this investigation.

In order to calculate the stresses on the mandrel using the steady state extrusion the design of experiments had to be conducted in two parts:

1. First, the 27 flow analysis DOE's needed to be conducted to obtain the flow stresses.

2. Second, the 27 forces developed due to the flow of aluminum were then mapped on the mandrel to conduct a die stress analysis.

The quarter-domain model consisted of 200,000 elements in the cavity filled work piece; and 200,000 elements in the mandrel both of which consisted of multiple mesh windows of higher mesh density to gain good accuracy in results of the critical features under investigation. For the flow analysis all tooling components were considered as rigid objects besides the billet which was modelled as a plastically deforming AA3003 aluminum. For the die stress analysis the mandrel was modelled as an elastic H-13 tool steel. The FEA model was considered to be isothermal as the main focus of this study was to obtain the stresses in the mandrel due to the flow of aluminum guided by the die cartridge.

The boundary conditions utilized in the both the Mandrel and Die Cartridge design of experiments simulations are summarized in the table below:

Table 4.4 DOE process paramters

FE Analysis Conditions	
Extrusion Condition	Value
Material of Billet	AA 3003
Material of Tools	H-13 Tool Steel
Billet Temperature	900 C
Tooling Temperature	900 C
Ram Velocity	1.034 in/sec
Friction Conditions	
Tooling & Billet Interface	Shear 1
Mandrel & Billet Interface	Coulomb 0.4
Die Plate & Billet Interface	Coulomb 0.4
Ram & Billet Interface	Shear 1

While conducting a DOE, it is important that all the boundary conditions in each of the 27 DOE simulations must be similar; therefore, to avoid the separation of nodes during the steady state iterations a sticking boundary condition using the shear friction model, with a friction factor of 1 (m = 1, sticking) was assigned to the billet mesh in

contact with the tooling components. Sticking boundary condition has also been reported in several literatures on the basis of experimental and industrial observations [7, 38, 61, 62]. A windows operating with 32GB of RAM and four 3.4Ghz Intel Core i7 processors was utilized to conduct the numerical simulation of the extrusion process in Deform. The total computational time for each simulation is 50 minutes.

4.5 Response Optimization

The Minitab response optimizer was utilized to help identify a specific combination of geometrical parameters under investigation that will help optimize a single response or a set of response.

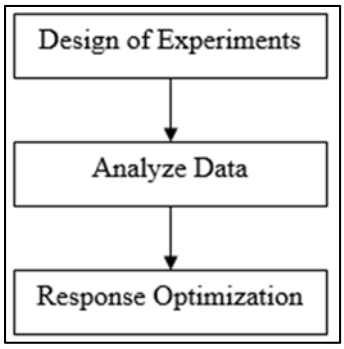

Figure 4.9 Minitab optimization process

Figure 4.9, shows the process utilized by Minitab to optimize a response. First, all the simulated values of welding pressure and effective stress obtained from the mandrel and die cartridge DOE's were inputted into Minitab worksheet. Second, a factorial design model using a 95% confidence interval was used to analyze the significance, main effects and interactions of each design parameter under investigation. Third, the analyzed DOE data was used by the optimizer to search for either a minimal, targeted or maximum optimal response.

4.6 Kriging Optimization

The response optimizer in Minitab analyzes the data set and picks either a global maxima or minima based on the objective of the optimization. As a result local points that could even further optimize the design are ignored. Therefore, a robust interpolation technique known as kriging was utilized to create a continuous function from a scattered data set provided by the design of experiments conducted in this thesis. In statistics, kirging is a robust interpolation technique that analyzes the variance patterns of the dataset to determine general trends in order to predict unknown values that have not been sampled[63]. In this method at every point where we do not have a sample, an estimated value ($\widehat{V_o}$) is predicted using a weighted (w_j) linear combination of the available samples (V_j), this is known as ordinary kriging.

$$\widehat{V_o} = \sum_{j=1}^{n} w_j \cdot V_j \tag{4.1}$$

This kriging optimization technique is calculated using the DACE (Design and Analysis of Computer Experiments) function which is a matlab toolbox used for constructing a kriging function based on data from the discretized domain of the design of experiments conducted.

5. RESULTS AND DISCUSSION

5.1 Material Flow

The material flow of aluminum through the modular die can be categorized into four stages: dividing, filling, welding and forming stage.

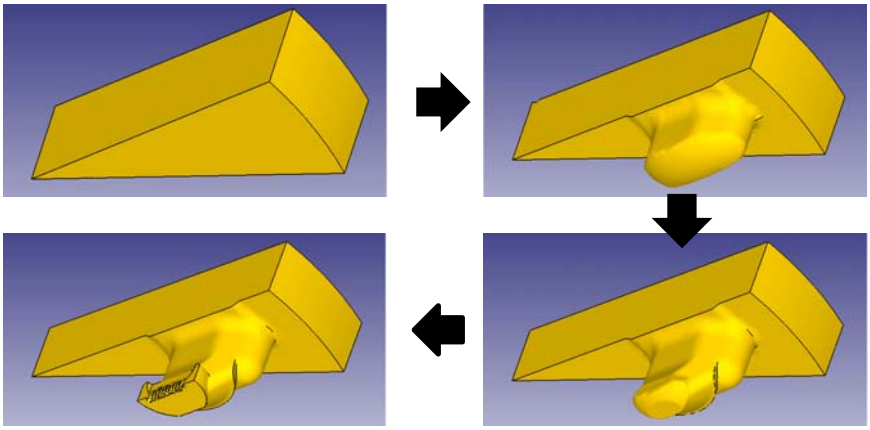

Figure 5.1 Modular die three dimensional forming process

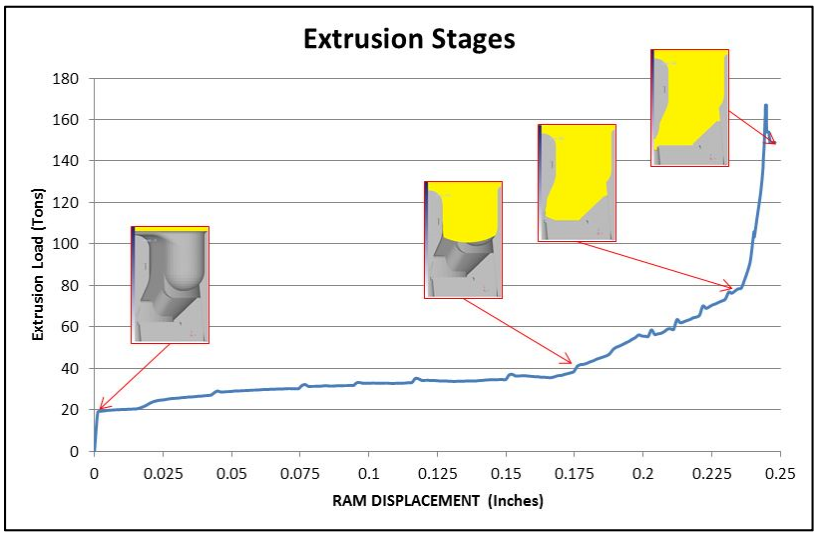

Figure 5.2 Modular die extrusion load

As the aluminum flows through the modular die, the cross sectional area of the die cavity reduces gradually which leads to an increase in the amount of load the ram has to exert on the deforming billet. This increase in load marks the beginning of each stage. First, increase in load is marked by the splitting of the billet into the porthole which gradual increase as the aluminum fills up the porthole. Second, filling stage, the load of the ram increase even further due to reduction in cross sectional area as the aluminum is forced to flow towards the mandrel. Third, Welding Stage, the divided aluminum flow will weld back together in the port opening of the mandrel to form the thin web walls of the MMP tube. Fourth, forming stage is marked by the peak value of extrusion load which forms the final shape of the MMP tube in the bearing area.

The welding of aluminum for the MMP tube initiates at the welding stage and is fully developed by the end of the forming stage where maximum force is exerted on the die by the aluminum flow. Therefore, to save computational time both, the mandrel and die cartridge design of experiments were simulated utilizing the steady state extrusion method in Deform 3D, which accurately models the extrusion process during the forming stage of the MMP tube. The results of the DOE's were then analyzed using Minitab a statistical software package that provides several analytical and graphical tools to help understand the results.

5.2 Mandrel DOE Results

The mandrel design of experiments were simulated using the cross sectional model established earlier in the chapter. The main objective of this study is to investigate the effects of port opening; port lead angle and port angle intercept distance on weld pressure, material velocity and effective stress of aluminum on the welding plane. In order to measure the data on the welding plane 100 equally distant sampling points were used form the entrance of the welding surface.

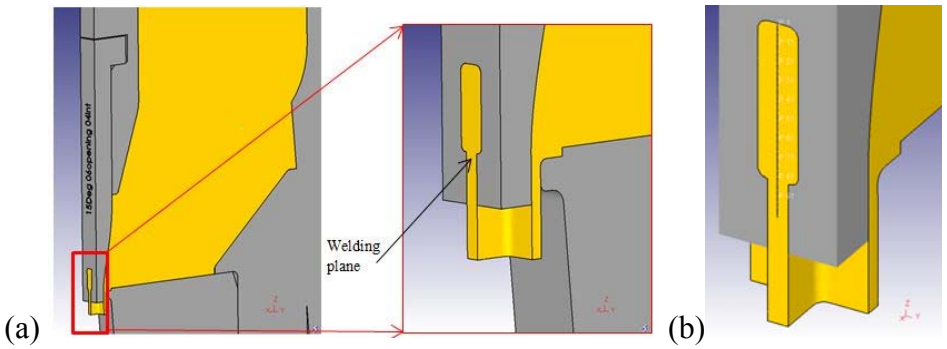

Figure 5.3 Mandrel DOE; (a) cross sectional model and (b) 100 sampling points on welding plane of port opening

5.2.1 Validation

In order to validate the results of the mandrel DOE, the distribution of welding pressure, and material velocity on the welding surface from one of the DOE simulations has been plotted and compared to the results Donati et al. [64] and Liu et al. [44].

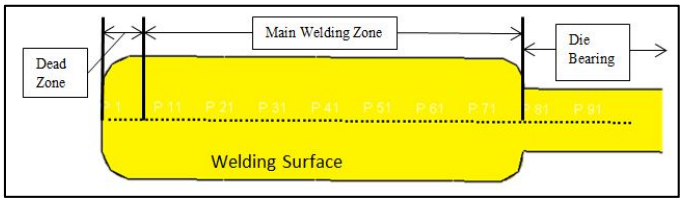

Figure 5.4 Welding surface sections

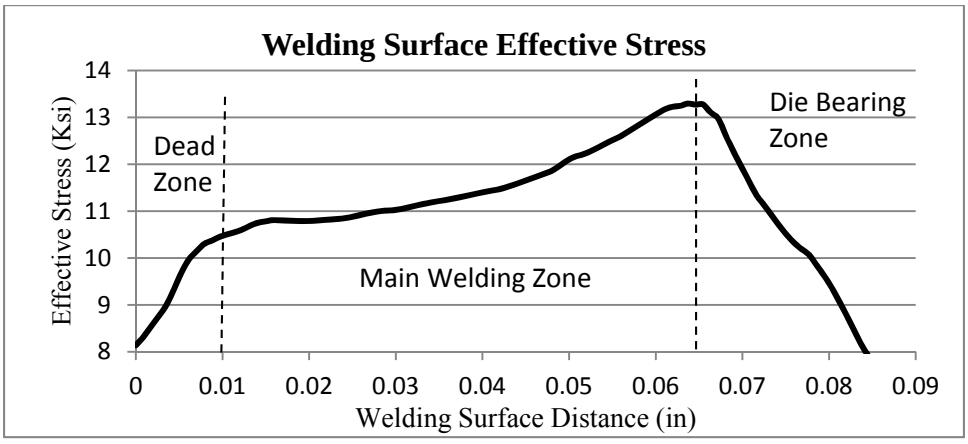

Figure 5.5 Effective stress on welding surface

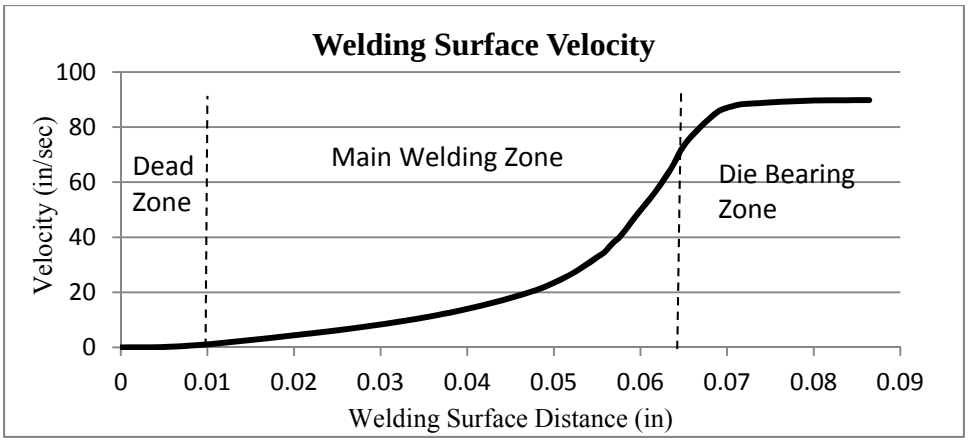

Figure 5.6 Material velocity on welding surface

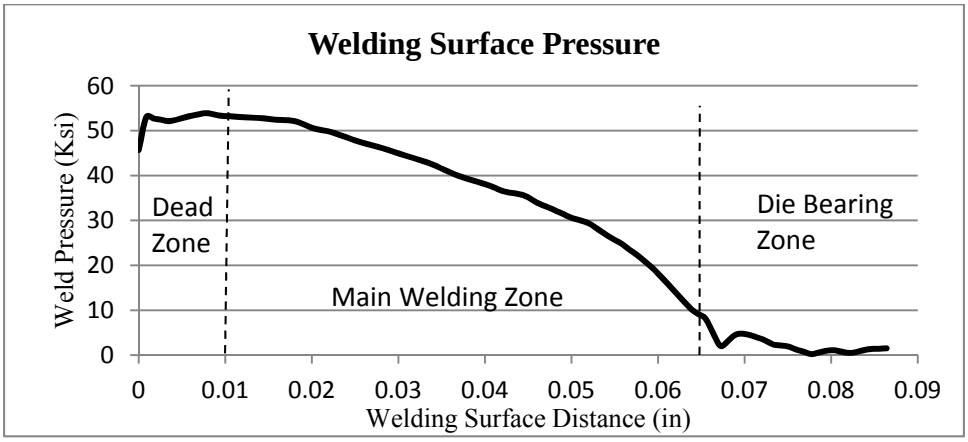

Figure 5.7 Welding pressure distribution on welding surface

The effective stress plotted in Figure 5.6, material velocity plotted in Figure 5.7, and welding pressure plotted in Figure 5.8 are consistent in each of the 27 design of experiments and is in good agreement with the results obtained by Donati et al. [64] and Liu et al. [44]. Based on similar results in their research the characteristics of effective stress, material velocity and weld pressure can be summarized by sectioning the welding surface into three regions:

1. Dead Zone: is formed right under the entrance to the port opening and is characterized by very low velocity, maximum welding pressure and a gradual increase in effective stress from a relatively low value.

2. Main Welding zone: is formed below the dead zone and is characterized by increase in material velocity while welding pressure decreases and effective stress gradually increases to a maximum value.
3. Die Bearing Zone: is the final region where the final shape of the MMP tube is formed and is characterized by highest velocity while the welding pressure is the lowest and effective stress gradually decreases from its maximum value at the beginning of the die bearing zone due to the maximum deformation state of the extrusion profile.

5.2.2 Effect of Port Opening

The purpose of the port opening is to allow the aluminum to weld back together before the thin walls of the condenser tube are formed.

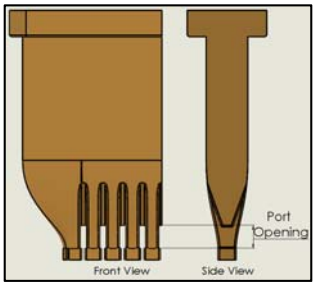

Figure 5.8 Mandrel port opening front and side view

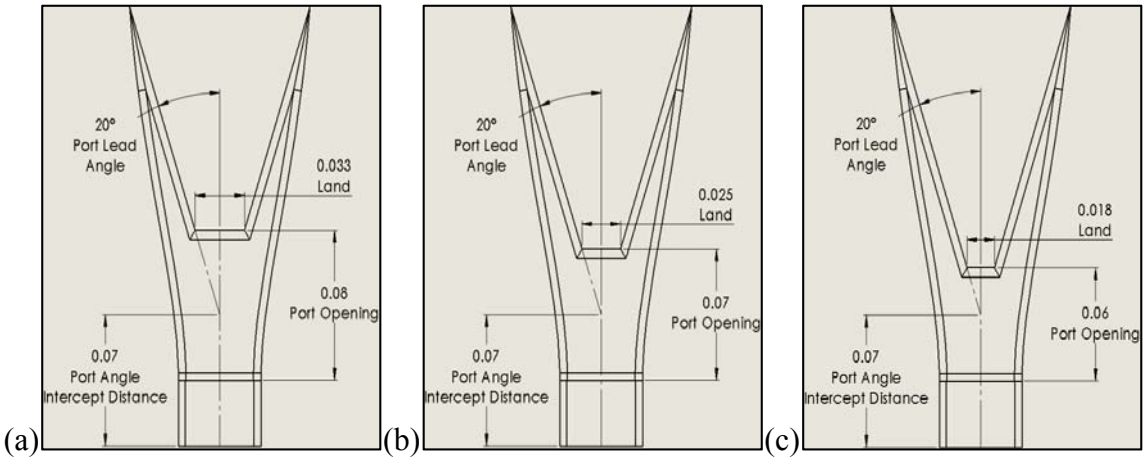

Figure 5.9 Port opening; (a) 0.06inch; (b) 0.07inch and (c) 0.08inch

Figure 5.9 shows the CAD geometry of the mandrel with varying port opening lengths. It is observed that the length of the land is 0.018 inches for 0.06 inch port opening length, 0.025 inches for 0.07 inch port opening length and 0.032 inches for 0.08 inch port opening length.

5.2.2.1 Effective Stress

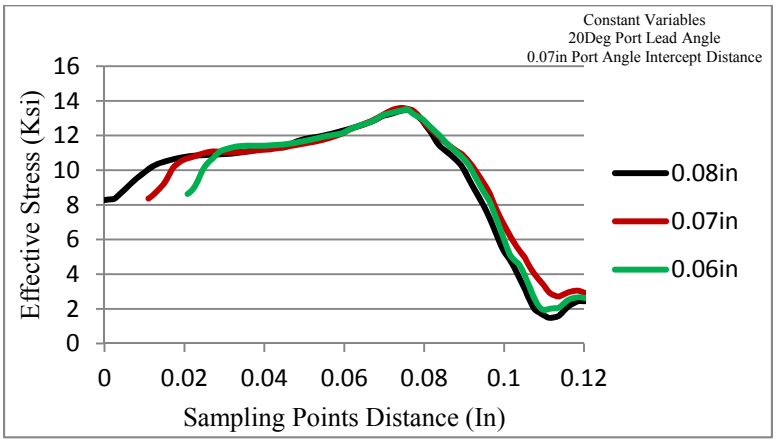

Figure 5.10 Effective stress vs. port opening on welding surface

Figure 5.10 compares the effective stress of the deforming aluminum on the welding surface by varying port opening lengths. It is observed that trend of effective stress in the dead zone, main welding zone and die bearing zone is similar in all port opening lengths. However, the length of the main welding zone decreases due to the decrease in port opening length.

5.2.2.2 Material Velocity

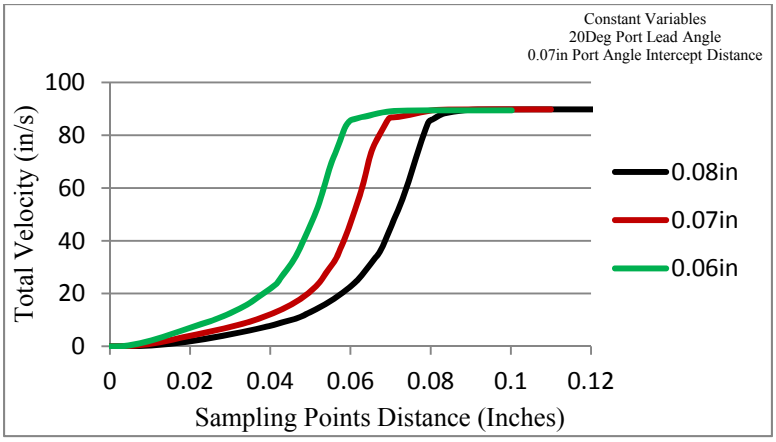

Figure 5.11 Velocity vs. port opening on welding surface

Figure 5.11 compares the flow of aluminum on the welding surface by varying port opening lengths. It is observed that the velocity of aluminum increases relatively faster when the length of the port opening decreases. The dead zone of aluminum increases as the port opening length increases. This behavior of aluminum flow is mainly dictated by the increase in length of land at the port opening entrance shown in Figure 5.9 which increases as the length of the port opening increase. However, the exit velocity of aluminum in all varying cases is similar due to the constant extrusion ratio.

$$Extrusion\ Ratio\ (ER) = \frac{Cross\ sectiona\ area\ of\ the\ billet\ (A_b)}{Cross\ sectional\ area\ of\ the\ profile\ (A_p)} \quad (5.1)$$

$$Exit\ Velocity\ (V_e) = Ram\ Velocity(V_r) \times ER \quad (5.2)$$

5.2.2.3 Welding Pressure

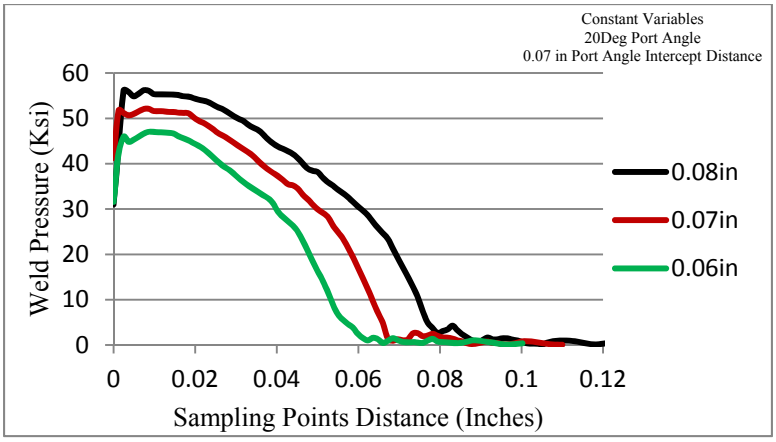

Figure 5.12 Weld pressure vs. port opening on welding surface

Figure 5.12 compares the weld pressure distribution of varying port opening lengths. It is observed that the welding pressure increases as the length of the port opening increases. This trend of weld pressure distribution is characterized by the combined effect of longer main welding zone observed in the effective stress distribution (Figure 5.10) and longer dead zones observed in the material velocity distribution (Figure 5.11) of varying port lengths. Therefore, 0.08 inch port opening length has the highest welding pressure distribution whereas, 0.06 inch port opening length has the lowest weld pressure distribution on the welding surface.

5.2.3 Effect of Port Lead Angle

The purpose of the port lead angle is to guide the aluminum flow from the porthole chamber into the port opening in order to gaining maximum weld. Figure 5.13 shows the CAD geometry of the mandrel with varying port lead angles. It is observed that increasing the port lead angle restricts the total volume of the porting.

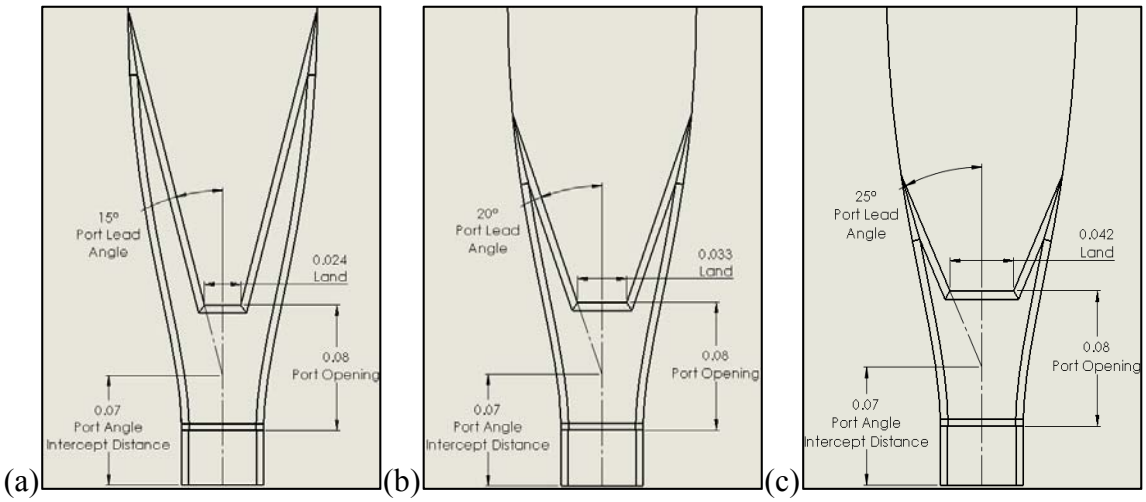

Figure 5.13 Port lead angles; (a) 15°; (b) 20° and (c) 25°

5.2.3.1 Effective Stress

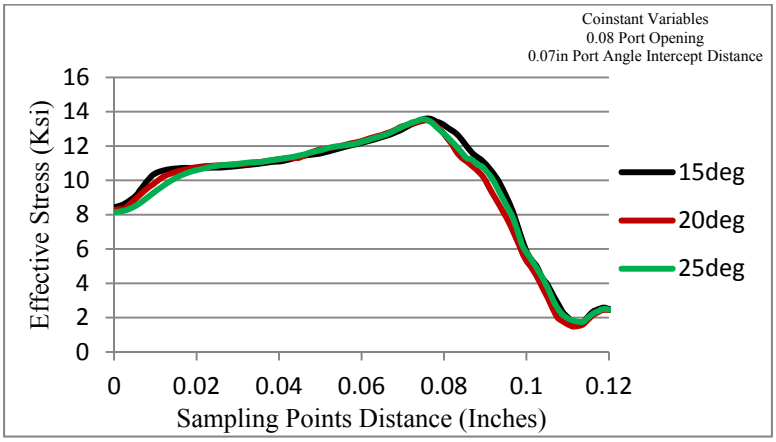

Figure 5.14 Effective stress vs. port lead angle on welding surface

Figure 5.14 compares the effective stress of the deforming aluminum on the welding surface by varying port lead angles. It is observed that the effective stress in the dead zone decreases with increasing port lead angle which gradually becomes constant over the main welding zone and then decreases in the die bearing zone as the port lead angle increases.

5.2.3.2 Material Velocity

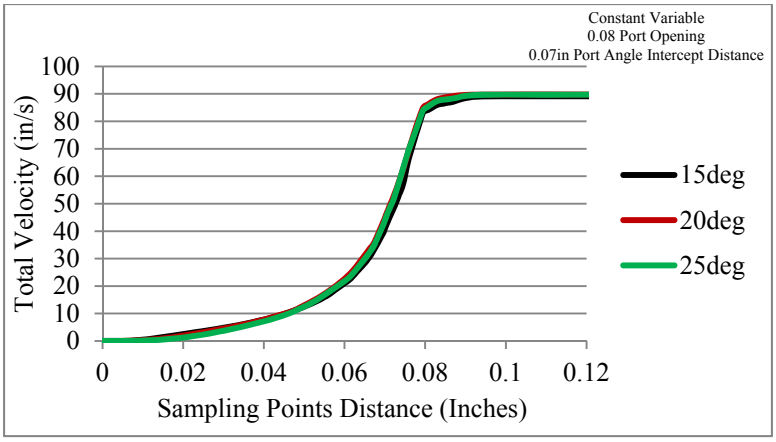

Figure 5.15 Velocity vs. port lead angle on welding surface

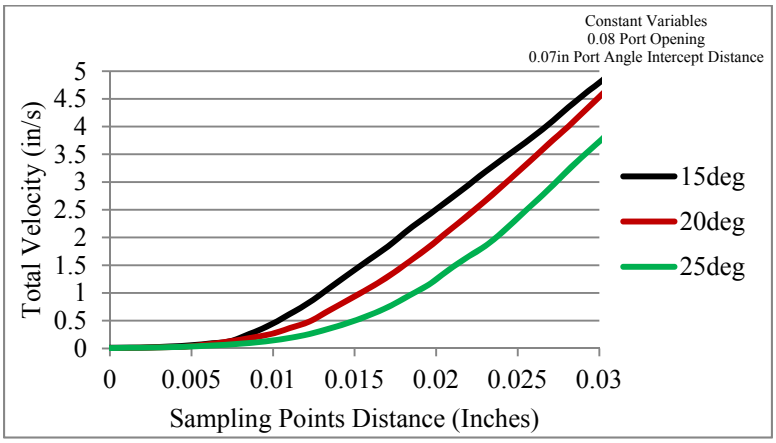

Figure 5.16 Velocity in dead zone vs. port lead angle on welding surface

Figure 5.15 compares the flow of aluminum on the welding surface by varying port lead angle. It is observed that the velocity profile over the entire welding surface follows a similar trend in all varying port lead angles. However, Figure 5.16 shows the dead zone increases with increasing angle due to the increase in length of the flat land shown in Figure 5.13.

5.2.3.3 Welding Pressure

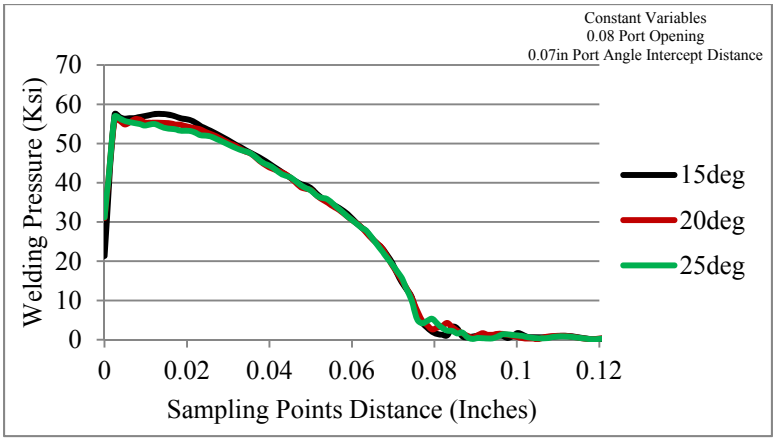

Figure 5.17 Weld pressure vs. port lead angle on welding surface

Figure 5.17 compares the weld pressure with the varying port lead angles on the welding surface. It is observed that the changes in weld pressure pertaining to the port lead angle is very minute, where the welding pressure for 25° port lead angle is 53.75 ksi, 20° port lead angle is approximately 55.14 ksi and 15° port lead angle is approximately 57.24 ksi. This trend of weld pressure observed at the entrance of the port opening on the welding surface is characterized by high effective stress and small dead zone of aluminum flow due to the increase of the port lead angle.

5.2.4 Effect of Angle Intercept Distance

The purpose of the port angle intercept distance is to hypothetically mark the point at which welding will commence in the port opening. This gives the die designer a rough idea of how big the dead metal zone will be in the port opening thus predicting weld formations.

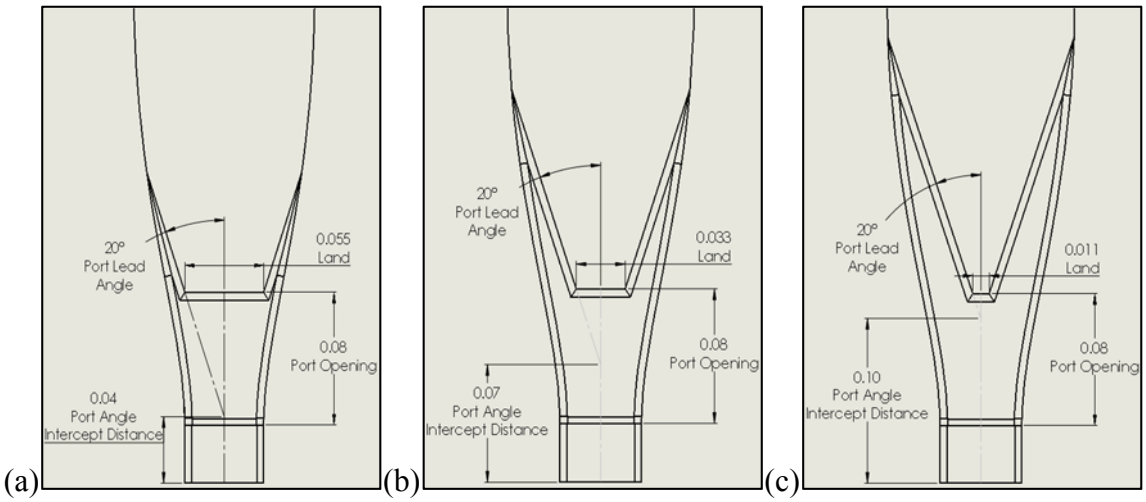

Figure 5.18 Angle intercept distance; (a) 0.04inch; (b) 0.07inch and (c) 0.1inch

Figure 5.18 shows the CAD geometry of the mandrel with varying angle intercept distance. It is observed that the length of the land increases that is 0.055 inches for 0.04 inch angle intercept distance, 0.033 inches for 0.07 inch angle intercept distance and 0.011 inches for 0.1 inch angle intercept distance.

5.2.4.1 Effective Stress

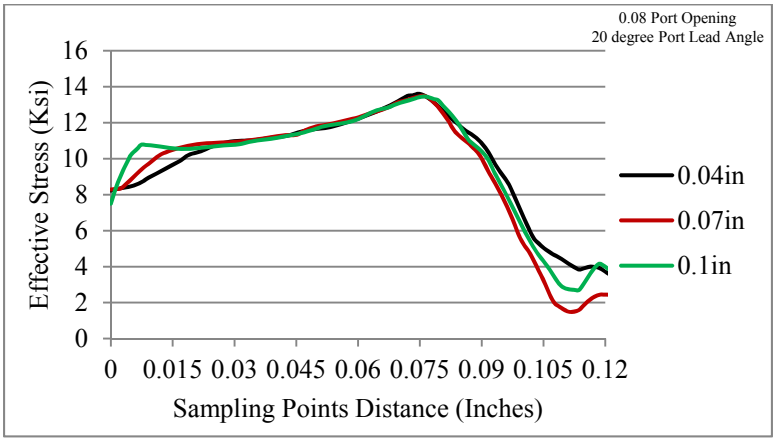

Figure 5.19 Effective stress vs. angle intercept distance on welding surface

Figure 5.19 compares the effective stress of aluminum by varying the angle intercept distance. The first peak in the effective stress graph marks the onset of the main

welding zone. It is observed that the length of the dead zone decreases as the angle intercept distance increases, whereas the length of the die bearing zone decreases.

5.2.4.2 Material Velocity

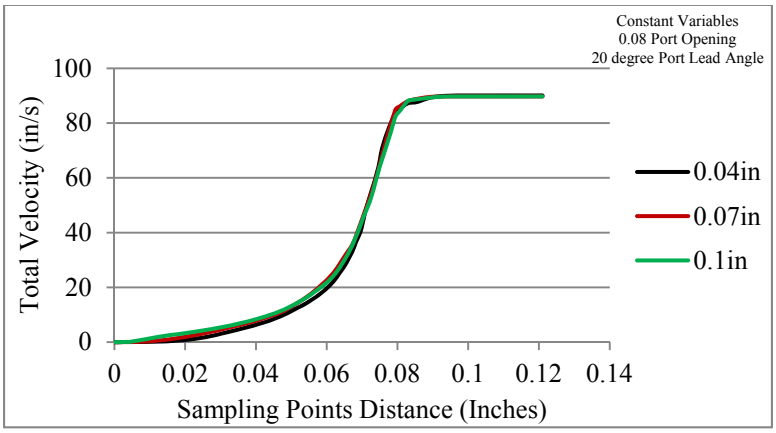

Figure 5.20 Velocity vs. angle intercept distance on welding surface

Figure 5.20 compares the velocity of aluminum by varying the angle intercept distance. It is observed that angle intercept distance does not significantly affect the aluminum velocity distribution. The 0.1inch angle intercept distance has the smallest land length shown in Figure 5.18; therefore, when comparing the aluminum flow in Figure 5.21 it is observed that the dead metal zone is the smallest for 0.1inch angle intercept distance and is the biggest for 0.04inch angle intercept distance.

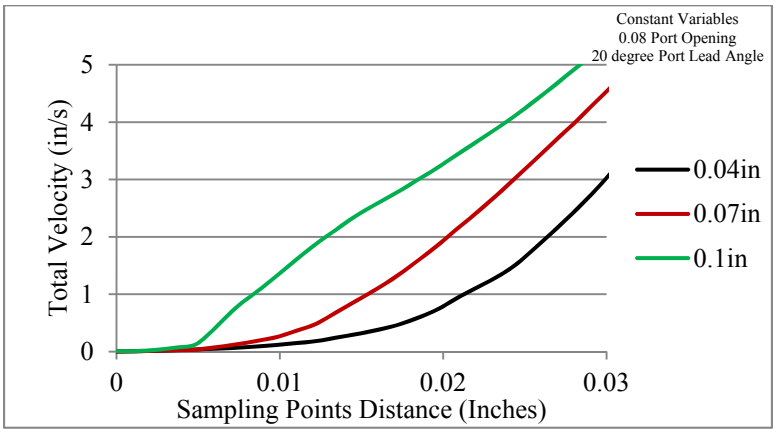

Figure 5.21 Velocity in dead zone vs. angle intercept distance on welding surface

5.2.4.3 Welding Pressure

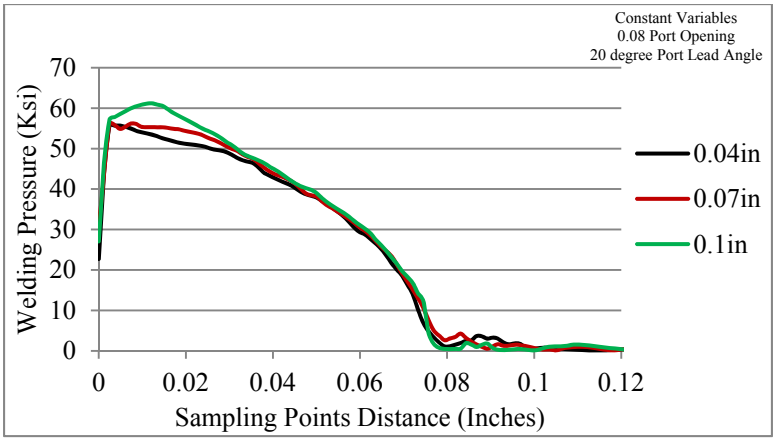

Figure 5.22 Weld pressure vs. angle intercept distance on welding surface

Figure 5.22, compares the weld pressure on the welding surface with varying angle intercept distance. The 0.1 inch angle intercept distance has a higher welding pressure of 60.56 ksi due to the combined effect of relatively high effective stress at the entrance of the port opening on the welding surface and a very small dead zone observed in the aluminum flow. The welding pressure observed for 0.07 inch angle intercept is 55.29 ksi and 0.04 inch angle intercept distance is 53.48 ksi. The maximum welding pressure achieved by the 0.1inch angle intercept distance is due to the smallest length of land, thus leading to the formation of a very small dead zone and a relatively long main welding zone.

5.2.5 Statistical Summary

A full factorial design of experiments was conducted and statistically analyzed using Minitab, to investigate the effects of mandrel port opening length, port lead angle and angle intercept distance on weld pressure. A main effects plot is an efficient visual tool in Minitab that summarizes the effect of each independent geometric parameter examined in all 27 mandrel DOE's

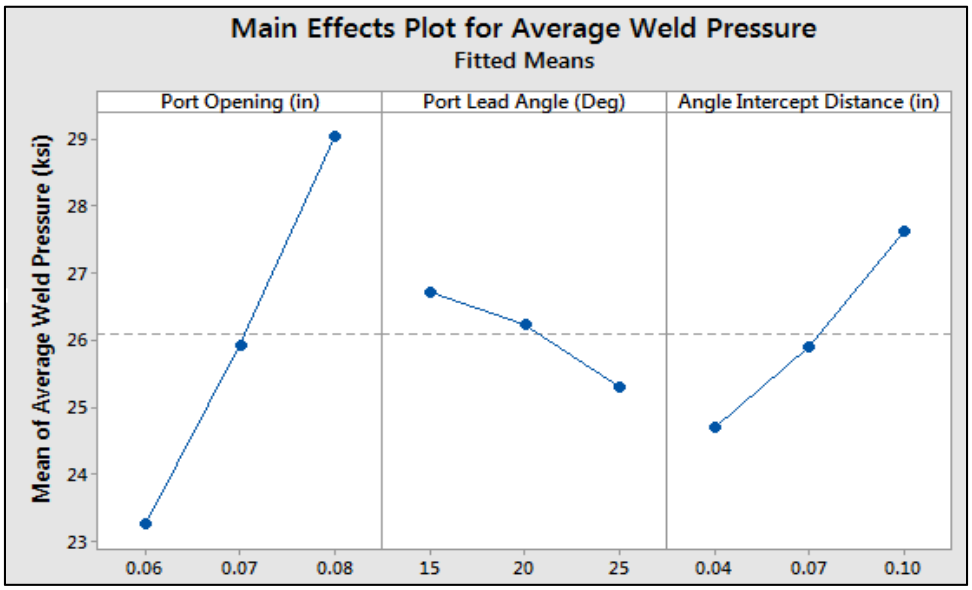

Figure 5.23 Main effects plot for average weld pressure

Figure 5.23 shows the main effects plot generated by analyzing the mean values of weld pressure at each level of varying port opening length, port lead angle and angle intercept distance. For example the mean weld pressure is 23.27 ksi for all 9 possible combinations of mandrel DOE with 0.06inch port opening length The average value of weld pressure for all 27 mandrel DOE's is 26.09 ksi, which is represented as a horizontal dashed line shown in the main effects plot. The left and right panel in the main effects plot indicates that increasing the length of the port opening and the angle intercept distance increases the weld pressure. However, the middle panel in the main effects plot indicates an inverse effect on the weld pressure which decreases as the port lead angle increases.

Although, the information provided by the main effects plot help guide the intuition of the die designer it is important to know which ones out of the three mandrel geometric parameters have a significant effect on welding pressure. To understand which mandrel geometric factors significantly affects the response of the weld pressure we compare the probability values also known as P-value generated through the full factorial analysis in Minitab. The definition of a P-value is the probability of either accepting or

rejecting a null hypothesis based on the threshold of a confidence interval which is typically 95% or a significance interval (α) of 0.05.

$$Confidence\ Interval = 100(1-\propto)\% \tag{5.3}$$

Source	P-Value
Model	0.000
Linear	0.000
Port Opening (in)	0.000
Port Lead Angle (Deg)	0.000
Angle Intercept Distance (in)	0.000
2-Way Interactions	0.001
Port Opening (in)*Port Lead Angle (Deg)	0.652
Port Opening (in)*Angle Intercept Distance (in)	0.000
Port Lead Angle (Deg)*Angle Intercept Distance (in)	0.012

Figure 5.24 Minitab general factorial regression model probability value

Figure 5.24 shows the P-value of all independent factors and their two-way interactions. It is observed that port opening length, port lead angle and angle intercept distance are statistically significant factors as their P-values are less than 0.05 as well as, the interaction of port opening and angle intercept distance. This means that changing any of these parameters has a significant effect on weld pressure.

5.3 Die Cartridge DOE Results

The die cartridge design of experiments were conducted in Deform 3D using a quarter domain model shown in Figure 5.25 which was established earlier in Section 5.

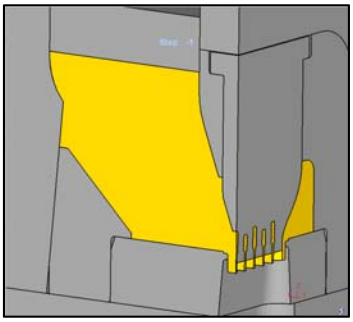

Figure 5.25 Die cartridge DOE quarter domain model

The main objective of this study is to investigate the effects of angle guide curve, die plate covering and bridge mandrel angle on the deformation of the mandrel teeth, particularly in the radius of the port opening entrance where previous failure modes were observed. Therefore, to evaluate the effects of the die cartridge geometric parameters in Minitab; an average value of effective-stress distribution for all 27 die cartridge DOE's was obtained through a top and bottom slicing plane histogram at the entrance of the port opening (Figure 5.26).

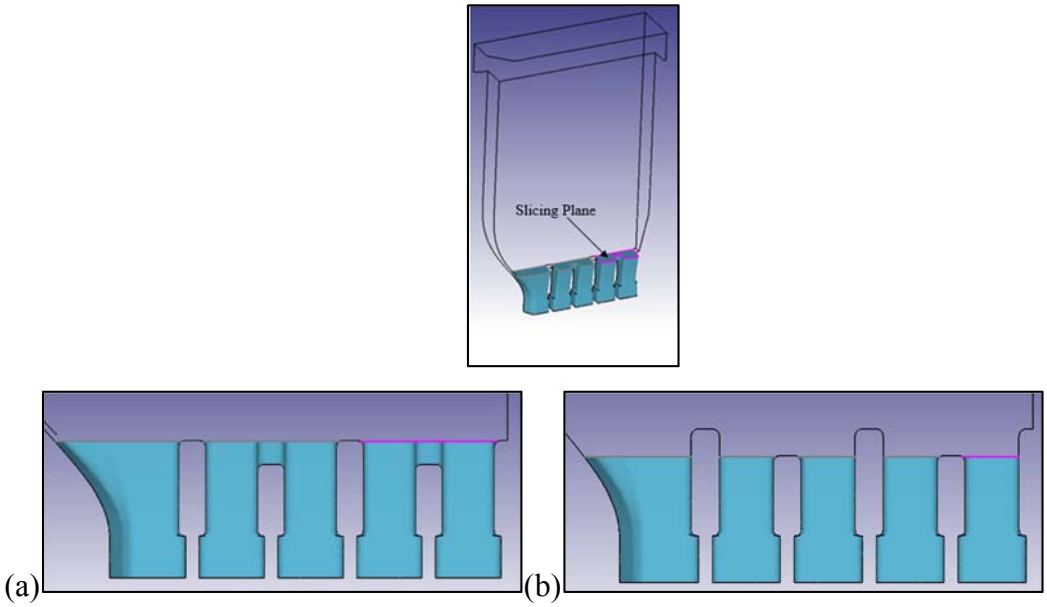

Figure 5.26 Slicing plane used to measure mandrel teeth stress; (a) top slicing plane and (b) bottom slicing plane

5.3.1 Validation

In order to validate the results of the die cartridge DOE, the aluminum velocity profile within the modular die was compared to the literature results found in Mooi et al. [61]; as well as, the etched surface of the modular die filled with aluminum obtained through a previous die trial run provided by an extrusion company.

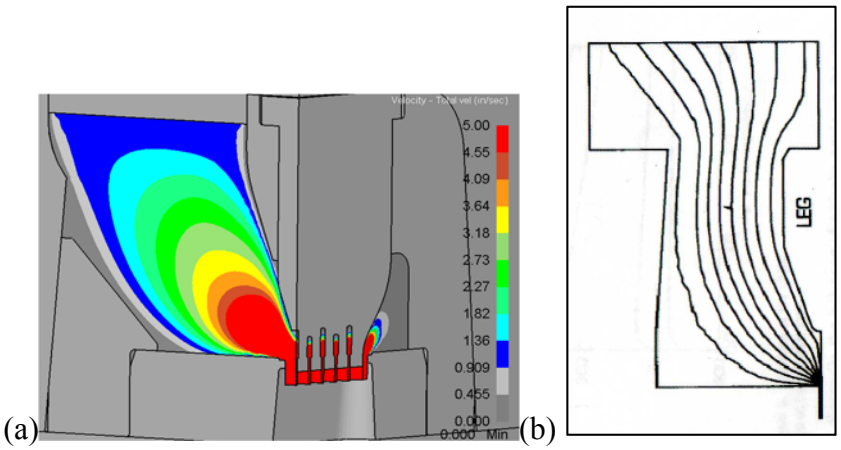

(a) (b)

Figure 5.27 (a) Aluminum velocity profile through the modular die and (b) velocity streamline around leg (reproduced from [61])

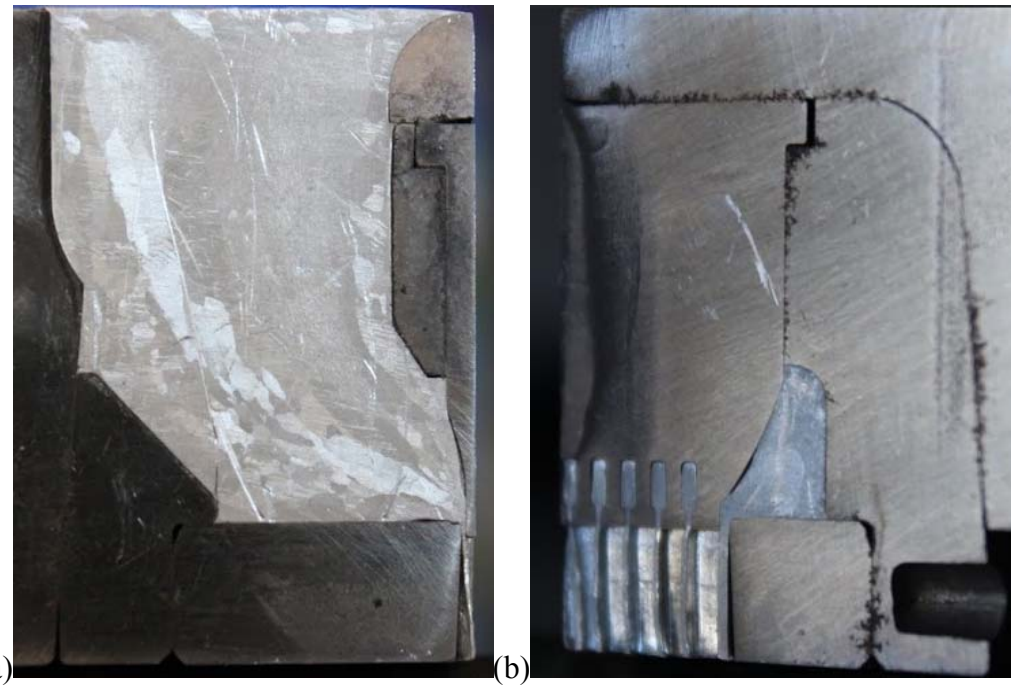

(a) (b)

Figure 5.28 Etched surface of aluminum filled modular die; (a) side view cross section and (b) front view cross section

Figure 5.27a show the velocity profile of aluminum through the modular die. From Figure 5.27b it is observed that aluminum sticks to the tooling components and flows faster in the center. A similar observation is made through the etched surface of aluminum filled modular die in Figure 5.28. The results from the simulation work done

by Mooi et al. [61] and the etched surface are in good agreement with the velocity profile generated through Deform 3D die cartridge DOE simulation.

5.3.2 Effect of Angle Guide Curve

The purpose of the Angle Guide Curve (AGC) is to help create a tapered surface to allow the die cartridge to seal better with the holder while guiding the flow of aluminum towards the mandrel.

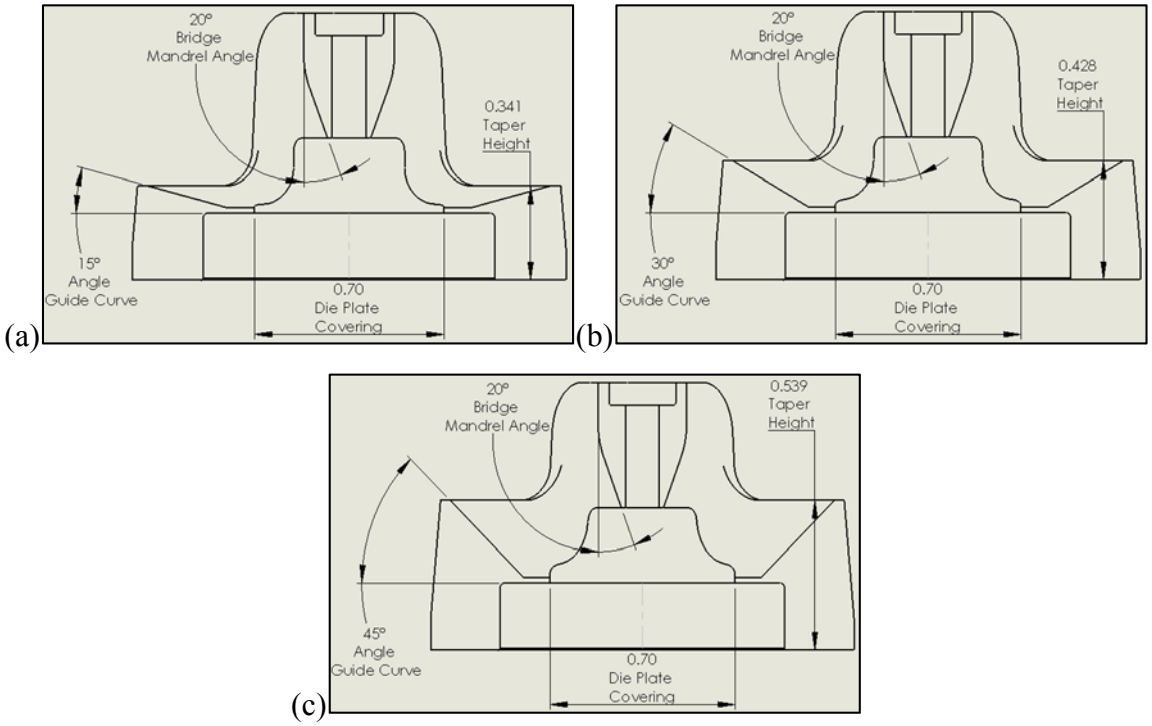

Figure 5.29 Angle guide curve; (a) 15°; (b) 30° and (c) 45˚

Figure 5.29 shows the difference in angle guide curve of the die cartridge CAD geometry. It is observed that decreasing the angle guide curve causes the taper height to decreases, thus the die cartridge with the 15˚ AGC will not seal as well as the 45˚ AGC.

5.3.2.1 Extrusion Load

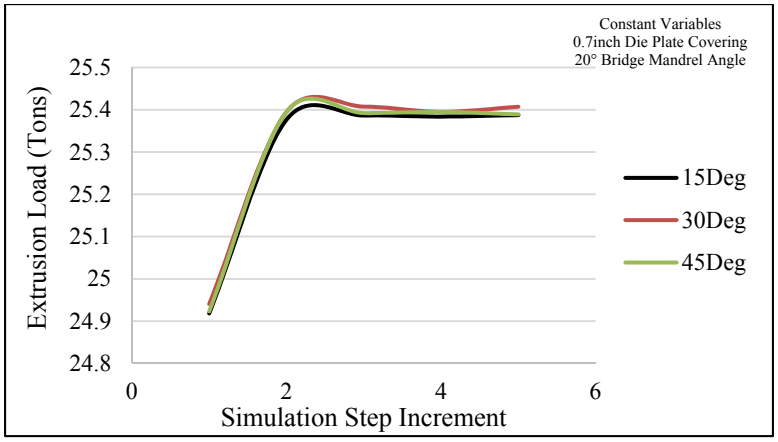

Figure 5.30 Extrusion load vs. varying angle guide curve; (a) 15°; (b) 30° and (c) 45°

Figure 5.30 compares the forces required by the ram to push the aluminum through the modular die with varying degrees of the angle guide curve. It is observed that variation of the angle guide curve has a minuscule effect on the extrusion load.

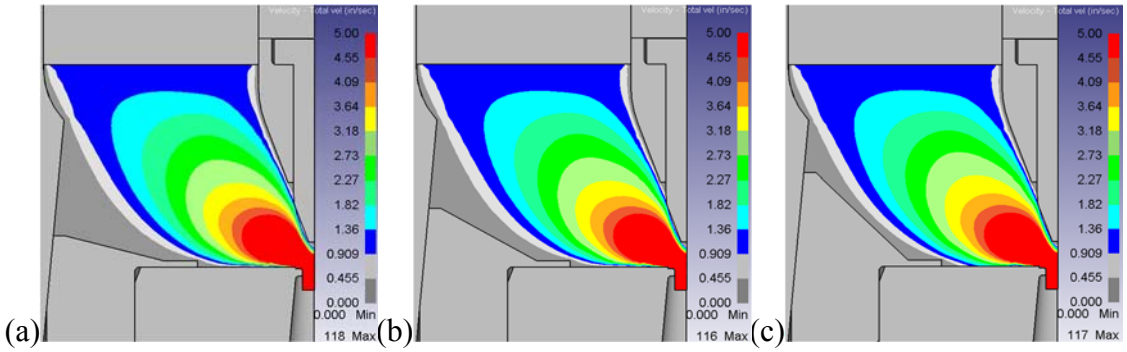

(a) (b) (c)

Figure 5.31 Aluminum velocity profile vs. varying angle guide curve; (a) 15°; (b) 30°; and (c) 45°

Figure 5.31 shows the velocity of extruding aluminum though the modular die. The areas in grey have a relatively slow velocity in the range of 0 in/s – 1 in/s; commonly known as the dead metal zone It is observed that the dead metal zone formed in the 15 degree angle guide curve is the largest whereas, it is the smallest in the 45° angle guide curve die cartridge.

Although, the volume of aluminum being pushed through the modular die increases with decreasing the angle, the velocity profile of aluminum through the modular die remains the same, while the volume of dead metal zone changes. This constant flow of aluminum with varying dead metal zones helps achieve a constant extrusion load, a similar observation has been made by Mahmoodkhani et al. [65]. Therefore, it can be concluded that varying the angle between 15° and 45° has a miniscule effect on the extrusion load; however, if the angle were to increase above 45° then it can be anticipated that the extrusion load will increase due to the constriction in aluminum flow.

5.3.2.2 Mandrel Effective Stress

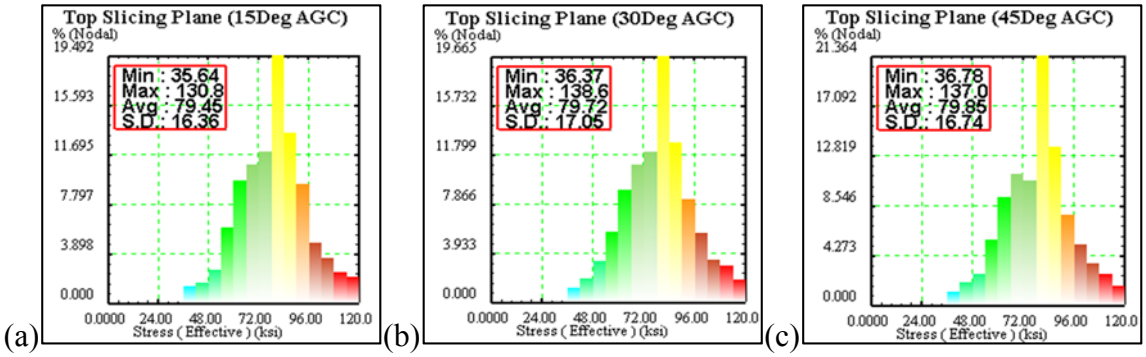

Figure 5.32 Mandrel effective stress histogram on top slicing plane Vs. varying angle guide curve; (a) 15°; (b) 30° and (c) 45°

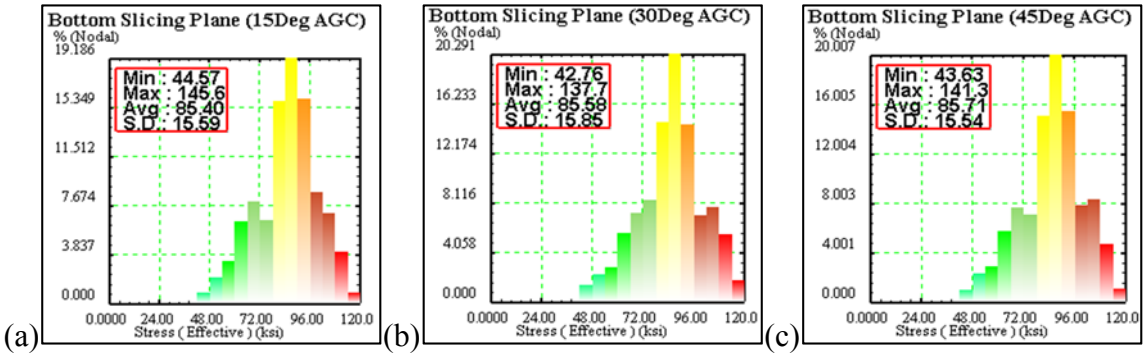

Figure 5.33 Mandrel effective stress histogram on bottom slicing plane vs. varying angle guide curve; (a) 15°; (b) 30° and (c) 45°

Figure 5.32 and 5.33 shows the histogram of the mandrel effective stress on the top and bottom slicing plane due to the varying angle guide curve of the die cartridge. It is observed that there is a maximum of 0.5% difference in effective stress; caused by the varying angle guide curve of the die cartridge on the mandrel teeth, which is very miniscule. However, comparing the histogram results of the top and bottom slicing planes it is noticed that the average effective stress of the bottom plane is 7.07% higher than the top plane. This behavior of a higher effective stress observed in the bottom slicing plane is due to the deflection of the longer mandrel tooth caused by the flow of aluminum.

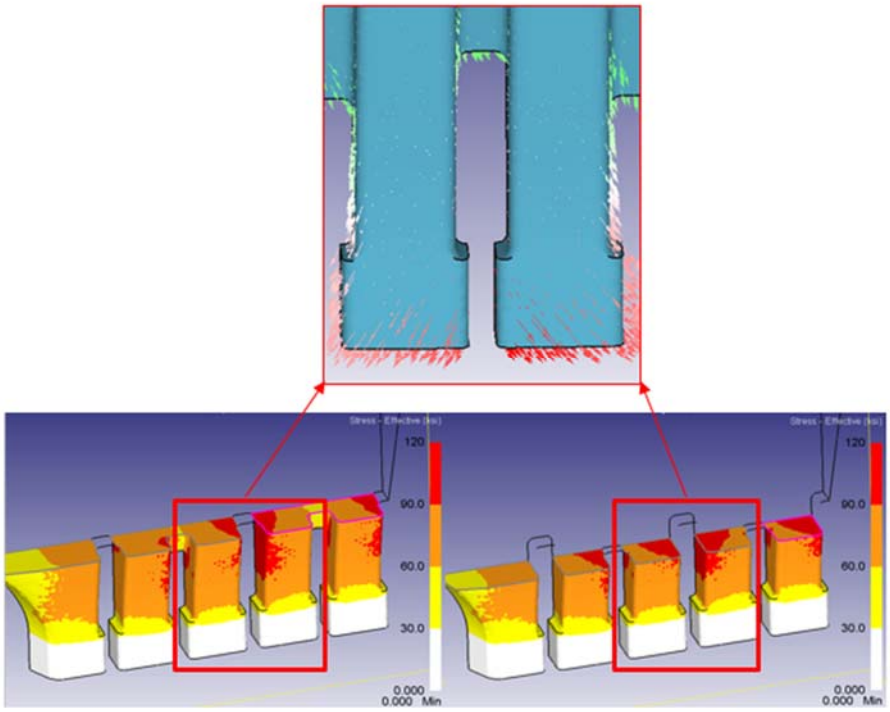

Figure 5.34 Mandrel teeth effective stress distribution due to displacement of teeth

5.3.3 Effect of Die Plate Covering

The purpose of the die plate covering is to cover the coating layer of the die plate from being worn away during the extrusion process.

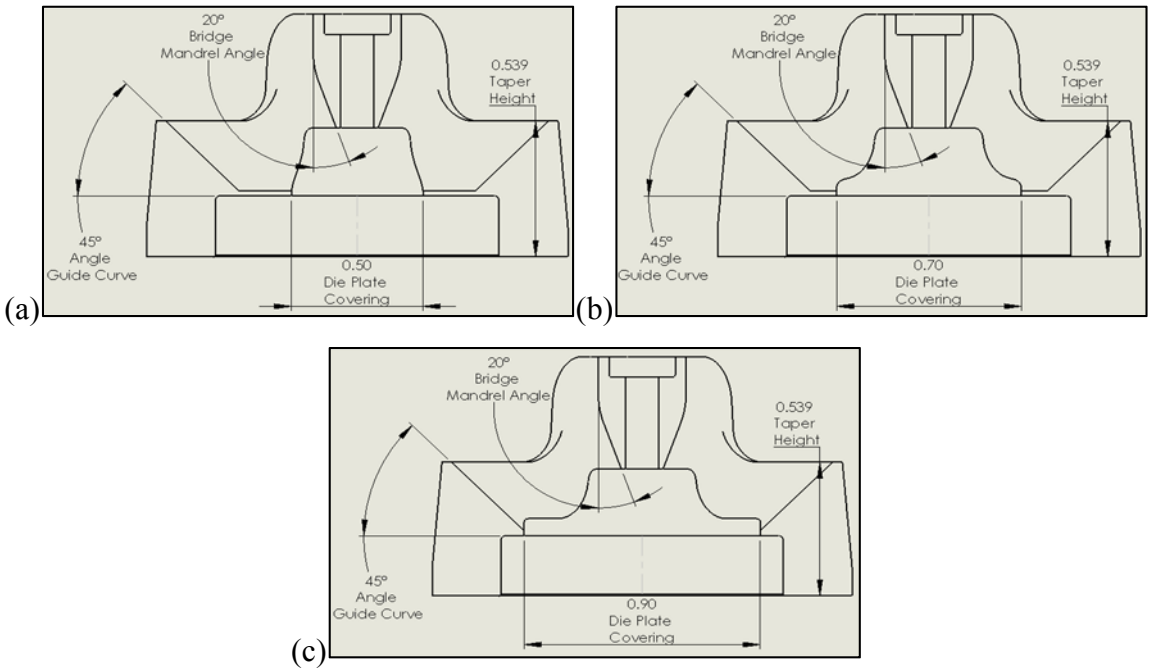

Figure 5.35 Die plate covering; (a) 0.5 inch; (b) 0.7 inch and (c) 0.9 inch

Figure 5.35 shows the difference in die cartridge CAD geometry with varying die plate covering dimensions utilized for the die cartridge design of experiments. Decreasing the length of the die plate covering increases the amount of die plate surface being covered during the extrusion process.

5.3.3.1 Extrusion Load

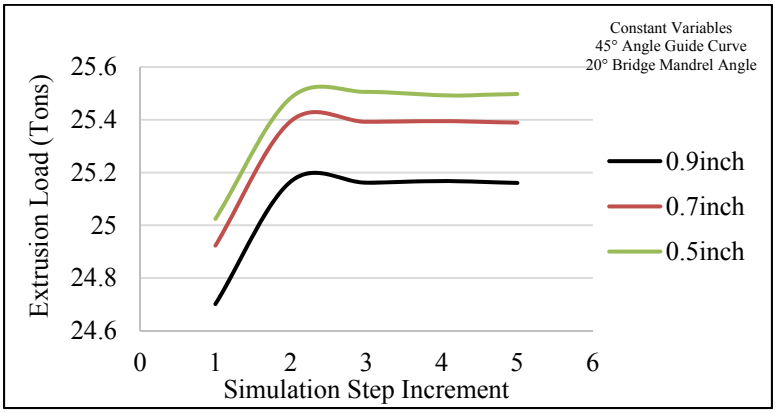

Figure 5.36 Extrusion load vs. die plate covering

Figure 5.36 compares the extrusion load required to push aluminum through the modular die by varying the die plate covering length. It is observed the highest extrusion force of 25.5 tons is required to push aluminum through the 0.5 inch die plate covering whereas, approximately 25.18 tons is required to push aluminum through 0.9 inch die plate covering of the modular die cartridge. Although the variation of extrusion force is miniscule, an inversely proportional behavior of die plate covering length and extrusion force is observed.

From Figure 5.37 it is observed that an increase in extrusion load is directly related to the flow of aluminum within the modular die. The 0.5 inch DPC length interrupts the flow of aluminum leading to the development of a smaller dead metal zone area as compared to the uninterrupted flow and larger dead metal zone area observed in the 0.9 inch DPC velocity profile. Therefore, the highest extrusion load is observed for the 0.5 inch DPC.

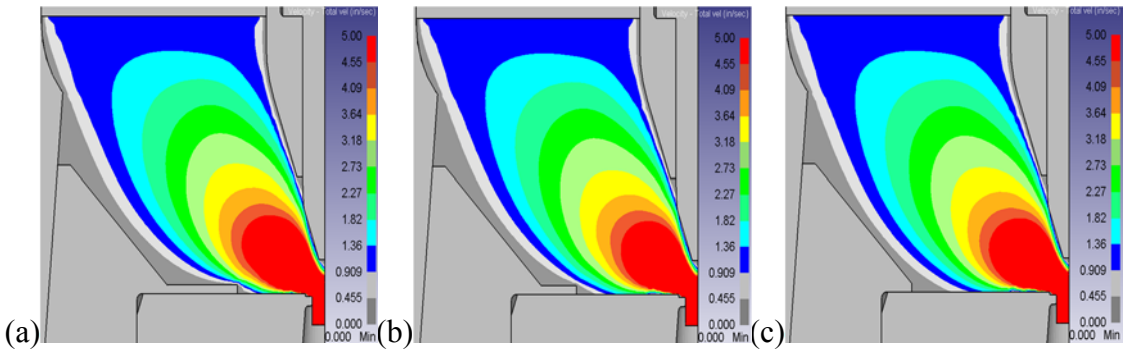

Figure 5.37 Aluminum velocity profile vs. die plate covering; (a) 0.5 inch; (b) 0.7 inch and (c) 0.9 inch

5.3.3.2 Mandrel Effective Stress

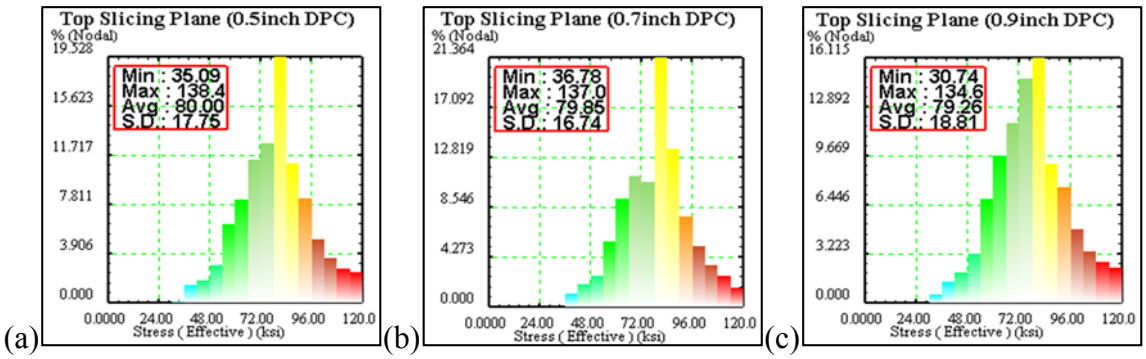

Figure 5.38 Mandrel effective stress histogram on top slicing plane vs. die plate covering; (a) 0.5 inch; (b) 0.7 inch and (c) 0.9 inch

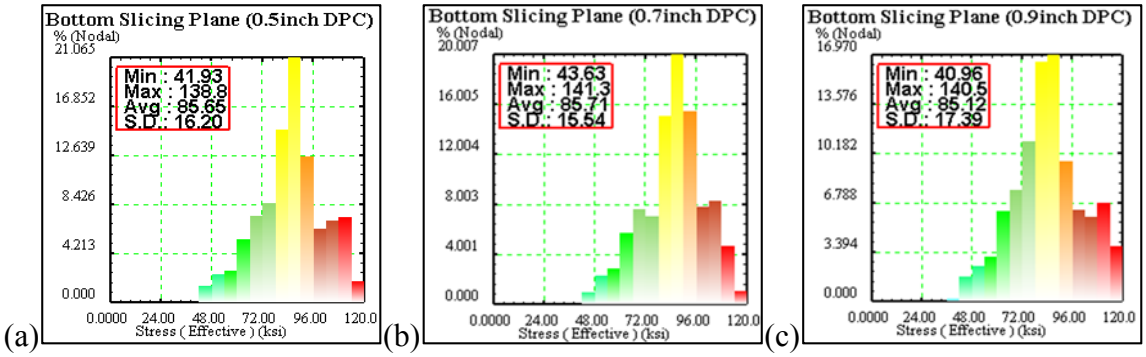

Figure 5.39 Mandrel effective stress histogram on bottom slicing plane vs. die plate covering; (a) 0.5 inch; (b) 0.7 inch and (c) 0.9 inch

Figure 5.38 and 5.39 compares the effective stress histogram on the top and bottom slicing plane of the mandrel due to the varying die plate covering lengths of the die cartridge. Similar to the extrusion load trend, it is observed that the 0.5 inch and 0.7 inch DPC length leads to a higher magnitude of average effective stress whereas, the 0.9 inch DPC length has the lowest value of average effective stress on the mandrel port opening.

5.3.4 Effect of Bridge Mandrel Angle

The purpose of the Bridge Mandrel Angle (BMA) is to guide the flow of aluminum towards the mandrel.

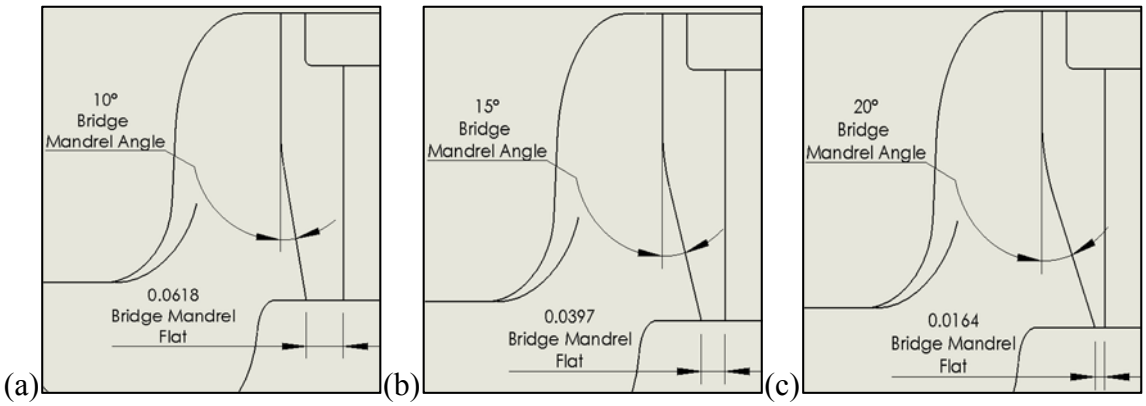

Figure 5.40 Bridge mandrel angle; (a) 10°; (b) 15° and (c) 20°

Figure 5.40 shows the CAD geometry of the die cartridge with varying Bridge Mandrel Angle (BMA), dimensioned from the vertical line of the die cartridge bridge. It is observed that the Flat at the end of the bridge mandrel increases in length when the bridge mandrel angle decreases. The length of the bridge mandrel flat for, 20° BMA is 0.0164 inch, 15° BMA is 0.0397 inch and 10° BMA is 0.0618 inch.

5.3.4.1 Extrusion Load

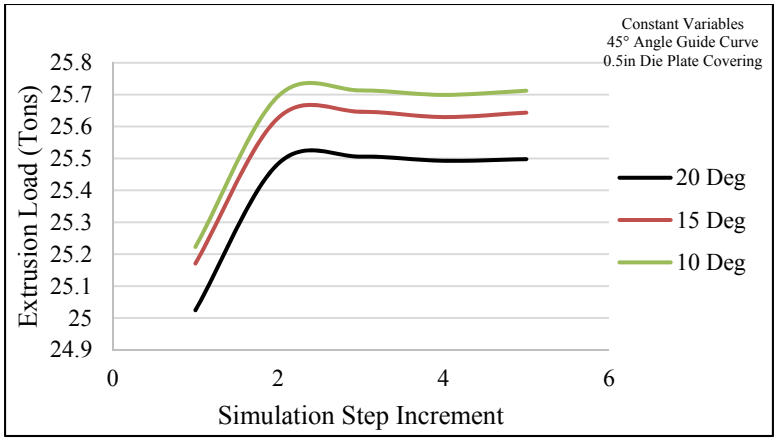

Figure 5.41 Extrusion load vs. bridge mandrel angle

Figure 5.41 compares the extrusion load required to extrude aluminum through the modular die by varying the bridge mandrel angle. Although, the variation in extrusion

load is miniscule it is observed that the extrusion load for 10° BMA is 25.4 tons, 15° BMA is 25.23 tons and 20° BMA is 25.16 tons.

As mentioned earlier, extrusion load is directly related to the flow of aluminum through the modular die. In Figure 5.42 it is observed that decreasing the bridge mandrel angle causes the length of the flat surface at the end of the bridge to increase, thus interrupting the flow path of aluminum in the modular die which leads to an increase in extrusion load. Another observation made is that the area of the dead metal zone increase due to the increase in length of the bridge mandrel flat. A larger dead metal zone creates a smaller area for the aluminum to flow through which results in an increase of extrusion load. Therefore, it can be summarized that an increase in bridge mandrel angle reduces the extrusion load.

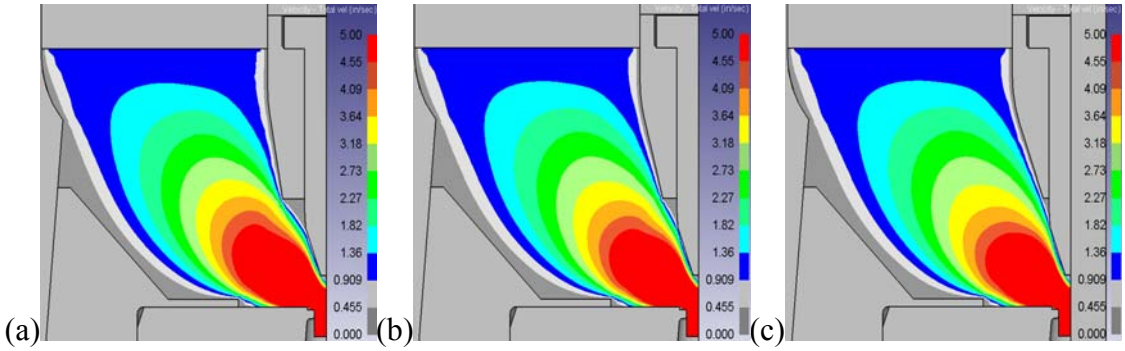

Figure 5.42 Aluminum velocity profile vs. bridge mandrel angle; (a) 10°; (b) 15° and (c) 20°.

5.3.4.2 Mandrel Effective Stress

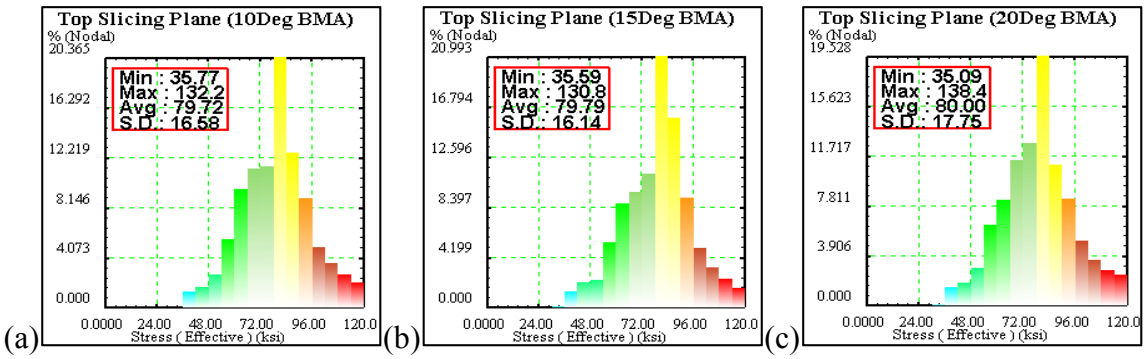

Figure 5.43 Mandrel effective stress histogram on top slicing plane vs. bridge mandrel angle; (a) 10°; (b) 15° and (c) 20°.

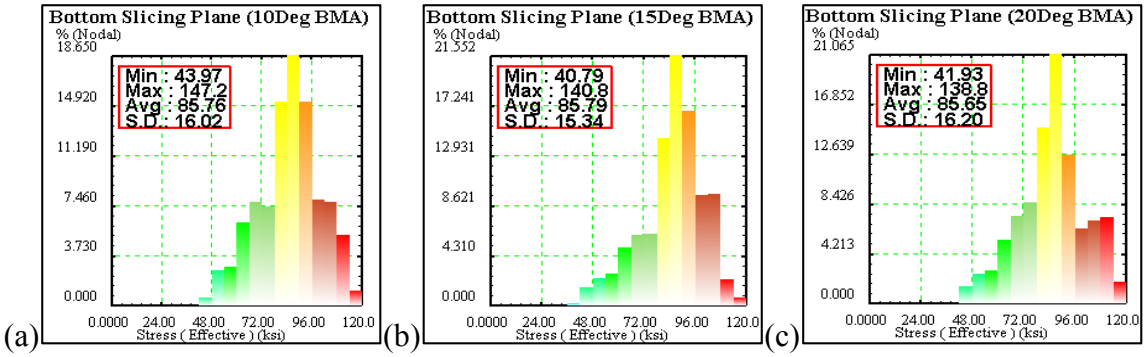

Figure 5.44 Mandrel effective stress histogram on bottom slicing plane vs. bridge mandrel angle; (a) 10°; (b) 15°; and (c) 20°.

Figure 5.43 and 5.44 compares the effective stress histogram on the top and bottom slicing plane of the mandrel by varying the bridge mandrel angle. It is observed that the mandrel effective stress on the top slicing plane is 79.72 ksi for 10° BMA, 79.79 ksi for 15° BMA and 80.00 ksi for 20° BMA, whereas, the effective stress observed on the bottom slicing plane is 85.76 ksi for 10° BMA, 85.79 ksi for 15° BMA and 85.65 ksi for 20° BMA. It is noticed that the decreasing the bridge mandrel angle causes a bigger dead metal zone to form which protects the mandrel from being deformed. However, the difference in average effective stress observed in both the top and bottom slicing plane due to varying angles of the bridge mandrel is very minute.

5.3.5 Statistical Summary

A full factorial design of experiments was conducted and statistically analyzed using Minitab, to help the die designer understand how stress distribution in the mandrel teeth is affected by changing the geometric parameters of the die cartridge.

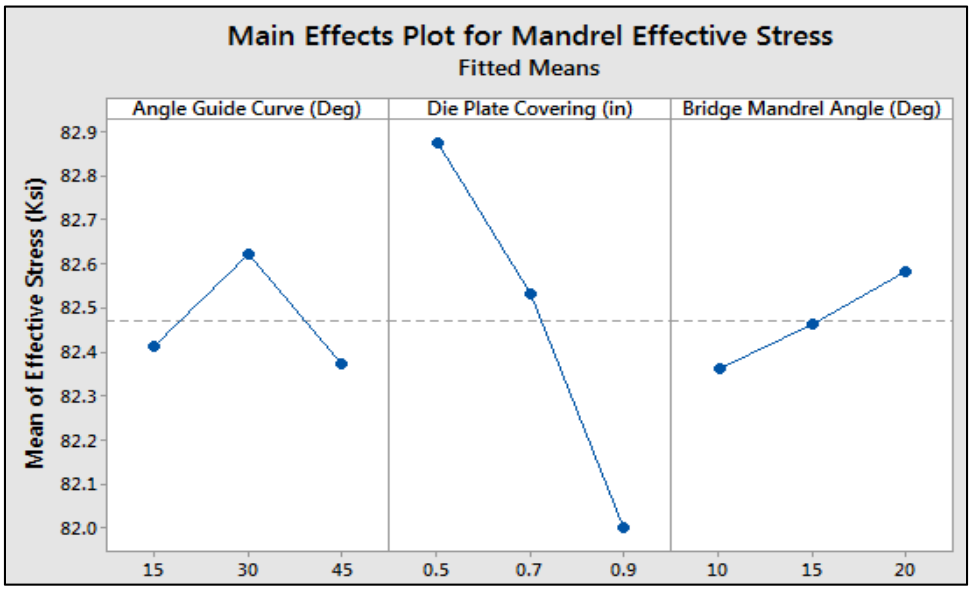

Figure 5.45 Main effects plot for mandrel effective stress

Figure5.45 shows the main effects plot for mandrel effective stress, which has been generated in Minitab by analyzing the mean values of effective stress for all 27 DOE's, at each level of varying angle guide curve, die plate covering and bridge mandrel angle of the die cartridge. In the left panel of the main effects plot, it is observed that the effective stress at 15° and 45° angle guide curve is lower than the effective stress of 30° angle guide curve. In the middle panel, it is observed that covering more surface area of the die plate leads to a higher effective stress of the mandrel teeth. In the right panel of the main effects plot, it is observed that effective stress increases as the bridge mandrel angle increases. It is observed from the main effects plots that increasing the length or angle of the three geometric parameters minutely increases or decreases the effective stress of the mandrel as the range of the effective stresses is approximately 1 ksi.

Source	P-Value
Model	0.056
Linear	0.005
Angle Guide Curve (Deg)	0.209
Die Plate Covering (in)	0.001
Bridge Mandrel Angle (Deg)	0.315
2-Way Interactions	0.856
Angle Guide Curve (Deg)*Die Plate Covering (in)	0.532
Angle Guide Curve (Deg)*Bridge Mandrel Angle (Deg)	0.705
Die Plate Covering (in)*Bridge Mandrel Angle (Deg)	0.962

Figure 5.46 Statistical significance of parameters affecting the mandrel effective stress

Based on the probability values generated through the general factorial regression model shown in Figure 5.46 for mandrel effective stress. It is observed that probability value (P-Value = 0.001 < 0.05) of the die plate covering has a significant effect on the mandrel effective stress as compared to the angle guide curve (P-Value = 0.209 > 0.05) or the bridge mandrel angle (P-Value = 0.315 > 0.05).

5.4 Optimization

This main focus of this section is the optimization of the mandrel and die cartridge design geometrical parameters using the Minitab response optimizer.

5.4.1 Mandrel Optimization

The optimization problem formulation for the Mandrel design of experiments is to maximize the weld pressure on the welding surface by finding an optimum combination of geometric parameter of the port opening (PO), port lead angle (PLA) and angle intercept distance (AID). The objective function for weld pressure is calculated in deform using the minimum work rate principle Equation (2.9).

$$\text{Maximize: Weld Pressure } f(PO, PLA, AID)$$
$$Contraints: 0.06 \leq PO \leq 0.08\ (inch)$$
$$15° \leq PLA \leq 25°\ (degree)$$
$$0.04 \leq PAID \leq 0.1\ (inch)$$

Once, the average value of the weld pressure on the welding surface was inputted into Minitab for all 27 design of experiments. The Minitab DOE response optimizer was utilized to find a combination of port opening, port lead angle and port angle intercept distance that would maximize the welding of the MMP tube on the welding plane.

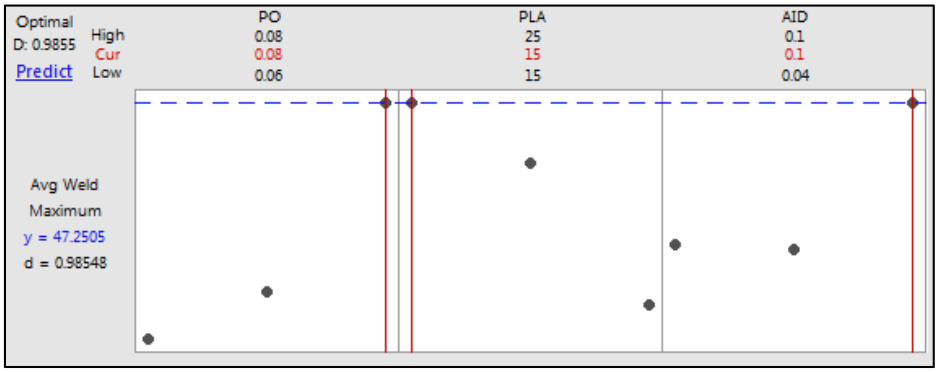

Figure 5.47 Mandrel DOE Minitab optimized response

Figure 5.47 shows 0.08 inch port opening 15° port lead angle and 0.1 inch angle intercept distance as the calculated optimized response combination for the mandrel geometric parameters that results in a maximum weld pressure of 47.2505 ksi. This optimized combination calculated in Minitab through the full factorial analysis of welding pressure for all the 27 mandrel design of experiments has a 98.54% accuracy of satisfying the optimization goal for maximizing welding pressure

5.4.1.1 Kriging Optimization

The kriging optimization technique was used to obtain the global maximum of weld pressure based on the unknown values within the discretized domain of the conducted design of experiments.

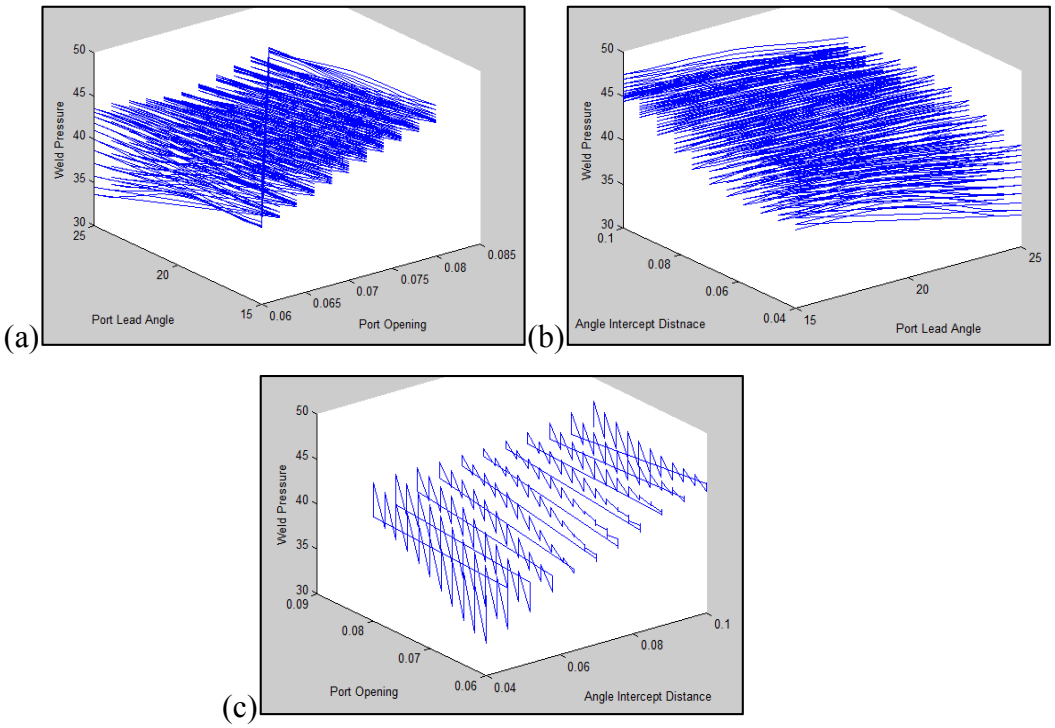

Figure 5.48 Continuous welding pressure kriging function; (a) port lead angle and port opening; (b) angle intercept distance and port lead angle and (c) port opening and angle intercept distance.

Figure 5.48 shows the continous kriging function predicted for each DOE parameter with respect to weld pressure.The optimum combination of port opening is 0.08 inch, port lead angel 15° port lead angle and 0.1 inch angle intercept distance that results with a maximum weld pressure of 47.4516 ksi. The results obtained from the kriging function match the results of the response optimization method. Thus, it is validated that the geometric parameters mentioned results in a global maximum of weld pressure.

5.4.2 Die Cartridge Optimization

The optimization problem formulation for the Die Cartridge design of experiments is to minimize the stress in the mandrel by finding an optimum combination of the angle guide curve (AGC), die plate covering (DPC) and bridge mandrel angle

(BMA). The objective function for minimization of mandrel stress is obtained through the force traction integral of the minimum work rate principle Equation (2.9) calculated in deform.

$$\text{Minimize: Mandrel Stress } f(AGC, DPC, BMA)$$
$$subject\ to: 15° \leq AGC \leq 45° \ (degree)$$
$$0.5 \leq DPC \leq 0.9 \ (inch)$$
$$10° \leq BMA \leq 20° \ (inch)$$

Deformation or die stress of the mandrel occurs due to the flow of aluminum through the modular die which is mainly influenced by the geometrical parameters of the die cartridge. The average value of the effective stresses generated on the top and bottom slicing planes of the mandrel for all 27 die cartridge design of experiments were inputted into the Minitab DOE response optimizer to find an optimum combination of the angle guide curve, die plate covering and bridge mandrel angle that would minimize the deformation of the mandrel during the extrusion of MMP tubes.

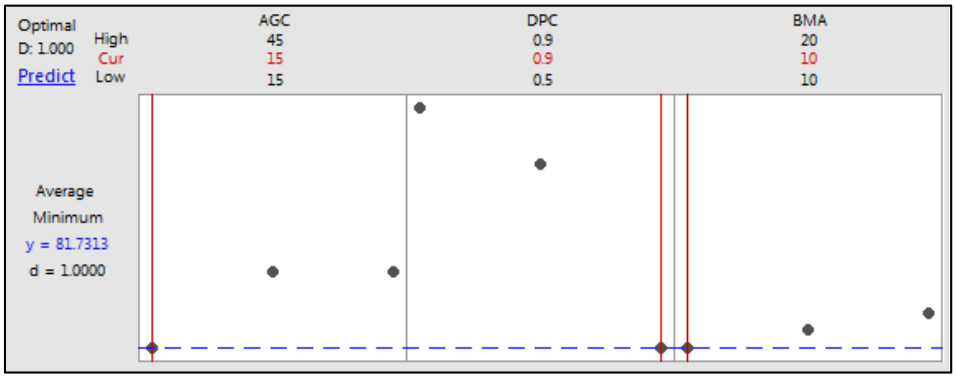

Figure 5.49 Die Cartridge DOE Minitab optimized response.

Figure 5.49 shows the optimization plot for the die cartridge geometrical parameters generated in Minitab through the full factorial analysis of the average effective stress in the mandrel top and bottom slicing plane. The optimized combination of 15° angle guide curve, 0.9 inch die plate covering and 10° bridge mandrel angle, calculated by Minitab has 95.46% accuracy, that will result in a minimum effective stress of 81.7313 ksi which is lower than the yield strength of H-13 tool steel (120 ksi @ 900°F)

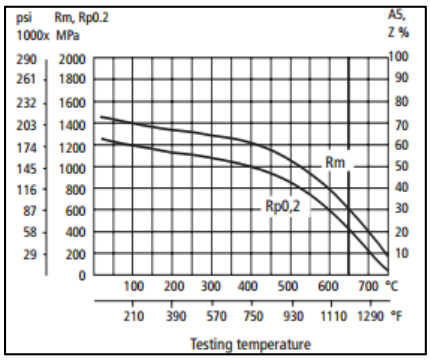

Figure 5.50 H-13 Tool steel strength at elevated temperature (reproduced from [66])

5.4.2.1 Kriging Optimization

The kriging optimization technique was used to obtain the global minimum of effective stress based on the unknown values within the discretized domain of the conducted die cartridge design of experiments.

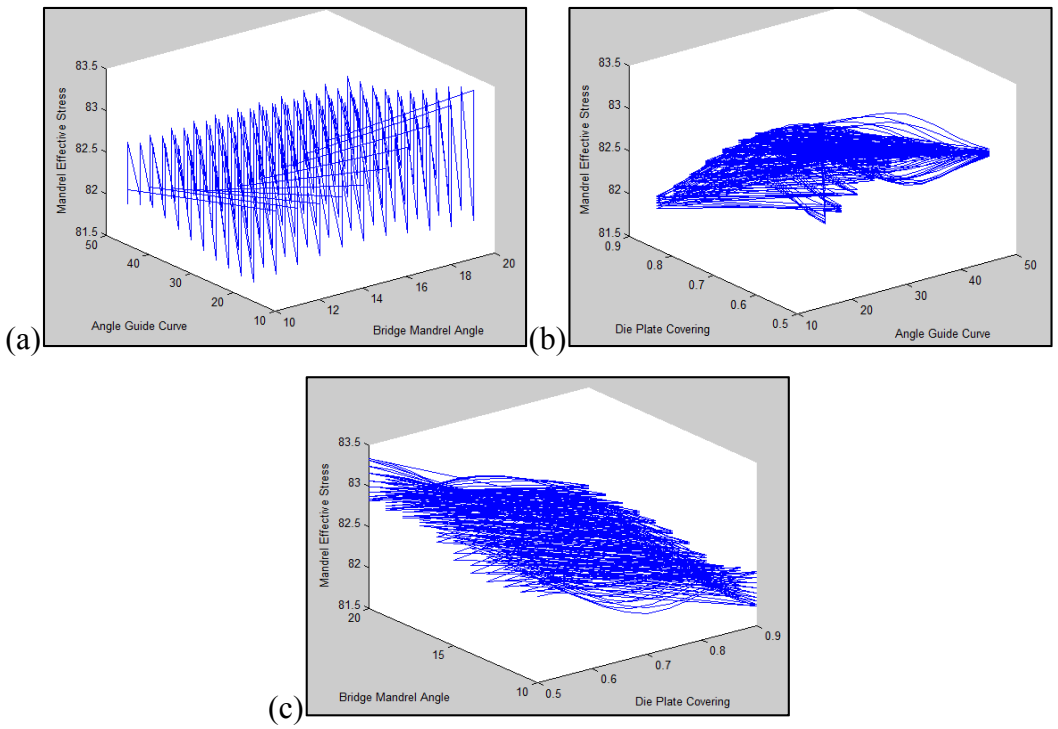

Figure 5.51 Continuous effective stress kriging function; (a) angle guide curve and bridge mandrel angle; (b) die plate covering and angle guide curve and (c) bridge mandrel angle and die plate covering.

Figure 5.51 shows the continous kriging function predicted for each die cartridge DOE parameter with respect to mandrel effective stress.The optimum combination of 15.214° angle guide curve, 0.9 inch die plate covering and 10° bridge mandrel angle results in the lowest effective stress of 81.74 ksi. The results obtained from the kriging function show that the true angle guide curve of 15.214° to be the global minimum parameter. However, this parameter cannot be manufactured and is close to the 15° value produced through the response optimization method.

6. CONCLUSION AND RECOMMENDATION

6.1 Conclusion

The main objective of the work presented, was to identify and use a suitable extrusion simulation package that can be used by the die designers, to help them visualize how changing a certain geometric parameter in the die design will influence aluminum flow and deformation of the die tooling components. The main contributions of this work are:

1. A methodological design framework using Deform 3D, a commercial extrusion simulation package was established for the analysis of die stress distribution and aluminum flow through the modular die for the production of AA3003 aluminum alloy Micro-Multiport tubes used for manufacturing of contemporary heat exchange applications.

2. Using the Archards wear model; based on abrasive wear theory. Reliable predictions on the mechanics of wear as well as, amount of wear depth, temperature distribution and stress concentration of each coating layer in the mandrel and die plate were analyzed. It was predicted that the service life of a bilayer coated mandrel is 12.07% higher than the non-coated mandrel, whereas the service life of the coated die plate is 6.63% higher than the non-coated die plate.

3. A design of experiments was conducted to understand the effects and interactions of port opening, port lead angle and port angle intercept distance; of the mandrel CAD geometry on weld pressure, velocity and effective stress of aluminum on the welding surface in the MMP tubes. Using Minitab a statistical analysis software

it was found that port opening and port angle intercept distance have a significant effect on the over quality of weld pressure.

4. A design of experiments was also conducted to understand the effects and interactions of angle guide curve, die plate covering and bridge mandrel angle; of the die cartridge CAD geometry leading to the deformation stresses of the mandrel teeth. Through the statistical analysis conducted for this DOE, it was found that die plate covering has a significant effect on the deformation of the mandrel teeth.

5. The Minitab response optimizer was utilized for the optimization of the geometric parameters for the mandrel and die cartridge. Which was validated by comparing the results with the Kriging optimization that provide the global optimized results.
    a. The optimum combination for the mandrel geometric parameters that resulted in a maximum weld pressure of 47.25 ksi is 0.08inch port opening, 15° port lead angle and 0.1inch angle intercept distance.
    b. The optimum combination for the die cartridge geometric parameters that resulted in a minimum deformation of the mandrel teeth is 15° angle guide curve, 0.9inch die plate covering and 10° bridge mandrel angle. The results of the die cartridge design of experiments ignore the effects of wear on the die plate. Hence 0.9inch die plate covering is feasible.

The main conclusion that can be drawn from this research is that extrusion die designers in the industry should not only rely on their intuition, personal judgment and experience when designing a die; they should rather validate their intuitions through the means of finite element simulations in order to have a better analytical and scientific understanding on the cause and effect of all the geometric parameters that define the die design.

6.2 Recommendations

Some of the recommended work that can be done in the future for further improvement of the modular die are:

1. Experimental Validation
    - To confirm the accuracy of the simulated results it necessary to conduct similar extrusion trials in a laboratory environment to record and compare, weld pressure, extrusion loads, and deformation of dies and wear of coating.

2. Coating Simulation
    - Conduct a friction test to predict an accurate wear coefficient rate (k) for the bilayer coating and H-13 tool steel that can be implemented in the Archards wear model.
    - Improve the Archard's wear model by utilizing temperature as a function of material hardness and wear rate coefficient.

3. Design of Experiments
    - Conduct a sensitivity test to examine the significance of all geometric parameters of the die cartridge and the mandrel as there could be other important parameters in each geometry that affect weld pressure and mandrel teeth effective stress.
    - Pick three or more significant factors from the sensitivity test to conduct a design of experiments to further optimize the die cartridge; either in terms of minimizing extrusion load or deformation stress.
    - The holder design of the modular die can further be improved by understanding how increasing or decreasing the dimension of the bridge affects stresses.
    - The three or four leg die cartridge designs can be optimized by conducting a DOE of varying lengths and width of the legs in order to minimize the stresses in the radiuses.
    - Optimizing the size of the radius under the armpit area of the die cartridge and holder.

LIST OF REFERENCES

LIST OF REFERENCES

[1] *Aluminum Extruders Council*. Available: http://www.aec.org/basics/basics.cfm. (Last Accessed Feb 2015)

[2] T. Björk, J. Bergström, and S. Hogmark, "Tribological simulation of aluminium hot extrusion," *Wear,* vol. 224, pp. 216-225, 2// 1999.

[3] "Fundamentals of Extrusion," *Aluminum Extrusion Technology,* 2000.

[4] P. K. Saha, "Thermodynamics and tribology in aluminum extrusion," *Wear,* vol. 218, pp. 179-190, 7// 1998.

[5] T. Moe, "Pressure and Strain Measurement During Hot Extrusion of Aluminum," Doctoral of Engineering Doctoral Thesis Department of Engineering Design and Materials, Norwegian University of Science and Technology, 2005.

[6] K. L. H.Stenger, *Extrusion*: American Society for Metals, 1976.

[7] I. Flitta and T. Sheppard, "Material Flow and Prediction of Extrusion Pressure When Extruding Through Bridge Dies Using FEM."

[8] E. Ceretti, L. Mazzoni, and C. Giardini, "3D FEM Geometry and Material Flow Optimization of Porthole-Die Extrusion," *AIP Conference Proceedings,* vol. 908, pp. 419-424, 05/17/ 2007.

[9] E. Ceretti, L. Mazzoni, and C. Giardini, "Simulation of metal flow and welding prediction in porthole die extrusion: the influence of the geometrical parameters," *International Journal of Material Forming,* vol. 2, pp. 101-104, 2009/08/01 2009.

[10] H. Chen, G. Zhao, C. Zhang, and Y. Guan, "Numerical simulation of extrusion process and die structure optimization for a hollow aluminum profile with thin wall," *Jixie Gongcheng Xuebao/Journal of Mechanical Engineering,* vol. 46, pp. 34-39, 2010.

[11] M. W. Fu, M. S. Yong, and T. Muramatsu, "Die fatigue life design and assessment via CAE simulation," *International Journal of Advanced Manufacturing Technology,* vol. 35, pp. 843-851, 2008.

[12] H. Valberg, "Metal flow in the direct axisymmetric extrusion of aluminium," *Journal of Materials Processing Technology,* vol. 31, pp. 39-55, 5// 1992.

[13] H. Valberg and T. Malvik, "An experimental investigation of the material flow inside the bearing channel in aluminium extrusion," *International Journal of Materials and Product Technology,* vol. 9, pp. 428-463, 01/01/ 1994.

[14] S. J. Yuan, F. Li, and Z. B. He, "Effects of guiding angle on plastic metal flow and defects in extrusion of aluminum alloy," *Journal of Materials Science & Technology,* vol. 24, pp. 256-260, Mar 2008.

[15] H. Sano, T. Ishikawa, and Y. Yoshida, "Study on Metal Flow in Extruded Billet," *ET Proceedings,* pp. 47-53, 2004.

[16] Y. T. Kim and K. Ikeda, "Flow behavior of the billet surface layer in porthole die extrusion of aluminum," *Metallurgical and Materials Transactions a-Physical Metallurgy and Materials Science,* vol. 31, pp. 1635-1643, Jun 2000.

[17] I. Flitta and T. Sheppard, "Nature of friction in extrusion process and its effect on material flow," *Materials Science and Technology,* vol. 19, pp. 837-846, Jul 2003.

[18] C. Zhang, G. Zhao, H. Chen, Y. Guan, and F. Kou, "Numerical simulation and metal flow analysis of hot extrusion process for a complex hollow aluminum profile," *The International Journal of Advanced Manufacturing Technology,* vol. 60, pp. 101-110, 2012/04/01 2012.

[19] J. M. Lee, B. M. Kim, and C. G. Kang, "Effects of chamber shapes of porthole die on elastic deformation and extrusion process in condenser tube extrusion," *Materials & Design,* vol. 26, pp. 327-336, 6// 2005.

[20] I. Flitta and T. Sheppard, "Temperature Changes and their effect on Deformation during Extrusion using FEM," *ET Proceedings,* pp. 269-283, 2004.

[21] I. Flitta and T. Sheppard, "Material flow during the extrusion of simple and complex cross-sections using FEM," *Materials Science and Technology,* vol. 21, pp. 648-656, 2005.

[22] P. Liu, S. Xie, and L. Cheng, "Die structure optimization for a large, multi-cavity aluminum profile using numerical simulation and experiments," *Materials & Design,* vol. 36, pp. 152-160, 4// 2012.

[23] P. Liu, S. Xie, and L. Cheng, "Die optimal design for a large diameter thin-walled aluminum profile extrusion by ALE algorithm," in *1st International Congress on Advanced Materials 2011, AM2011, May 13, 2011 - May 16, 2011*, Jinan, China, 2011, pp. 459-462.

[24] J. E. Jam and M. G. Zadeh, "3D Simulation of the cold extrusion process of non-symmetric section of Tellurium-Lead," *Association of Metallurgical Engineers of Serbia,* vol. 19, pp. 11-21, 2012.

[25] A. Hosseini, K. Farhangdoost, and M. Manoochehri, "Modelling of extrusion process and application of Taguchi method and ANOVA analysis for optimization the parameters," *MECHANIKA,* vol. 18, pp. 301-305, 2012.

[26] D. Tang, W. Fang, X. Fan, D. Li, and Y. Peng, "Effect of Die Design in Microchannel Tube Extrusion," *Procedia Engineering,* vol. 81, pp. 628-633, // 2014.

[27] G. Fang, J. Zhou, and J. Duszczyk, "Extrusion of 7075 aluminium alloy through double-pocket dies to manufacture a complex profile," *Journal of Materials Processing Technology,* vol. 209, pp. 3050-3059, 3/19/ 2009.

[28] J. X. Xie, T. Murakami, K. Ikeda, and H. Takahashi, "Experimental simulation of metal flow in porthole-die extrusion," *Journal of Materials Processing Technology,* vol. 49, pp. 1-11, 2/1/ 1995.

[29] J. Lof, "Developments in finite element simulations of aluminum extrusion," University Twente, Netherlands, 2000.

[30] S. Kobayashi, S. Oh, and T. Altan, *Metal forming and the finite element method.*, 1989.

[31] P. Kathirgamanathan, "Parameter Optimization of the Process of AA6xxxx and AA7xxx Series Aluminum Extrusion," Doctor of Philosophy in Mechanical Engineering, Mechanical Engineering, Auckland University of Technology, New Zealand, 2013.

[32] S. Oh, W. Wu, J. Tang, and A. Vedhanayagam, "Capabilities and applications of FEM code DEFORM: the prespective of the developer," *Journal of Materials Processing Technology,* vol. 27, pp. 25-42, 1991.

[33] C. Linder, "An Arbitrary Lagrangian-Eulerian Finite Element Formulation for Dynamics and Finite Strain Plasticity Models," Masters of Science, Department of Structural Mechanics, University Stuttgart, 2003.

[34] S. A. Savidis, D. Aubram, and F. Rackwitz, "Arbitrary lagrangian-eulerian finite element formulation for geotechnical construction process," *Journal of Theoretical and Applied Mechanics,* vol. 38, pp. 165-194, 2008.

[35] *Properties and Selection of Metals*, 8 ed. vol. 1. Ohio: American Society of Metals, 1961.

[36] Y. F. He, S. S. Xie, L. Cheng, G. J. Huang, and Y. Fu, "FEM simulation of aluminum extrusion process in porthole die with pockets," *Transactions of Nonferrous Metals Society of China,* vol. 20, pp. 1067-1071, Jun 2010.

[37] G. Li, J. T. Jinn, W. T. Wu, and S. I. Oh, "Recent development and applications of three-dimensional finite element modeling in bulk forming processes," *Journal of Materials Processing Technology,* vol. 113, pp. 40-45, 6/15/ 2001.

[38] L. Wang and H. Yang, "Friction in aluminium extrusion—part 2: A review of friction models for aluminium extrusion," *Tribology International,* vol. 56, pp. 99-106, 12// 2012.

[39] L. Wang, "Modelling of friction for high temperature extrusion of aluminium alloys," Master of Engineering, Engineering, Harbin Institute of Technology, 2012.

[40] H. Sofuoglu and H. Gedikli, "Physical and numerical analysis of three dimensional extrusion process," *Computational Materials Science,* vol. 31, pp. 113-124, 9// 2004.

[41] M. Arentoft, Z. Gronostajski, A. Niechajowicz, and T. Wanheim, "Physical and mathematical modelling of extrusion processes," *Journal of Materials Processing Technology,* vol. 106, pp. 2-7, 10/31/ 2000.

[42] W. Xianghong, Z. Guoqun, L. Yiguo, and M. Xinwu, "Numerical simulation and die structure optimization of an aluminum rectangular hollow pipe extrusion process," *Materials Science and Engineering: A,* vol. 435–436, pp. 266-274, 11/5/ 2006.

[43] Y. Aue-u-lan and K. Khansai, "3D Numerical Simulation to Investigate the Influential Factors Causing Die Failure in Hot Aluminum Extrusion of Square Hollow Profile," *International Journal of Science and Engineering,* vol. 2, pp. 11-17, 2012.

[44] J. Liu, G.-y. Lin, D. Feng, Y.-m. Zou, and L.-p. Sun, "Effects of process parameters and die geometry on longitudinal welds quality in aluminum porthole die extrusion process," *Journal of Central South University of Technology,* vol. 17, pp. 688-696, 2010/08/01 2010.

[45] U. Stahlberg and J. Hallstrom, "A Comparison Between Two Wear Models," *Material Process Technology,* vol. 87, pp. 223-229, 1999.

[46] T. Sobis, U. Engel, and M. Geiger, "A theoretical study on wear simulation in metal forming processes," *Journal of Materials Processing Technology,* vol. 34, pp. 233-240, 9// 1992.

[47] *Friction, Lubrication and Wear Technology* vol. 18: ASM International 1992.

[48] D. Kopeliovich. (2014). *Mechanisms of wear*. Available: http://www.substech.com/dokuwiki/doku.php?id=mechanisms_of_wear. (Last Accessed Feb 2015)

[49] C. Zhang, G. Zhao, T. Li, Y. Guan, H. Chen, and P. Li, "An Investigation of Die Wear Behavior During Aluminum Alloy 7075 Tube Extrusion," *Journal of Tribology,* vol. 135, pp. 011602-011602, 2012.

[50] A. G. Changhyok Choi, Taylan Altan∗, "Estimation of plastic deformation and abrasive wear in warm forging dies," *Journal of Materials Processing Technology,* vol. 2, 2012.

[51] G. A. Lee and Y. T. Im, "Finite-element investigation of the wear and elastic deformation of dies in metal forming," *Journal of Materials Processing Technology,* vol. 90, pp. 123-127, May 19 1999.

[52] T. Björk, R. Westergård, S. Hogmark, J. Bergström, and P. Hedenqvist, "Physical vapour deposition duplex coatings for aluminium extrusion dies," *Wear,* vol. 225–229, Part 2, pp. 1123-1130, 4// 1999.

[53] K. Lugscheider, T. Hornig, M. Maes, "Increasing the lifetime of aluminum and magnesium pressure die casting molds by arc ion plating PVD coatings.," presented at the 6th International Tooling Conference, Germany.

[54] S. Andersson, "Wear Simulation," in *Advanced Knowledge Application in Practice*, I. Fuerstner, ed, 2010.

[55] SFTC, "DEFORM V11.0.1 System Documentation," ed, 2014.

[56] T. Altan and M. Deshpande, "Selection of die materials and surface treatments for increasing die life in hot and warm forging," *Tech conference,* 2011.

[57] S. Paskvale, "Properties of PVD hard coatings," Mathematics and Physics, UNIVERSITY OF LJUBLJANA, Slovenia, 2007.

[58] C. Wu and M. S. Hamada, *Experiments: Planning, Analysis and Optimization*, second ed. New Jersey: John Wiley & Sons, Inc, 2011.

[59] K. Fang, R. Li, and A. Sudjianto, *Design and Modeling for Computer Experiments*: Chapman & Hall/CRC, 2006.

[60] S. H. Lee, J. M. Lee, H. H. Jo, H. Jo, and B. M. Kim, "Process analysis and die design in 12 cells condenser tube extrusion of Al3003," *Journal of Materials Processing Technology,* vol. 201, pp. 53-59, 5/26/ 2008.

[61] H.G.Mooi, A.J. Den Bakker, K.E. Nilsen, and J.Huetink, "Simulation of Aluminum Extrusion based on a Finite Element Method (FEM)," 1991.

[62] L. Donati and L. Tomesani, "Analysis of material flow and welding in aluminum extrusion of hollow sections," *V AITEM Conference,* pp. 678-698, 2001.

[63] (2015). *An overview of Kriging*. Available: http://php.scripts.psu.edu/users/s/d/sdq107/index_files/Geog486/lesson_5.htm. (Last Accessed Feb 2015)

[64] L. Donati and L. Tomesani, "The prediction of seam welds quality in aluminum extrusion," *Journal of Materials Processing Technology,* vol. 153–154, pp. 366-373, 11/10/ 2004.

[65] Y. Mahmoodkhani, M. A. Wells, N. Parson, and W. J. Poole, "Numerical modelling of the material flow during extrusion of aluminium alloys and transverse weld formation," *Journal of Materials Processing Technology,* vol. 214, pp. 688-700, 3// 2014.

[66] Uddeholm Orvar 2M/ AISI H13 Data Sheet [Online]. Available: http://www.bucanada.ca/media/orvar2m.pdf. (Last Accessed Feb 2015)